Universidade do Minho
Escola de Ciências

Weina Hou

Molecular Mechanisms of *Agrobacterium* Recognition and Defense Activation in Recalcitrant Plants

Dezembro de 2018

UMinho | 2018 Weina Hou **Molecular Mechanisms of *Agrobacterium* Recognition and Defense Activation in Recalcitrant Plants**

Universidade do Minho
Escola de Ciências

Weina Hou

Molecular Mechanisms of *Agrobacterium* Recognition and Defense Activation in Recalcitrant Plants

International Doctoral Program: Biological Sciences, Agricultural Production Chains-From Fork to Farm (AgriChains)

Supervisors:

Professor Doctor Alberto Carlos Pires Dias

Doctor Franklin Gregory

December 2018

DECLARATION

I declare that this thesis is an original report of my research, has been written by me and has not been submitted for any previous degree. The experimental work is almost entirely my own work; the collaborative contributions have been indicated clearly and acknowledged. Due references have been provided on all supporting literatures and resources.

I declare that I have acted with integrity in the elaboration of this thesis. I confirm that in all the work leading to its elaboration did not resort to the practice of plagiarism or any form of falsification of results.

I further declare that I have become aware of the University of Minho Code of Ethics.

Universidade do Minho, __1_/__12_/__2018____

WEINA HOU

Assinatura: _____Weina Hou__

The present work benefited from the following support:

The author acknowledges the financial support provided by the FCT-Portuguese Foundation for Science and Technology (SFRH/BD/52561/2014), under the Doctoral Programme "Agricultural Production Chains – from fork to farm" (PD/00122/2012).

Acknowledgements

I would like to take this opportunity to express my gratitude to everyone who supported me throughout the PhD journey both personally and professionally, without any of you I could not complete this wonderful trip of my life.

I am sincerely grateful to my family, my parents and my younger sister, for their disinterested supports, trust and encouragement as always. 感谢我家人一如既往的无条件的支持，信任以及鼓励。

I am sincerely thankful

To my supervisor Prof. Alberto Dias, I appreciate that he accepted me as his PhD student, and appreciate his constant support both scientifically and personally, especially the full trustfulness to allow me to design and organize the PhD work, empowering my independent thinking and creation, exercising my optimistic and positive attitude, as well as supervision and guide the PhD generally and helping me out when I need anytime.

To my co-supervisor Dr. Franklin Gregory, I appreciate he accepted me as his PhD student and let me complete my PhD project.

To my tutor Prof. Ana Cunha, I appreciate her friendly advices, warm concerns and professional support during the PhD journey.

To Prof. Francisco Tenllado, (the Biological Research Center, Spanish National Research Council, CIB-CSIC, Madrid, Spain), I appreciate he accepted me to join his lab for a part work of the PhD project. I appreciate his exemplary guidance, valuable knowledge as well as constant support on publications.

To my best close Portuguese colleague and friend Viviana, thanks for your meticulous concern and help from scientific advices and discussion, practical scientific knowledge to personal selfless care. And to my best close Portuguese colleague and friend Catarina, thanks for sharing the happiness and tears and support to each other to common growth in the past four years as a wonderful experience of my life. Thanks for both of you introduce me into your families and take care of me as a member of your families.

To my best Indian colleague and friend Rupesh, thanks for your valuable scientific discussions and views on related to the work. And thanks for sharing with me your happy moments of your life.

To my best Chinese colleague and friend Pan Zhao, thanks for his unconditional support from scientific work and encouragements.

To my best Croatian colleagues and friends Nikola and Iva, thanks for accompanying me during our PhD period, sharing the happiness, experiences and views.

To my dear colleagues and friends from LBV, Henrique, thanks for your truthful and illuminating views on a number of issues related to the project and thanks for sharing your sweet cat with me. And to all of my colleagues and friends from LBV, Richard, António, Jorge, Rose, Luis, Angélica, Bárbara, Catarina, Vanessa, etc., thanks for all of your kindly support during my PhD from the lab.

To the groups from CIB-CSIC, to Prof. Tomas Canto for his exemplary guidance and valuable knowledge in subcellular localization by confocal microscope. To my best Spanish colleagues and friends Emmanuel, Fran and Irene, thanks for your friendship, enthusiasm, concerns and truthful views on my work and my life.

To AgriChains' board team and all the professors and colleagues; to Prof. Eduardo Rosa for offering the opportunity to recruit the students from all over the world to join the AgriChains PhD program; to Prof. Amélia Silva for her hard work in the program and Ms Lígia Pinto for assisting the program as the AgriChains secretariat. To all of our AgriChains colleagues who've gone through together for these four excellent years.

And I appreciate Prof. Maria Teresa Almeida for kindly sharing the plant growth room. I am also grateful the support of the technicians Mr. Luis and Ms. Paula from the Department of Biology.

Molecular Mechanisms of *Agrobacterium* Recognition and Defense Activation in Recalcitrant Plants

Abstract

Hypericum perforatum L. is a reservoir of high-value secondary metabolites, with a rapidly increasing interest for both researchers and the pharmaceutical industry. Hence, improving the production of these compounds via genetic manipulation is a challenging task. However, a major drawback is the recalcitrance of *H. perforatum* L. to *Agrobacterium tumefaciens*-mediated transformation. Hence, in the presented study, *H. perforatum* L. was chosen as model plant to investigate the molecular mechanisms underlying plant recalcitrance to bacterial infection, by identifying and characterizing key genes involved in these responses. *Phenolic oxidative coupling protein* (*Hyp-1*), a pathogenesis-related (PR) class 10 family gene, was selected from a forward subtractive cDNA library from *H. perforatum* L. suspension cells elicitated with *A. tumefaciens*. The role of *Hyp-1* in defense against *A. tumefaciens* was analyzed in transgenic *Nicotiana tabacum* and *Lactuca sativa* plants overexpressing *Hyp-1*, and in *Catharanthus roseus* silenced for the homologous *Hyp-1* gene, *CrIPR*. Results showed that transformation efficiency of *A. tumefaciens* was greatly decreased in tobacco and lettuce plants overexpressing *Hyp-1*. However, silencing of *CrIPR* in *C. roseus* led to induction of *CrPR-5* and an increased resistance to *Agrobacterium* infection. Moreover, the expression of core genes regulating several defense pathways was analyzed in *Hyp-1* transgenic tobacco plants. Overall, overexpressing of *Hyp-1* led to an ample down-regulation of key genes involved in auxin signaling (*NtaTIR1*, *NtaAFR8)*, microRNA(miR)-based gene silencing (*NtaAGO1*, *Nta*miR*160*, *NtamiR164ab)*, detoxification of reactive oxygen species (*NtaFe-SOD*), phenylpropanoid pathway (*NtaPAL1*, *NtaPAL4* and *NtaCHS*) and PRs (*NtaPR10* and *NtaPR1)*. Moreover, Hyp-1 was detected in the nucleus, plasma membrane and the cytoplasm of epidermal cells by confocal microscopy. In parallel, a *Polygalacturonase inhibiting protein* (*PGIP*) from *H. perforatum* L. was selected from the same cDNA library. The role of *HpPGIP* in defense against *A. tumefaciens* was analyzed in transgenic *N. tabacum* plants overexpression *HpPGIP*, and in *Nicotiana benthamiana* heterogeneous silenced for the homologous *BoPGIP*. Results showed that the transformation efficiency of *A. tumefaciens* was greatly decreased in tobacco overexpressing *HpPGIP*. However, silencing of *BoPGIP* in *N. benthamiana* led to induction of *NbPRs* and increased resistance to *A. tumefaciens*. Moreover, the expression of core genes regulating several defense pathways was analyzed in *HpPGIP* transgenic tobacco plants.

Overall, plants overexpressing *HpPGIP* showed increased expression of the key genes involved in the synthesis of secondary metabolites lignin and flavonoids (*NtaPAL1,4*, *NtaCCR* and *NtaCHS*), ROS pathway (*NtaAPX* and *NtaFe-SOD*), as well as microRNA-mediated gene silencing pathway (*NtaAGO1* and *NtamiR164c*). Additionally, plants overexpression *Hyp-1-PGIP,* showed enriched secondary metabolism and ROS defense pathways, by especially up-regulating *NtaCAD* and *NtaCAT*, respectively. The expression of genes from JA signaling pathway (*NtaLOX*) and miroRNA-mediated gene silencing pathway (*NtaAGO1*) was also upregulated in these plants. In the present study, it was also demonstrated that HpPGIP protein localizes at plasma membrane, cytoplasm and nucleus. To further understand the molecular mechanisms involved in *A. tumefaciens* and *H. perforatum* L. interaction, the expression of core genes involved in plant defense pathways including secondary metabolism, gene silencing, ROS pathways and other defense genes (*Hyp-1* and *HpPGIP*) was investigated. Results indicated that resistance of *H. perforatum* L. cells to infection by *A. tumefaciens* involves the induction of several genes encoding key enzymes of secondary metabolism, including those mediating not only the synthesis of xanthones (*HpPAL* and *HpBPS*), but also hypericin (*HpOKS* and *HpPKS2*) and melatonin (*HpIGPS*), ROS pathway (*HpAOX*) and other defense genes (*Hyp-1* and *HpPGIP*). Moreover, transcript levels of *RDR6* and *SGS3* associated to the gene silencing pathway, sense-post-transcriptional gene silencing (S-PTGS) and trans acting siRNAs (ta-siRNA) pathway, together with *HpAGO5*, were not affected during the defense response. This study was complemented by quantifying the expression of these defense genes in *H. perforatum* L. plants with or without dark glands, which are known to accumulate large amounts of secondary metabolites, hence contributing to plant defense ability. Results supported the key role of these glands in gifting the host plant with resistance to pathogens, by highly accumulating secondary metabolites like xanthone (*HpPAL* and *HpBPS*) and hypericin (*HpOKS* and *HpPKS2*), together with a stimulation of the ROS pathway (*HpCAT*) and of the expression of other genes directly associated to the defense response (*HpHyp-1* and *HpPGIP*). In summary, the present study provided a better understanding on the functional roles of *Hyp-1* and *HpPGIP*, enlightening their role in plant defense and on the network of events underlying the molecular responses of *H. perforatum* L. upon interaction with *A. tumefacien.*

Mecanismos Moleculares de Reconhecimento de *Agrobacterium* e de Ativação de Sistemas de Defesa em Plantas Recalcitrantes

Resumo

Hypericum perforatum L. é uma planta com um vasto reservatório de metabolitos secundários de valor acrescentado, suscitando um crescente interesse na investigação científica e na indústria farmacêutica. Desta forma, melhorar a produção destes compostos através da manipulação genética é uma tarefa desafiadora. No entanto, um dos maiores entraves a esta tarefa consiste na recalcitrância de *H. perforatum* L. à transformação mediada por *Agrobacterium tumefaciens*. No presente estudo, *H. perforatum* L. foi selecionado como modelo para investigar os mecanismos moleculares que estão na base da recalcitrância das plantas à infecção bacteriana, através da indentificação e caracterização de genes-chave envolvidos na resposta ao stresse biótico. Uma *Phenolic oxidative coupling protein* (*Hyp-1*), pertencente à família *pathogenesis-related (PR) class 10* foi selecionada de uma biblioteca subtrativa de cDNA de suspensões celulares de *H. perforatum* L. elicitadas com *A. tumefaciens*. A função de *Hyp-1* na defesa contra *A. tumefaciens* foi analisada em plantas transgénicas de tabaco e de alface com sobrexpressão deste gene, e em plantas de *Catharanthus roseus* com o gene homólogo *CrIPR* silenciado. Os resultados mostraram que a eficiência de infeção de *A. tumefaciens* diminuiu drasticamente em plantas de tabaco e de alface com sobrexpressão do *Hyp-1*. No entanto, o silenciamento do gene *CrIPR* em *C. roseus* resultou numa indução do gene *CPR-5* e conduziu a um aumento da resistência à infecção por *Agrobacterium*. Adicionalmente, a expressão de gene-chave reguladores dos mecanismos de defesa da planta foram analisados nas plantas de tabaco com sobrexpressão do gene *Hyp-1*. De um modo geral, estas plantas apresentaram uma repressão na expressão de genes envolvidos na sinalização das auxinas (*NtaTIR1*, *NtaAFR8)*, no silenciamento de genes mediado por microRNAs (*NtaAGO1*, *Nta*miR*160*, *NtamiR164ab)*, na destoxificação de espécies reativas de oxigénio (*NtaFe-SOD*), na via fenilpropanóide (*NtaPAL1*, *NtaPAL4* e *NtaCHS*) e em genes da família *PR* (*NtaPR10* e *NtaPR1)*. Verificou-se ainda que a proteína Hyp-1 está localizada no núcleo, na membrana plasmática e no citosol de células da epiderme, como observado por microscopia de fluorescência de proteínas de fusão. Em paralelo, uma *Polygalacturonase inhibiting protein* (*PGIP*) de *H. perforatum* L. foi também selecionada da mesma biblioteca de cDNA. O papel do *HpPGIP* na defesa contra *A. tumefaciens* foi analizada em plantas tabaco com sobrexpressão deste gene, e em plantas *Nicotiana benthamiana* com silenciamento do gene homólogo,

BoPGIP. Os resultados mostraram que a eficiência de infeção de *A. tumefaciens* diminuiu significativamente nas plantas com sobrexpressão do *HpPGIP*. No entanto, o silenciamento do gene *BoPGIP* em *N. benthamiana* conduziu a uma indução da expressão de *NbPRs*, bem como do aumento da resistência a *A. tumefaciens*. Foi ainda estudada a expressão de genes-chave da regulação das vias de defesa em plantas transgénicas de tabaco sobrexpressando o gene *HpPGIP*. Verificou-se que estas plantas apresentavam uma sobrexpressão de genes envolvidos na biossíntese de metabolitos secundários como a lenhina e os flavonóides (*NtaPAL1,4*, *NtaCCR* e *NtaCHS*), na via dos ROS (*NtaAPX* e *NtaFe-SOD*), e no silenciamento de genes mediado por microRNAs (*NtaAGO1* e *NtamiR164c*). Foi observada ainda a indução da expressão dos genes *NtaCAD* e *NtaCAT*, bem como de genes envolvidos nas vias de sinalização do ácido jasmónico (*NtaLOX*). No presente estudo verificou-se que a proteína HpPGIP está localizada na membrana plasmática, no citoplasma e no núcleo das células. Para melhor compreender os mecanismos envolvidos neste processo, a expressão de genes-chave envolvidos na resposta da planta ao stress biótico foi determinada em suspensões celulares de *H. perforatum* L. elicitadas com *A. tumefaciens*, incluindo genes das vias do metabolismo secundário, de silenciamento de genes, do metabolismo dos ROS e de outras vias de defesa, incluindo o *Hyp-1* e *HpPGIP*. Os resultados mostraram diferenças na expressão de vários genes envolvidos nas vias de biossíntese de xantonas (*HpPAL* e *HpBPS*), hipericina (*HpOKS* e *HpPKS2*) e melatonina (*HpIGPS*), bem como no metabolismo dos ROS (*HpAOX*), e na defesa da planta (*Hyp-1* e *HpPGIP*). Foi ainda observado que os níveis de transcritos dos genes *RDR6* e *SGS3* associados à via de silenciamento de genes não foram afetados, bem como do gene *S-PTGS* e *HpAGO5*. O presente estudo foi complementado pela quantificação da expressão destes genes em plantas de *H. perforatum* com ou sem estruturas glandulares, onde se acumulam grandes quantidades de metabolitos secundários, contribuindo assim para a capacidade de defesa da planta. Os resultados suportaram o papel fundamental destas estruturas na resposta da planta ao stresse biótico, verificando-se sobrexpressão de genes da via de produção de xantonas (*HpPAL* e *HpBPS*) e hipericina (*HpOKS* e *HpPKS2*), bem como uma estimulação da via dos ROS (*HpCAT*) e dos genes caracterizados neste estudo (*HpHyp-1* e *HpPGIP*). Em suma, o presente trabalho contribuiu para melhor compreender o papel dos genes *Hyp-1* e *HpPGIP* na defesa da planta contra stresse biótico, e a sua influência na regulação da rede de eventos moleculares que estão na base da recalcitrância de *H. perforatum* L. à infeção por *A. tumefaciens.*

List of original publications

This thesis is based on the following papers:

Publications

1. **Weina Hou**, Preeti Shakya and Gregory Franklin (2016) A perspective on *Hypericum perforatum* genetic transformation. Front. Plant Sci., 24 June 2016 doi.org/10.3389/fpls.2016.00879
2. Singh RK, **Weina Hou**, Franklin G. (2016) Construction of hypericin gland-specific cDNA library via Suppression subtractive hybridization. Methods Mol Biol. 2016; 1391:317-34. doi: 10.1007/978-1-4939-3332-7_22
3. **Weina Hou**, Rupesh Kumar Singh, Pan Zhao, Viviana Martins, Emmanuel Aguilar, Tomás Canto, Franklin Gregory, Francisco Tenllado, Alberto Carlos Pires Dias. (2018) Transgenic expression of *Hyp-1* gene from *Hypericum perforatum* L. alters expression of defense-related genes and modulates recalcitrance to *Agrobacterium tumefaciens*. *Plant Science* (submitted).
4. **Weina Hou**, Rupesh Kumar Singh, Viviana Martins, Emmanuel Aguilar, Tomás Canto, Franklin Gregory, Francisco Tenllado, Alberto Carlos Pires Dias. (2018) Evidence for the involvement of a *Polygalacturonase-inhibiting protein* from *Hypericum perforatum* L. in its recalcitrance to *Agrobacterium tumefaciens*-mediated transformation. *Planta* (submitted).
5. **Weina Hou**, Rupesh Kumar Singh, Viviana Martins, Francisco Tenllado, Alberto Carlos Pires Dias. (2018) Transcriptional responses of *Hypericum perforatum* L. cells upon co-cultivation with *Agrobacterium tumefaciens* and comparison of gene expression in *Hypericum perforatum* L. leaves and glands. To be submitted.

Congress abstracts

1. RK Singh, **Weina Hou**, ACP Dias and G Franklin (2014) *Agrobacterium*-elicited *Hypericum perforatum* cell methanolic extract shows antibacterial activity against human pathogens. Planta Med 2014; 80 - P1L4. doi: 10.1055/s-0034-1394698
2. RK Singh, **Weina Hou**, G Marslin, ACP Dias and G Franklin (2014) Lignin and flavonoid content increases in *Hypericum perforatum* cell wall after *Agrobacterium tumefaciens* co cultivation. Planta Med 2014; 80 - P1M22. doi: 10.1055/s-0034-13945

Table of Contents

DECLARAÇÃO II

Acknowledgements VII

Abstract IX

Resumo XI

List of original publications XIII

Table of Contents XV

Abbreviations and Acronyms XIX

List of Figures XXIII

Chapter 1 General introduction 2

1.1 ***Hypericum perforatum*** **L.** 2

1.2 **Induction of plant defense responses by** ***Agrobacterium*** **elicitation** 4

1.3 ***A. tumefaciens*** **defense genes** ***Phenolic oxidative coupling protein*** **(*Hyp-1*) and** ***Polygalacturonase inhibiting protein*** **(*PGIP*)** 5

1.3.1 ***A. tumefaciens*** **defense gene** ***Hyp-1*** 6

1.3.2 ***A. tumefaciens*** **defense gene** ***PGIP*** 7

1.4 **Virus-induced gene silencing** 8

1.5 **Objectives of study** 9

1.6 References 10

Chapter 2 Materials and methods 16

2.1 **Plant material and plant growth conditions** 16

2.1.1 **Seeds sterilization and germination** 16

2.1.2 **Plant growth condition** 16

2.2 **Elicitation of** ***H. perforatum*** **L. cells with** ***A. tumefaciens*** 17

2.3 **Suppression subtraction hybridization (SSH) and cDNA library construction** 17

2.4 **Plasmid construction and site-directed mutagenesis** 18

2.4.1 **Constructions of** ***Hyp-1*** **related plasmids** 18

2.4.2 Constructions of *HpPGIP* related plasmids 19

2.4.3 Construction of plasmids for VIGS 19

2.5 *Agrobacterium*-mediated genetic transformation 21

2.6 *Agrobacterium*-mediated transient expression 22

2.7 Plant total RNA isolation and quantitative real-time RT-PCR 22

2.7.1 Plant total RNA isolation 22

2.7.2 Quantitative real-time RT-PCR 23

2.8 Semiquantitative RT-PCR 30

2.8.1 Semiquantitative RT-PCR in *C. roseus* 30

2.8.2 Semiquantitative RT-PCR in *N. benthamiana* 30

2.9 GUS staining assays 31

2.10 Subcellular localization 32

2.11 Virus-induced gene silencing 32

2.11.1 VIGS in *C. roseus* 32

2.11.2 VIGS in *N. benthamiana* 33

2.11.3 VIGS in *H. perforatum* L. 33

2.12 Plant virus inoculation 33

2.13 Western blotting 34

2.14 Statistical analysis 34

2.15 References 34

Chapter 3 Transgenic expression of *Hyp-1* gene from *H. perforatum* L. alters expression of defense-related genes and modulates recalcitrance to *A. tumefaciens* 38

3.1 Summary 38

3.2 Introduction 39

3.3 Results 44

3.3.1 Overexpression of *Hyp-1* in *N. tabacum* and *L. sativa* 44

3.3.2 Subcellular localization studies 49

3.3.3 Overexpression of *Hyp-1* alters expression of multiple defense-related genes 51

3.3.4 Virus-induced gene silencing in *C. roseus* 54

3.3.5 Virus-induced gene silencing in *H. perforatum* L. 55

3.4 Discussion 58

3.5 Acknowledgements 62

3.6 References 62

Chapter 4 Evidence for the involvement of a *Polygalacturonase-inhibiting protein* from *H. perforatum* L. in its recalcitrance to *A. tumefaciens*-mediated transformation 74

4.1 Summary 74

4.2 Introduction 75

4.3 Results 77

4.3.1 Cloning and characterization of *HpPGIP* 77

4.3.2 Overexpression of *HpPGIP* in *N. tabacum* 77

4.3.3 Subcellular localization assays 82

4.3.4 *HpPGIP* alters gene expression of multiple defense pathways 83

4.3.5 Virus-induced gene silencing in *N. benthamiana* 88

4.4 Discussion 90

4.5 Acknowledgments 94

4.6 References 95

Chapter 5 Transcriptional responses of *H. perforatum* L. cells upon co-cultivation with *A. tumefaciens* and comparison of gene expression in *H. perforatum* L. leaves and glands 102

5.1 Summary 102

5.2 Introduction 103

5.3 Results 105

5.3.1 Expression of key genes involved in the defense of *H. perforatum* L. cells to *A. tumefaciens* elicitation 105

5.3.2 Comparison the expression of key genes involved in the defense of *H. perforatum* L. plants in glands 111

5.4 Discussion 115

5.5 Acknowledgements 117

5.6 References 117

Chapter 6 General discussion and future prospects 124

6.1 General discussion 124

6.1.1 Hyp-1 localizes to the plasma membrane, cytoplasm and nucleus and overexpression of *Hyp-1* alters expression of defense-related genes to modulates recalcitrance to *A. tumefaciens* ..124

6.1.2 PGIP localizes to the plasma membrane, cytoplasm and nucleus and overexpression of *HpHGIP* alters expression of defense-related genes to modulates recalcitrance to *A. tumefaciens* 126

6.1.3 A networking of genes involved in secondary metabolism, ROS pathways and other defense mechanisms is recruited in *H. perforatum* L. upon elicitation with *A. tumefaciens* ... 129

6.2 Future prospects 131

6.3 References 132

Abbreviations and Acronyms

4CL-4-Coumarate: CoA ligase

18SrRNA-18S ribosomal RNA

aa-Amino acid

ABA-Abscisic acid

AGO-ARGONAUTE protein

APX-Ascorbate peroxidase

ARF-Auxin responsive factor

AS-Acetosyringone

BA-6-Benzylaminopurine

bp-Base pair

BPS-Benzophenone synthase

CAD-Cinnamyl alcohol dehydrogenase

CAT-Catalase

CCR-Cinnamoyl CoA reductase

cDNA - Complementary DNA

ChlH-Catharanthus *roseus* protoporphyrin IX magnesium chelatase subunit H

CHS-Chalcone synthase

CMV-*Cucumber mosaic virus*

CrIPR-*C. roseus* is intracellular pathogenesis related protein

CTAB- Cetyltrimethylammonium bromide

DCLs-Dicer-like protein

DTT-1,4-Dithiothreitol

EDTA- Ethylenediaminetetraacetic acid

EF-1α-Elongation factor 1α

FDA-Fluorescein diacetate

GAPDH-Glyceraldehyde-3-phosphate dehydrogenase A subunit

GFP-Green fluorescent protein

GUS: β-glucuronidase

Hyp-1-Phenolic oxidative coupling protein

IAA-Indole-3-acetic acid

IBA- Indole-3-butyric acid

IGPS-Indole-3-glycerol phosphate synthase

JA-Jasmonate

kDa-kilodalton

L25-L25 ribosomal protein

LB – Luria-Bertani medium

LOX-Lipoxygenases

MAPKs-Mitogen- activated protein kinases

MES-2-(N-morpholino) ethanesulfonic acid

mRNA-Messenger RNA

MS-Murashige and Skoog

nt-Nucleotides

OD600-Optical density at 600 nm

OGs-Oligogalacturonides

OKS-Octaketide synthase

ORF-Open reading frame

PAL-Phenylalanine ammonia-lyase

PAMPs-Pathogen-associated molecular patterns

PAT-Phosphoribosylanthranilate transferase

PG-Polygalacturonase

PGIP-Polygalacturonase inhibiting protein

PI-Propidium iodide

PKS-Type III polyketide synthases

PPV-*Plum pox virus* tagged

PRs-Pathogenesis related proteins

PTGS-Posttranscriptional gene silencing

PTI-PAMP-triggered immunity

PVDF-poly- vinylidene difluoride

PVP-Polyvinylpyrrolidone

PVX-*Potato virus X*

qRT-PCR (qPCR)-Quantitative real-time RT-PCR

RDR6-RNA-dependent RNA polymerases 6

RISC-RNA-induced silencing complex

ROS-Reactive oxygen species

RSP9-40S ribosomal protein S9

RT-PCR - Reverse transcriptase-PCR

SA-Salicylic acid

SD-Standard deviation

SDS- Sodium dodecyl sulfate

SEM-Standard error of the mean

SGS3-Suppressor of Gene Silencing 3

SOD-Superoxide dismutase

S-PTGS-Sense-post-transcriptional gene silencing

SSH-Suppressive subtractive hybridization

T-DNA-Transfer DNA

TIR-Transport inhibitor response

TRV-*Tobacco rattle virus*

TuMV-*Turnip mosaic virus*

MeJA-Methyl jasmonate

NAA- Naphthaleneacetic acid

VIGS-Virus-induced gene silencing

x *g*-Relative centrifugal force (or times the Earth's gravitational acceleration)

List of Figures

Fig. 1.1 *H. perforatum* L. plant (A) and glands on flowers (B) and leaves (C) and the arrows indicate the glands. 3
Fig. 1.2 Changes in *H. perforatum* L. suspension cells in response to *A. tumefaciens* co-cultivation.... 5
Fig. 3.1 Generation of *N. tabacum* GFP-Hyp-1 overexpressing plants..... 45
Fig. 3.2 Detection of *Agrobacterium*-mediated expression in GFP-Hyp-1 tobacco T2 lines by GUS staining. 46
Fig. 3.3 Generation of *L. sativa* BL *Hyp-1* overexpression plants. 47
Fig. 3.4 Generation of *L. sativa* SBR *Hyp-1* overexpression plants..... 47
Fig. 3.5 Detection of *Agrobacterium*-mediated expression in Hyp-1 *L. sativa* BL T1 lines by GUS staining. 48
Fig. 3.6 Detection of *Agrobacterium*-mediated expression in Hyp-1 *L. sativa* SBR T1 lines by GUS staining. 49
Fig. 3.7 Detection of *Agrobacterium*-mediated expression in GFP-Hyp-N tobacco T2 lines by GUS staining. 49
Fig. 3.8 Subcellular localization of GFP-Hyp-1 at the plasma membrane, nucleus and cytoplasm. 50
Fig. 3.9 Fluorescence microscopy and western blot analysis in GFP-Hyp-1 transgenic lines..... 51
Fig. 3.10 Quantitative real time PCR to assess core genes involved in different plant defense pathways in GFP-Hyp-1 transgenic tobacco plants. 53
Fig. 3.11 Phylogenetic relationships of Hyp-1 homologs in plants, constructed using the program MEGA 6..... 56
Fig. 3.12 Silencing of *CrIPR* in *C. roseus* results in enhanced tolerance to *A. tumefaciens*..... 57
Fig. 3.13 Symptoms of *N. benthamiana* plants infected with viruses..... 58
Fig. 4.1 cDNA and amino acid sequence of *HpPGIP* from *H. perforatum* L..... 79
Fig. 4.2 Phylogenetic analysis of *HpPGIP* and other homologous genes..... 80
Fig. 4.3 Generation of *HpPGIP* overexpressed tobacco T2 plant lines. 81
Fig. 4.4 Detection of *Agrobacterium*-mediated gene expression in T2 HpPGIP tobacco lines by GUS staining. 82
Fig. 4.5 Subcellular localization of GFP-PGIP in the nucleus, plasma membrane and cytoplasm..... 83
Fig. 4.6 Quantitative real time RT-PCR to assess core genes involved in different plant defense pathways in PGIP transgenic tobacco plants..... 86
Fig. 4.7 Quantitative real time RT-PCR to assess core genes involved in different plant defense pathways in Hyp-1-PGIP transgenic tobacco plants. 87
Fig. 4.8 TRV-mediated silencing of *PGIP* in *N. benthamiana*. 89

Fig. 5.1 Gene expression of key genes involved in secondary metabolites defense pathway detected by qRT-PCR. 107
Fig. 5.2 Putative secondary metabolite synthesis pathway and fold variation in relative key genes from those pathways in *H. perforatum* L. 108
Fig. 5.3 Gene expression variation of key genes involved in gene silencing pathway. 109
Fig. 5.4 Gene expression variation in ROS pathway. 110
Fig. 5.5 Gene expression variation of *Agrobacterium* defense genes. 110
Fig. 5.6 Comparison the accumulation of core value genes from secondary metabolites pathways in *H. perforatum* L. leaves and glands by qRT-PCR. 112
Fig. 5.7 Fold variation in comparison of relative level expression of transcripts in flavonoids, xanthone, hyperforin, hypericin, and melatonin biosynthesis pathways in *H. perforatum* L. 113
Fig. 5.8 Comparison of relative level expression of genes from gene silencing pathway in *H. perforatum* L. leaves and glands by qRT-PCR. 113
Fig. 5.9 Comparison of relative level expression of ROS pathway genes transcripts in *H. perforatum* L. leaves and glands by qRT-PCR. 114
Fig. 5.10 Comparison of relative level expression of *Agrobacterium* defense genes in *H. perforatum* L. leaves and glands by qRT-PCR. 114

Chapter 1

General Introduction

Part of the content of this chapter is included in those following publications:

Weina Hou, Rupesh Kumar Singh, Pan Zhao, Viviana Martins, Emmanuel Aguilar, Tomás Canto, Franklin Gregory, Francisco Tenllado, Alberto Carlos Pires Dias. (2018) Transgenic expression of *Hyp-1* gene from *Hypericum perforatum* L. alters expression of defense-related genes and modulates recalcitrance to *Agrobacterium tumefaciens*. *Plant Science* (submitted).

Weina Hou, Rupesh Kumar Singh, Viviana Martins, Emmanuel Aguilar, Tomás Canto, Franklin Gregory, Francisco Tenllado, Alberto Carlos Pires Dias. (2018) Evidence for the involvement of a *Polygalacturonase-inhibiting protein* from *Hypericum perforatum* L. in its recalcitrance to *Agrobacterium tumefaciens*-mediated transformation. *Planta* (submitted).

Chapter 1 General introduction

1.1 *Hypericum perforatum* L.

H. perforatum L. is one of the oldest medicinal plants with a history of more than 2000 years, popularly known as St. John's wort. It belongs to the Guttiferae family, and around 450 known species of *Hypericum* are widely distributed in Europe, North America, Australia, New Zealand, Eastern Asia and South America (Karppinen, 2010). *H. perforatum* L. normally is 50-100 cm height and mostly grows at sunny and well-drained roadsides, slopes, wood borders or stone quarries. The flowers of *H. perforatum* L. are bright yellow, star-shaped, clustered in a trio and have five petals (Fig. 1.1). Different types of secretory structures including dark glands, translucent glands and various secretory canals characterize *H. perforatum* L. (Zobayed *et al.*, 2006; Karppinen, 2010; Raak *et al.*, 2012). The dark glands are black or dark-red multicellular nodules appear at leaf margins, stems, flower petals and stamens. The translucent glands make leaves look perforated, and they are visible in sepals and petals of flowers and all leaves. Additionally, there are three different types of secretory canals have been described in *H. perforatum* L. tissues (Karppinen, 2010).

In addition, *H. perforatum* L. contains a broad range of bioactive secondary metabolites that belong to different chemical groups. Hypericin, hyperforin, xanthones, essential oils, phenolic acids and a series of flavonoids, have been identified in extracts of the plant (Butterweck *et al.*, 2003; Patočka J, 2003; Tatsis *et al.*, 2007; Saddiqe *et al.*, 2010). The hypericin is one of the most interesting compounds of *H. perforatum* L. and many pharmacological effects of hypericin have been described (Saddiqe *et al.*, 2010). In *H. perforatum* L., hypericin abundantly presents in flowers and leaves, and accumulates in black glands. Although the function of hypericin in *Hypericum* species is still not clear, it is proposed that it serves as a defensive role against plant pathogens. It is reported that hypericin levels of two *Hypericum* species (*H. perforatum* L. and *H. pruinatum*) increased significantly in response to inoculation with two fungal pathogens (Cirak *et al.*, 2005). In our present study, the transcript level of the hypericin synthesis pathway genes *type III Polyketide synthases 2* (*PKS2*) and *Octaketide synthase* (*OKS*) both were increased in *H. perforatum* L. suspension cells elicited with *A. tumefaciens* for 12 h (as detailed in chapter 5). Hyperforin widely distributes in *H. perforatum* L. and occurs in flowers, fruits and leaves. The benefit of hyperforin to the plant still remains unclear, but it has

antimicrobial properties are expected to response to plant biotic stress (Bruni and Sacchetti, 2009; Karppinen, 2010). Xanthones have a wide range of pharmacological and biological properties, such as antioxidant and antimicrobial. It has been reported that the accumulation of xanthones is highly increased when *H. perforatum* L. culture elicited with *Colletotrichum gloeosporioides* and *A. tumefaciens* (Conceição *et al.*, 2006; Franklin *et al.*, 2009). In the present study, the two xanthones synthesis pathway genes *Phenylalanine ammonia-lyase* (*PAL*) and *Benzophenone synthase* (*BPS*) were increased significantly when *H. perforatum* L. suspension cells incubation with *A. tumefaciens* 12 h, as detailed in chapter 5. The pharmacological studies have confirmed that hypericin, hyperforin and xanthones make mainly contribution to the antidepressant activity of the species through various mechanisms of action (Tatsis *et al.*, 2007; Karppinen, 2010).

H. perforatum L. has attracted attention as a medicinal plant with pharmacological properties like antidepressant, anti-inflammatory, antiviral, anti-cancer, and antibacterial. However, little genetic information is available for this species, especially that concerning the genetic transformation and gene functional research for this species.



Fig. 1.1 *H. perforatum* L. plant (A) and glands on flowers (B) and leaves (C) and the arrows indicate the glands. Adapted from Araújo PV (2018) *H. perforatum* L., Flora-On: Flora de Portugal Interactiva, Sociedade Portuguesa de Botânica. www.flora-on.pt.

1.2 Induction of plant defense responses by *Agrobacterium* elicitation

Agrobacterium tumefaciens is a gram-negative, soil-born bacterium which has a broad range of host in plants, especially dicot species. In the natural environment, wild type *A. tumefaciens* infect the plant cells by integration of a transfer DNA (T-DNA) by the help of Ti plasmid and produce crown gall disease on host species. This feature of *A. tumefaciens* has been widely exploited to introduce candidate gene into plant, fungi and even animal cells in laboratory conditions (Gelvin, 2005; 2010).

Agrobacterium-mediated genetic transformation is the most preferred strategy to produce stable gene transfer for desirable traits into crop plants. The advantages like simplicity, cost affordable, lower transgene rearrangement, ability of long DNA segments transfer, and preferential integration of foreign genes into transcriptionally active regions make *Agrobacterium*-mediated transformation into an attractive method (Kumar *et al.*, 2013).

However, as a bacterium that is pathogenic to plants, *Agrobacterium* induces a series of defense responses in infected plant cells (Pitzschke, 2013). The recognition of pathogen-associated molecular patterns (PAMPs) by the plant's innate immune system represents the first layer of defense against pathogenic bacterial attack. The recognition of PAMPs and the subsequent plant defense responses are also referred to as PAMP-triggered immunity (PTI). The cellular responses associated with PTI include rapid ion fluxes across the plasma membrane, the generation of reactive oxygen species (ROS), activation of mitogen- activated protein kinases (MAPKs) and the gene expression is changed rapidly, such as the expression of pathogenesis related (PR) genes are induced and hormonal adjustments (Postel *et al*,. 2009; Pitzschke, 2013). Obviously, by employing *Agrobacterium* as a vehicle for genetic transformation, a series of plant defense responses will be induced during the infection.

Supporting this defense response, Franklin and co-workers (2008) reported the incompatible interaction of *A. tumefaciens* with *H. perforatum* L., resulting in 99% mortality of *A. tumefaciens* within 12 h of co-cultivation, while *H. perforatum* L. cells did not undergo an obvious apoptotic process (Fig. 1.2). This result revealed that *H. perforatum* L. defense response quickly reduced *Agrobacterium* viability and affected the transformation process during co-cultivation.

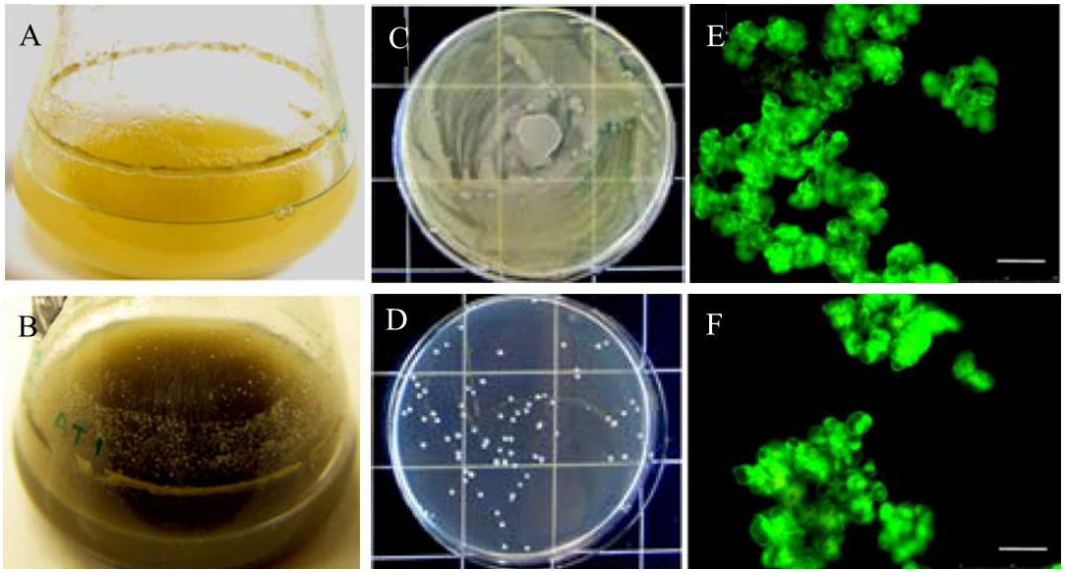


Fig. 1.2 Changes in *H. perforatum* L. suspension cells in response to *A. tumefaciens* co-cultivation. (A) *H. perforatum* L. suspension cells. (B) *H. perforatum* L. suspension cells co-cultivation with *A. tumefaciens* in 12 h. (C-D) Growth of bacteria after co-cultivation with *H. perforatum* L. cells in 0 and 12 h, respectively. (E-F) Fluorescein diacetate (FDA) and propidium iodide (PI) double staining to check cell viability in 0 and 12 h, respectively. Adapted from Franklin *et al*. 2008.

1.3 *A. tumefaciens* defense genes *Phenolic oxidative coupling protein* (*Hyp-1*) and *Polygalacturonase inhibiting protein* (*PGIP*)

To understand the mechanism of *H. perforatum* L. defense against *A. tumefaciens*, the defense response genes from *H. perforatum* L. has been identified and characterized in this present study. The forward subtractive cDNA library was performed by employing suppressive subtractive hybridization (SSH). SHH is a highly sensitive PCR-based cDNA subtraction method, widely used in the study of differential gene expression to identify novel genes (Suzuki *et al.*, 2007), especially in species for which limited genomic information available (as in the case of *Hypericum* spp). It selectively amplifies differentially expressed cDNA fragments while suppressing non-target cDNA amplification so that genes of relatively low abundances could be identified. In this work, RNAs isolated from *H. perforatum* L. suspension culture challenged with *A. tumefaciens* as tester and RNAs from control cultures were served as driver to construct the forward subtracted cDNA library and two highly expressed genes *Phenolic oxidative coupling protein* (*Hyp-1*) and *Polygalacturonase inhibiting protein* (*PGIP*) were selected.

1.3.1 *A. tumefaciens* defense gene *Hyp-1*

The *Hyp-1* gene encodes the phenolic coupling protein was cloned and characterized for the first time from *H. perforatum* L. cell cultures by Bais and co-workers (2003). In their work, the *Hyp*-1 was identified by setting up a cDNA library and showed that the full-length cDNA sequence of *Hyp*-1 is 782 nucleotides with an open reading frame (ORF) which is 477 nucleotides that code a protein of 159 amino acids residues with a molecular weight of 17.8 kDa, share 45.1% homology to Bet.v.1 class allergens. Remarkably, their results demonstrated that Hyp-1 is the solely enzyme catalyze emodin to hypericin in *H. perforatum* L. *in vitro*. Unfortunately, the authors were not able to confirm the catalytic activity of this protein in other studies. On the contrary, Čellárová and co-workers (2007) detected expression levels of *Hyp-1* gene by qRT-PCR in different organs, including root, stem, shoot apex, intact leaf, leaf lamina free of leaf margins containing dark glands, in early stages of development of *H. perforatum* L. Surprisingly, the results showed the highest expression level of *Hyp-1* was found in roots where there were no dark glands. Moreover, no significant differences in *Hyp-1* expression were observed in roots and in the leaf containing dark glands, compromising the role of the *Hyp-1* gene in the biosynthesis of hypericin. Later on, the same team (2011) further demonstrated there was no clear correlation between the production of hypericin and *Hyp-1* expression since the *Hyp-1* gene is expressed in both "hypericin producing" (HYCIN+) species and "hypericin lacking" species (HYCIN–). On the other hand, almost at the same time, Jaskolski and the coworkers (2008; 2010) studied on crystal structure of Hyp-1 and their results demonstrated Hyp-1 structurally belongs to the family of plant pathogenesis-related class 10 (PR-10) proteins, since the well-defined PR-10 fold, which contains a hydrophobic cavity, was found in crystal structure of Hyp-1. Interestingly, the cavity of Hyp-1is compatible with binding of two emodin molecules or of one hypericin molecule, which suggested that Hyp-1 serves as a vehicle for hypericin storage or transport in stand of synthesis. Čellárová and co-workers (2013) provided the genetic evidences to confirm the classification of *Hyp-1* as a PR-10 family protein. In order to concern the *Hyp-1* reaction in plant defense which is reported the function of PR-10 proteins, in their work they localized the intron sequence in the coding region strictly conserved position of codon 62, which is a typical feature of the dicot PR-10 subfamily, and observed the response of the *Hyp-1* gene to abiotic and biotic stresses include, wounding, ABA and *A. tumefaciens*, as well as known that PR-10 proteins are induced when plant response to the factors described as above. In addition, together with the sequence homology (Bais *et al.*, 2003), the highest

expression in roots (Košuth *et al.*, 2007) which is typical for PR-10 proteins (Lebel *et al.*, 2010; Meyer *et al.*, 2012; Han *et al.*, 2015), Hyp-1 classified in the PR-10 protein family. Furthermore, in Hohtola and co-workers (2016) the first time they examined the expression of *Hyp-1* gene in a cellular level by *in situ* RNA localization and the results shown neither the location of the hyp-1 mRNA nor Hyp-1 protein in dark glands or accumulation of the protein via transportation to the dark glands. As reported in Chapter 3 of the present thesis, *Hyp-1* gene is highly expressed in the samples of *H. perforatum* L. cell suspension culture treated with *A. tumefaciens* for 12 hours (Hou *et al*., unpublished results).

1.3.2 *A. tumefaciens* defense gene *PGIP*

PGIP are a group of plant cell wall proteins, which are from the leucine-rich repeat (LRR) superfamily and defense against pathogens, and widely exist in the plant kingdom. Plant grown in natural environment is exposed to risk multiple pathogens, the cell wall functions as the first barrier that plant utilize to defend themselves against pathogenic microorganisms. It has been reported that fungi such as, *Botrytis cinerea* (Sicilia, 2005), *Bipolaris sorokiniana* (Janni *et al.*, 2008), *Sclerotinia sclerotiorum* (Bashi *et al.*, 2013), *Verticillium dahliae* and *Fusarium oxysporum* f. sp. *vasinfectum* (Liu *et al.*, 2017), and bacteria such as *A. tumefaciens* (Rodriguez-Palenzuela *et al.*, 1991) and *Pectobacterium carotovorum* subsp. *carotovorum* (Hwang *et al.*, 2010) could secret polygalacturonase (PG) the first cell wall degrading enzyme, while PGIP produced by plant could specially recognize and inhibit those PGs. The PG-PGIP interaction limits the destructive potential of PGs, which could release the elicitors of immunity identified as oligogalacturonides (OGs) and lead to the accumulation of OGs during microbial infections. OGs activate a wide range of defense responses, including the accumulation of phytoalexins and lignin, the expression of defense-related genes, and the production of ROS (Srivastava, 2013). Recently, the importance of PGIP in plant defense has been studied from molecular biological level. For instance, overexpression of a bean *PGIP* gene *PvPGIP2* in wheat, the resistance to fungi *B. sorokiniana* was enhanced in transgenic plant (Janni *et al.*, 2008). Overexpression of a Chinese cabbage *PGIP* gene *BrPGIP2* in tobacco and Chinese cabbage, the transgenic plants confer the increased resistance to bacterial soft rot caused by pathogen *P. carotovorum ssp. carotovorum* (Hwang *et al.*, 2010). Overexpression of pepper *PGIP* gene *CaPGIP1* in tobacco increased resistance to fungi *Alternaria alternate* and *Colletotrichum*

nicotianae (Wang *et al.*, 2013). Moreover, the expression of *NtPGIP* was up-regulated under the biotic and abiotic stresses including *Phytophthora nicotianae* incubation and salicylic acid (SA), abscisicacid (ABA), salt, and cold treatments. The recombinant NtPGIP could successfully inhibit the PG activity of *Phytophthora capsici* (Zhang *et al.*, 2016). Furthermore, the similar pattern has been reported in cotton, that the purified GhPGIP1 inhibits *V. dahliae* and *F. oxysporum* f. sp. *vasinfectum*, which cause cotton wilt. The transcript level of *GhPGIP1* was up regulated to response the abiotic and biotic stresses including methyl jasmonate (MeJA), SA, H_2O_2, wounding, and inoculation with *V. dahliae* and *F. oxysporum* f. sp. *vasinfectum*. *GhPGIP1* overexpressed transgenic *Arabidopsis* conferred the defense by accumulation of the expression of *PRs*, *Isochorismate synthase 1* (*ICS1*), *Enhanced disease susceptibility 1* (*EDS1*), and *Phytoalexindeficient 4* (*PAD4*) genes. And *GhPGIP1* knock out cotton was highly susceptible to the pathogens infection (Liu *et al.*, 2017). As shown in Chapter 4 of the present thesis, the transcript level of *HpPGIP* is highly induced in *H. perforatum* L. suspension culture challenged with *A. tumefaciens* therefore to be selected as *A. tumefaciens* defense gene (Hou *et al*., unpublished results).

1.4 Virus-induced gene silencing

Virus-induced gene silencing (VIGS) has been developed as a well-known technique to knock down the expression of endogenous genes by utilizing recombinant viruses (viral vectors) based on post-transcriptional gene silencing (PTGS). In this technique, the plant natural defense mechanism against viral attack though especially degrading the viral genome-derived RNAs is used as the principle. The viral vector carries host-derived homologous sequence or heterologous sequence of endogenous genes to silence the corresponding genes in infected plants by a homology-dependent RNA degradation mechanism (Gedling *et al.*, 2018). VIGS serves as a powerful and efficient approach for functional genomic studies and has been wildly applied due to the obvious advantages compared with others, including simple, fast, cost less, no need of stable transgenic transformation, only partial sequences are available for vector construction and serves as both forward and reverse genetics approaches (Ramegowda *et al.*, 2014).

Tobacco rattle virus (TRV) derived VIGS as one of the successfully developed VIGS vectors has been wildly used for gene suppression in plants (Liu *et al.*, 2002; Ramegowda *et al.*, 2014). TRV is a bipartite positive sense RNA virus, the features of vigorous spread in all plant organs,

weak infection symptoms and a numerous range of host species make the TRV derived VIGS assays rapidly become an efficient tool for gene silencing in a diverse array of plant species. TRV-VIGS is employed to knocked out the two *Agrobacterium* defense genes *Hyp-1* and *HpPGIP* to characterize the gene functions in this PhD project.

1.5 Objectives of study

Within this scientific framework it was our goal, the identification and characterization of the *H. perforatum* L. genes involved in resistance against *A. tumefaciens* to develop crown gall disease prevention strategies for economically important crops in order to contribute to the European bio-economy. In addition, being an important medicinal plant, *H. perforatum* L. with many pharmaceutically important compounds such as hypericin, hyperforin, xanthones, flavonoids, understanding their biosynthetic pathways is mandatory to broaden the availability of industrially exploitable bioactive compounds, which is one of the societal challenges of Horizon2020 by European Commission (2014-2020). However, functional genomic studies of *H. perforatum* L. secondary metabolic pathways are hindered due to the absence of transgene expression tools, the understanding thoroughly the pathogens defense mechanisms of *H. perforatum* L. could be benefit for investigation of *H. perforatum* L. transgenic expression.

To understand the mechanism of *H. perforatum* L. defense against *A. tumefaciens*, in this PhD project, identification of the *H. perforatum* L. genes involved in resistance against *A. tumefaciens* has been carried out by construction of a forward subtractive cDNA library from *A. tumefaciens*-treated *H. perforatum* L. suspension cells and two highly significant expression genes *Hyp-1* and *HpPGIP* have been selected. Therefore, three major objectives were outlined in the present thesis, namely:

1. Elucidation of the functional relevance of *A. tumefaciens* defense gene *Hyp-1*;
2. Elucidation of the functional relevance of *A. tumefaciens* defense gene *HpPGIP*;
3. Unravelling the mechanisms of *H. perforatum* L. resistance to *A. tumefaciens*.

Regarding the first goal, the biological function of *Hyp-1* in defense against *A. tumefaciens* was analyzed in transgenic *N. tabacum* and *L. sativa* plants overexpressing *Hyp-1*, and in *C. roseus* silenced for the *Hyp-1* homologous gene. The expression of core genes regulating several defense pathways was analyzed in *Hyp-1* overexpressing lines. And Hyp-1 was detected in the nucleus, plasma membrane and cytoplasm of epidermal cells by confocal microscopy. All

findings suggest that *Hyp-1* from *H. perforatum* L. modulates tolerance to *A. tumefaciens* as part of defense mechanisms against pathogen infection. This work is reported in chapter 3 of the present thesis.

Regarding goal 2, the functional characterization of *HpPGIP* in *A. tumefaciens* defense was assessed in transgenic *N. tabacum* plants overexpressing *HpPGIP* and in *N. benthamiana* plants silenced for the *HpPGIP* homologous gene. The expression of core genes regulating several defense pathways was analyzed in *HpPGIP* overexpressing lines. Additionally, HpPGIP was detected in the nucleus, plasma membrane and cytoplasm of epidermal cells by confocal microscopy. Results indicated that *HpPGIP* from *H. perforatum* L. modulates tolerance to *A. tumefaciens* as part of defense mechanisms against pathogenic infection. This work is reported in chapter 4 of the present thesis.

In addition, to further contribute to understand the mechanisms of *H. perforatum* L. defense against *A. tumefaciens* (goal 3), the transcripts of the core genes encoding enzymes involved in the plant defense pathways were analyzed by quantitative real-time PCR in *H. perforatum* L. cell suspensions challenged with *A. tumefaciens* and in dark glands obtained from *H. perforatum* L. seedlings. This work is reported in chapter 5 of the present thesis.

Overall, the present study provided a solid functional characterization of *Hyp-1* and *HpPGIP* genes from *H. perforatum* L., and contributed towards understanding the molecular mechanisms underlying *H. perforatum* L.-*A. tumefaciens* interaction.

1.6 References

Bais, H.P., Vepachedu, R., Lawrence, C.B., Stermitz, F.R. and Vivanco, J.M. (2003) Molecular and biochemical characterization of an enzyme responsible for the formation of hypericin in St. John's wort (Hypericum perforatum L.). *J. Biol. Chem.* **278**, 32413–32422.

Bashi, Z.D., Rimmer, S.R., Khachatourians, G.G. and Hegedus, D.D. (2013) Brassica napus polygalacturonase inhibitor proteins inhibit Sclerotinia sclerotiorum polygalacturonase enzymatic and necrotizing activities and delay symptoms in transgenic plants. *Can. J. Microbiol.* **59**, 79–86.

Bruni, R. and Sacchetti, G. (2009) Factors affecting polyphenol biosynthesis in wild and field grown St. John's Wort (Hypericum perforatum L. Hypericaceae/Guttiferae). *Molecules* **14**,

682–725.

Butterweck, V., Christoffel, V., Nahrstedt, A., Petereit, F., Spengler, B. and Winterhoff, H. (2003) Step by step removal of hyperforin and hypericin: Activity profile of different Hypericum preparations in behavioral models. *Life Sci.* **73**, 627–639.

Cirak, C., Aksoy, H.M., Ayan, A.K., Saglam, B. and Kevseroglu, K. (2005) Enhanced hypericin production in Hypericum perforatum and Hypericum pruinatum in response to inoculation with two fungal pathogens. *Plant Prot. Sci.* **41**, 109–114.

Conceição, L.F.R., Ferreres, F., Tavares, R.M. and Dias, A.C.P. (2006) Induction of phenolic compounds in Hypericum perforatum L. cells by Colletotrichum gloeosporioides elicitation. *Phytochemistry* **67**, 149–155.

Fernandes, H., Konieczna, M., Kolodziejczyk, R., Bujacz, G., Sikorski, M. and Jaskolski, M. (2008) Crystallization and preliminary crystallographic studies of Hyp-1, a St John's wort protein implicated in the biosynthesis of hypericin. *Acta Crystallogr. Sect. F Struct. Biol. Cryst. Commun.* **64**, 405–408.

Franklin, G., Conceição, L.F.R., Kombrink, E. and Dias, A.C.P. (2008) Hypericum perforatum plant cells reduce Agrobacterium viability during co-cultivation. *Planta* **227**, 1401–1408.

Franklin, G., Conceição, L.F.R., Kombrink, E. and Dias, A.C.P. (2009) Xanthone biosynthesis in Hypericum perforatum cells provides antioxidant and antimicrobial protection upon biotic stress. *Phytochemistry* **70**, 60–68.

Gedling, C.R., Ali, E.M., Gunadi, A., Finer, J.J., Xie, K., Liu, Y., Yoshikawa, N., Qu, F. and Dorrance, A.E. (2018) Improved apple latent spherical virus-induced gene silencing in multiple soybean genotypes through direct inoculation of agro-infiltrated Nicotiana benthamiana extract. *Plant Methods* **14**, 1–10.

Gelvin, S.B. (2005) Agricultural biotechnology: Gene exchange by design. *Nature* **433**, 583–584.

Gelvin, S.B. (2010) Plant Proteins Involved in *Agrobacterium*-Mediated Genetic Transformation. *Annu. Rev. Phytopathol.* **48**, 45–68.

Han, J.H., Lee, J.H. and Lee, O.R. (2015) Leaf-specific pathogenesis-related 10 homolog,

PgPR-10.3, shows in silico binding affinity with several biologically important molecules. *J. Ginseng Res.* **39**, 406–413.

Hwang, B.H., Bae, H., Lim, H.S., Kim, K.B., Kim, S.J., Im, M.H., Park, B.S., Kim, D.S. and Kim, J. (2010) Overexpression of polygalacturonase-inhibiting protein 2 (PGIP2) of Chinese cabbage (Brassica rapa ssp. pekinensis) increased resistance to the bacterial pathogen Pectobacterium carotovorum ssp. carotovorum. *Plant Cell. Tissue Organ Cult.* **103**, 293–305.

Janni, M., Sella, L., Favaron, F., Blechl, A.E., Lorenzo, G. De and D'Ovidio, R. (2008) The expression of a bean PGIP in transgenic wheat confers increased resistance to the fungal pathogen *Bipolaris sorokiniana*. *Mol. Plant-Microbe Interact.* **21**, 171–177.

Karppinen, K. (2010) Biosynthesis of hypericins and hyperforins in Hypericum perforatum L.(St. John's wort)—precursors and genes involved.

Karppinen, K., Derzsó, E., Jaakola, L. and Hohtola, A. (2016) Molecular cloning and expression analysis of hyp-1 type PR-10 family genes in Hypericum perforatum. *Front. Plant Sci.* **7**, 526.

Košuth, J., Hrehorová, D., Jaskolski, M. and Čellárová, E. (2013) Stress-induced expression and structure of the putative gene hyp-1 for hypericin biosynthesis. *Plant Cell. Tissue Organ Cult.* **114**, 207–216.

Košuth, J., Katkovčinová, Z., Olexová, P. and Čellárová, E. (2007) Expression of the hyp-1 gene in early stages of development of Hypericum perforatum L. *Plant Cell Rep.* **26**, 211–217.

Košuth, J., Smelcerovic, A., Borsch, T., Zuehlke, S., Karppinen, K., Spiteller, M., Hohtola, A. and Čellárová, E. (2011) The hyp-1 gene is not a limiting factor for hypericin biosynthesis in the genus Hypericum. *Funct. Plant Biol.* **38**, 35–43.

Kumar, N., Gulati, A. and Bhattacharya, A. (2013) L-glutamine and l-glutamic acid facilitate successful agrobacterium infection of recalcitrant tea cultivars. *Appl. Biochem. Biotechnol.* **170**, 1649–1664.

Lebel, S., Schellenbaum, P., Walter, B. and Maillot, P. (2010) Characterisation of the Vitis vinifera PR10 multigene family. *BMC Plant Biol.* **10**, 184.

Liu, N., Zhang, X., Sun, Y., Wang, P., Li, X., Pei, Y., Li, F. and Hou, Y. (2017) Molecular evidence for the involvement of a polygalacturonase-inhibiting protein, GhPGIP1, in enhanced resistance to Verticillium and Fusarium wilts in cotton. *Sci. Rep.* **7**, 1–18.

Liu, Y., Schiff, M., Marathe, R. and Dinesh-Kumar, S.P. (2002) Tobacco Rar1, EDS1 and NPR1/NIM1 like genes are required for N-mediated resistance to tobacco mosaic virus. *Plant J.* **30**, 415–429.

Meyer, C.A., Lee, O.R., Pulla, R.K., Kim, Y.J., Devi Balusamy, S.R. and Yang, D.C. (2012) Expression and stress tolerance of PR10 genes from Panax ginseng. *Mol. Biol. Rep.* **39**, 2365–2374.

Michalska, K., Fernandes, H., Sikorski, M. and Jaskolski, M. (2010) Crystal structure of Hyp-1, a St. John's wort protein implicated in the biosynthesis of hypericin. *J. Struct. Biol.* **169**, 161–171.

Patočka, J. (2003) The chemistry, pharmacology, and toxicology of the biologically active constituents of the herb Hypericum perforatum L. *J. Appl. Biomed.* **1**, 61–70.

Pitzschke, A. (2013) Agrobacterium infection and plant defense—transformation success hangs by a thread. *Front. Plant Sci.* **4**, 1–12.

Raak, C., Büssing, A., Gassmann, G., Boehm, K. and Ostermann, T. (2012) A systematic review and meta-analysis on the use of Hypericum perforatum (St. John's Wort) for pain conditions in dental practice. *Homeopathy* **101**, 204–210.

Ramegowda, V., Mysore, K.S. and Senthil-Kumar, M. (2014) Virus-induced gene silencing is a versatile tool for unraveling the functional relevance of multiple abiotic-stress-responsive genes in crop plants. *Front. Plant Sci.* **5**.

Rodriguez-Palenzuela P, Burr TJ, Collmer A. (1991) Polygalacturonase is a virulence factor in Agrobacterium-tumefaciens biovar 3. *J. Bacteriol.* **173 (20)**, 6547–6552

Saddiqe, Z., Naeem, I. and Maimoona, A. (2010) A review of the antibacterial activity of Hypericum perforatum L. *J. Ethnopharmacol.* **131**, 511–521.

Sandra Postel, B.K. (2009) Management and control of shipping around Shetland. *Mar. Policy* **17**, 371–379.

Senthil-Kumar M, Hema R, Anand A, Kang L, Udayakumar M, Kirankumar S. Mysore.

(2007) A systematic study to determine the extent of gene silencing in Nicotiana benthamiana and other Solanaceae species when heterologous gene sequences are used for virus-induced gene silencing. New Phytol 176: 782–791.

Sicilia, F. (2005) The Polygalacturonase-inhibiting protein PGIP2 of phaseolus vulgaris has evolved a mixed mode of inhibition of endopolygalacturonase PG1 of botrytis cinerea. *Plant Physiol.* **139**, 1380–1388.

Srivastava, N. and Meshram, A. (2013) An insight into the molecular structure and function of Polygalacturonase inhibiting protein (PGIP). *Journal of Proteins and Proteomics*. **4**, 175–181.

Suzuki, K., Yano, A., Nishiuchi, T., Nakano, T., Kodama, H., Yamaguchi, K. and Shinshi, H. (2007) Comprehensive analysis of early response genes to two different microbial elicitors in tobacco cells. *Plant Sci.* **173**, 291–301.

Tatsis, E.C., Boeren, S., Exarchou, V., Troganis, A.N., Vervoort, J. and Gerothanassis, I.P. (2007) Identification of the major constituents of Hypericum perforatum by LC/SPE/NMR and/or LC/MS. *Phytochemistry* **68**, 383–393.

Wang, X., Zhu, X., Tooley, P. and Zhang, X. (2013) Cloning and functional analysis of three genes encoding polygalacturonase-inhibiting proteins from Capsicum annuum and transgenic CaPGIP1 in tobacco in relation to increased resistance to two fungal pathogens. *Plant Mol. Biol.* **81**, 379–400.

Zhang, C., Feng, C., Wang, J., Kong, F. and Sun, W. (2016) Cloning , expression analysis and recombinant expression of a gene encoding a polygalac- turonase-inhibiting protein from tobacco , Nicotiana tabacum. *Hly*.

Zobayed, S.M.A., Afreen, F., Goto, E. and Kozai, T. (2006) Plant-environment interactions: Accumulation of hypericin in dark glands of Hypericum perforatum. *Ann. Bot.* **98**, 793–804.

Chapter 2

Materials and Methods

Chapter 2 Materials and methods

2.1 Plant material and plant growth conditions

2.1.1 Seeds sterilization and germination

Seeds of *N. tabacum* were surface sterilized by immersion in 1.5% (v/v) bleach for 7 min, washed four times with sterile distilled water and sown onto 1% agar containing 1/2 Murashige and Skoog (MS) medium. Seeds of *L. sativa*, varieties Batavia Laura (BL) and Salad bowl rossa (SBR) of were surface sterilized by immersion in 6% (v/v) NaClO for 15 and 10 min, respectively. Then washed four times with sterile distil water and sown onto 1% agar containing 1/2 MS medium. Seeds of *H. perforatum* L. variety "Helos" (Richters seeds, ON, Canada) were placed in 2.0 ml Eppendorf tubes containing 1.0 ml sterile water with 10 µl of Tween® 20 (Sigma-Aldrich, USA) and kept in the dark at 4 °C. After 4 h, the solution was removed and the seeds were washed four times with sterilized distilled water followed by 6% active chlorine for 3 min followed by washing in sterilized distilled water. Seeds were germinated on 1/2 MS medium containing 1% agar.

All steps were done in sterile flow chamber and seeds were grown in the tissue culture room at 25 °C with a 16-h light/8-h dark photoperiod.

2.1.2 Plant growth condition

Control and transgenic plants of *N. tabacum* and *L. sativa* and five-weeks old *N. tabacum* plants used for infiltration were grown in the growth chamber at 25 °C with a 16-h light/8-h dark photoperiod.

Wild type *C. roseus* seeds for VIGS were germinated and grown in the plant growth chamber at 25 °C with a 16-h light/8-h dark photoperiod. *C. roseus* plants having two pairs of fully developed leaves (3-6 weeks old) with a stem sturdy enough to be able to sustain infection, were used for agroinfiltration.

Brassica oleracea var. *oleracea* seeds were germinated and grown in the plant growth chamber

at 18 °C with a 16-h light/8-h dark photoperiod. Five-week-old *N. benthamiana* plants were grown in a grow chamber at 25 °C with a 16-h light/8-h dark photoperiod.

Seedlings of *H. perforatum* L. were grown in a tissue culture room at 25 °C with a 16-h light/8-h dark photoperiod for 2 weeks. Samples of leaf margins were collected and denoted as with glands (HpWith Glands) while middle part of leaf served as without glands (HpWithout Glands).

2.2 Elicitation of *H. perforatum* L. cells with *A. tumefaciens*

H. perforatum L. cell suspensions were elicited with *A. tumefaciens* and the details of the experimental procedure were described previously (Franklin *et al.*, 2008). Briefly, *H. perforatum* L. cell suspension cultures were established by using the variety "Helos" (Richters seeds, ON, Canada) as described by Dias *et al*. (2001). Suspended *H. perforatum* L. cell suspensions were collected in a sterile beaker with the final concentration about 5,000 cells ml^{-1} in 80 ml MS medium with 100 µM acetosyringone (AS), after 5 days of subculture. Then the flakes of *H. perforatum* L. cell suspensions were inoculated with the *A. tumefaciens* stock with optical density at 600 nm (OD_{600}) around 1.0. Cell samples were collected after co-cultivation periods of 12 h (Hp-AT 12 h) and 24 h (Hp-AT 24 h). A control condition corresponding to *H. perforatum* L. suspensions only: 0h (Hp-AT 0 h) was included. All the treatment and control cultures were incubated under 16-h light/8-h dark photoperiod at 25 °C in a growth chamber during co-cultivation.

2.3 Suppression subtraction hybridization (SSH) and cDNA library construction

Suspension cells of *H. perforatum* L. were treated with *A. tumefaciens* as described previously, and forward subtractive cDNA library was performed by using the PCR-Select cDNA Subtraction kit (Clontech, USA) according to the manufacturer's instructions. RNAs isolated from *Hypericum* suspension culture challenged with *A. tumefaciens* was served as tester, and RNAs derived from control cultures as driver. The details of the experimental procedure have been described previously (Singh *et al.*, 2016). Briefly, 2 µg Poly A+ RNA from tester and driver was used to prepare cDNA pools. Both cDNA was digested with Rsa I to obtain shorter, blunt ended molecules, followed by phenol/chloroform extraction, ethanol precipitation and

finally resuspended in RNase free water. Tester cDNAs were split into two pools equally, each of which was suitable for ligation with a different adapter supplied in the kit. After first and second hybridizations, the purified subtracted cDNAs were cloned in to pGEM-T easy cloning vector (Promega, Madison, WI, USA) for transformation into DH5α competent *Escherichia coli* cells and selected with suitable antibiotics. Individual colonies were screened by PCR for size of inserts and fragments above 150 bp were subjected to single-pass sequencing. Vector contamination was removed using the Vecscreen bioinformatics tool (http://www.ncbi.nlm.nih.gov/tools/vecscreen). The sequence similarity of obtained ESTs was analyzed by BLASTN and BLASTX and compared in different databases.

2.4 Plasmid construction and site-directed mutagenesis

2.4.1 Constructions of *Hyp-1* related plasmids

For gene overexpression, pBI121-GFP-Hyp-1 and pBI121-Hyp-1 were constructed. Full-length cDNA of Green fluorescence protein (GFP) was amplified from pGE vector (Received from Prof. Jim E. Brandle, Canada) (Conley *et al.*, 2009) by Platinum Taq DNA Polymerase High Fidelity (Invitrogen, USA) with the following forward and reverse primers: BamH I-GFP-F and GFP-Spe I-Sac I-R. After sequencing, the *GFP* cDNA was digested with BamH I/Sac I and inserted downstream of the *Cauliflower mosaic virus* (CaMV) 35S promoter in the binary vector pBI121 (GenBank Accession No. AF485783) to generate pBI121-GFP. To produce *Hyp-1* cDNA, a 480-nucleotide fragment (GenBank Accession No. GU324243.1) was RT-PCR-amplified from the total RNAs of *H. perforatum* L. suspension culture elicited with *A. tumefaciens* by Maxima First Strand cDNA Synthesis Kit (Thermo Scientific, USA) using Platinum Taq DNA Polymerase High Fidelity. The primers used were as follow: SpeI-Hyp-1-F and Hyp-1-SacI-R. The sequenced *Hyp-1* cDNA was finally cloned into the plasmid pBI121-GFP described above by digestion with Spe I/Sac I to achieve pBI121-GFP-Hyp-1.

For the construction of pBI121-Hyp-1, the *GFP* gene was removed from pBI121-GFP-Hyp-1 by digestion with BamH I/Spe I. The Klenow Fragment of DNA Polymerase I (Invitrogen, USA) was used for producing blunt ends, and then the termini were ligated by T4 DNA Ligase (Thermo Scientific, USA).

To construct pBI121-GFP-Hyp-1-N, three stop codons (TAG TAA TGA) were added at 240 bp after the second ATG (nt 203) in Hyp-1 sequence. To prepare the template pT-Spe I-Hyp-1-Sac I, the plasmid pBI121-GFP-Hyp-1 and self- ligated pT easy vector were digested by Spe I/Sac I respectively and then ligated by T4 ligase. To achieve pBI121-GFP-Hyp-1-N, the circled, sequenced plasmid pT-Spe I-Hyp-1-Sac I and the site-directed mutagenesis primers: STOP-Hyp-F and STOP-Hyp-R were used to amplify pT-Stop codon-Hyp-1-N by Platinum Taq DNA Polymerase High Fidelity. After the self-ligation, the plasmid pT-Stop codon-Hyp-1-N was double digested with Spe I/Sac I and inserted into pBII121-GFP digested with the same restriction enzymes downstream of GFP sequence.

2.4.2 Constructions of *HpPGIP* related plasmids

For gene overexpression studies, a 945-nucleotide fragment of *PGIP* (GenBank Accession No. MK290240) was amplified by reverse transcriptase-PCR from the total RNAs of *H. perforatum* L. suspension culture elicited with *A. tumefaciens*. The sequenced PGIP cDNA was finally cloned downstream of the 35S promoter in the plasmid pBI121 by digestion with Sma I/Sac I to provide pBI121-PGIP. The primers were: Sma I-PGIP-F and PGIP-Sac I-R. For constructing pBI121-GFP-PGIP, the PGIP fragment was amplified by RT-PCR from total RNA of *A. tumefaciens* treated *H. perforatum* L. suspension culture cells using the primers Spe I-PGIP-F and PGIP-Sac I-R. After digestion by Spe I/Sac I, the sequenced PGIP fragment was inserted into pBI121-GFP which was digested by the same pair of the restriction enzymes. To construct pBI121-Hyp-1-PGIP, the forward primer Sac I-PGIP-F together with PGIP-Sac I-R described above were used to amplify Sac I-PGIP-Sac I by RT-PCR from total RNA of *A. tumefaciens* treated *H. perforatum* L. suspension culture cells. Then, pBI121-Hyp-1 was employed as the destination vector to insert the Sac I digested PGIP fragment just behind Hyp-1 to achieve pBI121-Hyp-1-PGIP.

All the primers were given in Table 1. All the purified recombinant plasmids were transformed into *A. tumefaciens* strain EHA105 by chemical transformation.

2.4.3 Construction of plasmids for VIGS

The homologous *Hyp-1* gene from *C. roseus Intracellular pathogenesis related protein* (*CrIPR*) (GenBank Accession No. Y10612.1) was selected to construct pTRV2: CrIPR. A 318-bp fragment from the 3´ terminus of CrIPR was used to synthesize cDNA by Superscript II reverse transcriptase (200 units) (Invitrogen, USA). The cDNA was amplified with primers Cr-IPR-F/R by High-fidelity Taq DNA Polymerase (Roche, Germany). The PCR product was first cloned in pGEM-T easy vector. After DNA sequencing, the EcoR I-digested CrIPR fragment was inserted into pTRV2:00 which was previously digested with EcoR I followed by dephosphorization with alkaline phosphatase (Roche, Germany) according to the manufacturer's instructions.

The homologous gene of *PGIP* from *B. oleracea* var. *oleracea* (*Polygalacturonase inhibitor 1-like (PGIP)*, GenBank Accession No. XM 013751645.1) was selected to construct pTRV2: BoPGIP. A 507 bp fragment from the 3´ terminus of BoPGIP was reverse transcribed by Superscript II reverse transcriptase (200 units) (Invitrogen, USA) and amplified by High-fidelity Taq DNA Polymerase (Rocha, Germany) with primers Bo-PGIP-1-F/R. The PCR products were first cloned in pGEM-T easy vector (Promega, Madison,WI, USA) for sequencing. The correct clone was digested by EcoR I and inserted into pTRV2-MCS, which was digested by the same restriction enzyme and followed by dephosphorization with alkaline phosphatase (Rocha, Germany) according to the manufacturer's instructions.

All primers were given in Table 1. All the recombinant plasmids for VIGS assays were transformed into *A. tumefaciens* strain GV3101 by electroporation.

Table 1 Gene-specific primers used for plasmid constructions

Gene	Primers **(5'-3')**
BamH I-GFP-F	Forward: GTGCA***CGGATCC***ATGGTGAGCAAGGGCGAG [a]
GFP-Spe I-SacI-R	Reverse: CT***GAGCTCACTAGT***CTTGTACAGCTCGTCC [b]
Spe I-Hyp-1-F	Forward: GTGCAC***ACTAGT***ATGGCGGCGTACACTATT [c]
Hyp-1-Sac I-R	Reverse: GTGCAC***GAGCTC***TTAAGCGAAAACTTCAGG [d]
STOP-Hyp-F	Forward: TAGTAATGATATTGCAAGTACAC
STOP-Hyp-R	Reverse: GAAATTTGCGGCATCAAT TTCAT

Gene	Primers **(5'-3')**
Sma I-PGIP-F	Forward: ACTGAC***CCCGGG***ATGAGAGCCCATTTCCTC [e]
PGIP-Sac I-R	Reverse: ACTCAC***GAGCTC***TTACTTGCAAGCTGGAAG [d]
Spe I-PGIP-F	Forward: GTGCAC***ACTAGT***ATGAGAGCCCATTTCCTC [c]
PGIP-Sac I-R	Reverse: ACTCAC***GAGCTC***TTACTTGCAAGCTGGAAG [d]
Sac I-PGIP-F	Forward: GTGCAC***GAGCTC***ATGAGAGCCCATTTCCTC [d]
Cr-IPR	Forward: CGGGATTCTCCAAGGAGATGGAGGTG
	Reverse: CGGTCTAGAATAATCTGGATTGGCTTGAA
Bo-PGIP-1	Forward: CGGGAATTCAGCTCTCTCGCTTTGTTACC
	Reverse: CGGTCTAGAAAGAATCAAATCTCTGAAG

[a]: The nucleotides in italic and bold indicate the introduced restrictive cleavage site BamH I

[b]: The nucleotides in italic and bold indicate the introduced restrictive cleavage sites Spe I-Sac I

[c]: The nucleotides in italic and bold indicated the introduced restrictive cleavage site Spe I

[d]: The nucleotides in italic and bold indicated the introduced restrictive cleavage sites Sac I

[e]: The nucleotides in italic and bold indicate the introduced restrictive cleavage site Sma I

2.5 *Agrobacterium*-mediated genetic transformation

Transgenic *N. tabacum* plants were generated by the leaf disc transformation method as described by Horsch *et al*. (1985). Briefly, *in vitro* grown *N. tabacum* leaves were cut into 4-6 pieces and laid on the MSIB medium (MS medium containing IAA 0.5 mg/L; BA 2.5 mg/L) for 2 days under the dark in the tissue culture room conditions described above. The explants were co-incubation with *A. tumefaciens* with OD_{600} of 0.5-0.8 for 8 min with vacuum. Explants were kept to the same medium in the dark for another two days. Then explants were transferred into shooting medium (MSIB medium containing 50 mg/L Kanamycin and 500 mg/L ticarcillin), re-cultured after each two-weeks. Shoots (3-4 cm) were transferred into tubes with

MS medium containing 0.5 mg/L IBA for root development.

For *L. sativa* transformation, two varieties Batavia Laura (BL) and Salad bowl rossa (SBR) were used in this study. Seedlings (4-6 days old) of *L. sativa* were punctured gently on the leaf surface near the petiolar region by scalpel blade, transferred to MS0.1BN (MS medium with 0.1 mg/L BA and 0.1 mg/L NAA) and incubated in 16-h light/8-h dark condition at 25 °C for 1 day. Explants were co-cultivated with *A. tumefaciens* suspension at OD_{600} around 0.5 kept vacuuming for 10 min. Explants were transferred to MS0.1BN plates under light for 5-7 days. Then explants were transferred to MS0.1BN medium with 50 mg/L Kanamycin + 500 mg/L ticarcillin), re-cultured in each two-weeks until initiation of shooting. Finally, explants were transferred to MS medium with 50 mg/L Kanamycin + 500 mg/L ticarcillin for rooting and waiting for harvesting the whole transgenic plants.

All the transgenic T1 plants were confirmed by PCR amplification of target genes and *NPTII* genes and expression of GFP fluorescence detected by microscopy (Leica-DM5000B + CTR5000 + ebq100, Germany). Progenies derived from self-fertilized T1 plants were germinated in MS medium containing 50 mg/L Kanamycin.

2.6 *Agrobacterium*-mediated transient expression

A. tumefaciens containing recombinant plasmids were grown overnight in Luria-Bertani (LB) medium containing antibiotic at 28 °C and resuspended in buffer containing10 mM $MgCl_2$, 10 mM MES (2-(N-morpholino) ethanesulfonic acid) and 0.15 mM AS, and adjusted the OD_{600} to 0.2-2 (based on different plant materials and experimental purposes). The prepared *Agrobacterium* strains were mixed equally and left at room temperature for 3-4 hours before inoculation, then injected into the plant leaves with a 1-ml syringe (Hou *et al.*, 2011).

2.7 Plant total RNA isolation and quantitative real-time RT-PCR

2.7.1 Plant total RNA isolation

Total RNAs of *N. tabacum*, *L. sativa* and *H. perforatum* L. were isolated by the CTAB method

as described (Gasic *et al.*, 2004). Briefly, samples (0.12-0.15g) were grounded in liquid nitrogen and mixed with 0.9 ml 65 °C extraction buffer containing 2% CTAB (w/v), 2% polyvinylpyrrolidone (PVP) K-30 (w/v), 100 mM Tris HCl (pH 8.0), 25 mM EDTA, 2.0 M NaCl and 2% β-mercaptoethanol (v/v). The homogenate was incubated at 65 °C for 10 min and 0.9 ml of chloroform/isoamyl alcohol (24:1, v/v) was added into the mixture, vortexed, centrifuged at 12,000 x *g* for 15 min at 4 °C. The resulting upper aqueous phase was transferred into another tube containing 100 µl 3 M sodium acetate (pH 5.5) and 600 µl isopropanol. The mixture was incubated at -80 °C for 30 min, followed by centrifugation at 12,000 x *g* for 30 min at 4 °C. The supernatant was decanted and the pellet was dried and dissolved in 250-375 µL RNase free TE (pH 8.0). Equal volume of 8 M LiCl was added, mixed well and incubated at -80 °C for 4-5 hours, followed by centrifugation at 13,000 rpm for 30 min at 4 °C. The supernatant was decanted and the pellet was rinsed with 75% ethanol and collected by centrifugation at 12,000 x *g* for 5 min at 4 °C. The dried pellet was finally dissolved in 45 µl of RNase-free water and stored at -80 °C. The RNeasy Mini Kit (Qiagen, Germany) was used to clean up RNA including the DNase treatment according to the manufacturer's instructions.

Total RNAs for microRNA detection were isolated with Trizol reagent (Invitrogen, USA) according to the instruction manual.

Total RNA from young leaves of *C. roseus* and *B. oleracea* were isolated using the NucleoSpin RNA Plant kit (Macherey-Nagel, Germany), and followed by DNase treatment with TURBO DNA-free kit (Ambion, USA).

The total RNAs were quantified by NanoDrop 1000 Spectrophotometer (NanoDrop Technologies, Inc., USA) at A260/A280 and structural integrities were checked by 1.0% agarose-gel electrophoresis.

2.7.2 Quantitative real-time RT-PCR

2.7.2.1 qRT-PCR to detect defense pathways gene expression

Gene expression was monitored by qRT-PCR in 96-well plates with 5x HOT FIREPol® EvaGreen® qPCR Mix Plus (ROX) (Solis Biodyne, Estonia). For each biological replicate, qRT-PCR reactions were performed in triplicates using 3 µl 5x EvaGreen® qPCR master mix,

200 nM of each primer, 1 µl 10x diluted cDNA template and nuclease-free water to a final volume of 15 µl. Amplification was performed on CFX96 Real-Time System C1000 Thermal Cycler (Bio-Rad Laboratories, Inc., USA) following the conditions: 95 °C for 15 min, 45 cycles of 95 °C for 15 s, 60 °C for 20 s and 72 °C for 20 s. Primers were designed to specifically anneal with each of the *N. tabacum* genes by using the online quantitative PCR primers design software QuantPrime (Arvidsson *et al.*, 2008). Gene expression in *N. tabacum* was normalized with internal control *Elongation factor 1α* (EF-1α) and *L25 ribosomal protein* (*L25*)gene primers (Schmidt and Delaney, 2010). Gene expression in *H. perforatum* L. was normalized with internal control *Glyceraldehyde-3-phosphate dehydrogenase A* subunit (*GAPDH*) and *18S ribosomal RNA* (*18SrRNA*) (Jepson *et al.*, 2014). The efficiency of primers was determined by using a 4-fold serial dilution of 1 µl 10x diluted cDNA template with 3 dilution points. The CFX Manager Software (Bio-Rad Laboratories, Inc., USA) was used to analyze the data. The relative quantification of PCR products was calculated by the $2^{-\Delta\Delta}$CT method.

2.7.2.2 qRT-PCR for microRNA detection

For microRNA detection, the method based on adding poly(A)-tailing to validate the expression of artificial microRNAs was employed (Shi *et al.*, 2012). For poly (A) tailing, 250 ng of total RNA, 1.25 µl 10mM ATP, 1 µl Yeast Poly(A) Polymerase (1 U/µl) (Applied Biological Materials Inc, Canada), 5 µl 5X Poly(A) Polymerase Buffer, 2.5 µl 25 mM $MnCl_2$ and Nuclease-free water up to 25 µl was mixed and the reaction mixture was incubated at 37 °C for 20 minutes, followed by 65 °C for 20 minutes to terminate the reaction. cDNA was synthesized as follows: 25 µl Poly(A) RNA was added to 25 pmol of polyT adapter (Shi *et al.*, 2010) and the mixture was incubated at 70 °C for 2 min followed by cooling on ice for 2 min. Then, the reactions were mixed with 8 µl of 5X First-Strand Buffer, 1 µl of dNTP Mix (10 mM each), 1 µl of DTT (20 mM), 0.5 µl SMARTScribe Reverse Transcriptase (Clontech, USA) (100 units/µl) and sterile water up to 40 µl. The reaction mixture was incubated at 42 °C for 1.5 hr. Diluted cDNA template (1 µl 5x) was used to process the qRT-PCR as described above with gene-specific primers. Gene expression was normalized to the *N. tabacum* 5.8S rRNA forward primer and Poly(T) adaptor reverse primer (Shi *et al.*, 2010). Data was analyzed as described above.

2.7.2.3 qRT-PCR for VIGS

To detect the relative accumulation of *CrPR-1* and *CrPR-5* genes, one-step qRT-PCR was carried out in the Rotor-Gene 6000 real-time PCR detection system (Corbett, Australia) using CrPR-1- and CrPR-5-specific primers. To ensure the absence of DNA template in the samples, qRT-PCRs with and without reverse transcriptase were run in parallel, and *C. roseus 40S ribosomal protein S9* gene (*CrRSP9*) was used to normalize gene expression. qRT-PCR was carried out at 50 °C for 10 min, 95 °C for 3 min, 40 cycles of 95 °C for 10 s, and 60 °C for 20 s. The efficiency of each pair of primers was determined by using a 5-fold serial dilution starting from 100 ng/µl RNA with five dilution points. The Rotor-Gene 6000 software was used to confirm the synthesis of cDNA products by melting curves.

To detect the relative accumulation of PR proteins genes in *N. benthamiana*, one-step qRT-PCR reactions were carried out in the Rotor-Gene 6000 real-time PCR detection system (Corbett, Australia). The RNAs was prepared as described above. In this study, each of two biological replicates were analyzed in triplicate. Each technical replicate was performed in 15 µl reaction mixture contained 7.5 µl brilliant III ultrafast qPCR master mix (Agilent, USA), 0.75 µl reverse transcriptase, 0.3 µM primers of *NbPR-1*, *NbPR-5* and *NbPR-10*, 30 ng RNAs, 0.15 µl 100 mM DTT, and nuclease-free water up to final volume. To ensure the absence of DNA template in the samples, qRT-PCR with and without reverse transcriptase was run in parallel, and *Nb18S rRNA* was used to normalize the gene expression. The program described as followed: 50 °C for 10 min, 95 °C for 3 min, 40 cycles of 95 °C for 10 s, and 60 °C for 20 s. The efficiency of each pair of primers was determined by using a 5-fold serial dilution of 100 ng/µl RNA with at least 5 dilution points. The Rotor-Gene 6000 software was used to confirm the synthesis of cDNA products by melting curves.

All primers were given in Table 2.

Table 2 Gene-specific primers used for gene expression analysis by quantitative real-time PCR

Gene	Primers **(5'-3')**
NtaEF-1α	Forward: TGAGATGCACCACGAAGCTC
	Reverse: CCAACATTGTCACCAGGAAGTG

Gene	Primers **(5'-3')**
NtaL25	Forward: CCCCTCACCACAGAGTCTGC
	Reverse: AAGGGTGTTGTTGTCCTCAATCTT
Hyp-1	Forward: GAACGCCTGGATTTAGTGGA
	Reverse: AAGCTTGTAGGTGGCCGTAA
HpPGIP	Forward: CTCAGATTCCTGAGGCTTGACT
	Reverse: ATCGACCCAGATAGCTTGTTGT
NtaTIR1	Forward: ACTCTTGGGCCGCTTGATACTG
	Reverse: CGCCGCAATTCTTTACAGTTCTCC
NtaARF8	Forward: GCTGCCTGCTCAAACTCAAATGG
	Reverse: GCTGATTGCCGACTTGTTGCTG
NtaLOX1	Forward: GCAGACACTGCTTGGCATTTCC
	Reverse: TGCCCGAGGTAAAGTGTATCCG
NtaPR-10	Forward: CTTGCCAATTCTACCGTCTATGCC
	Reverse: ATTAGCCGAGCTGGACGCAAAC
NtaPR-1	Forward: AGGCGTGGAACCATTAACTTGGG
	Reverse: GCAGTCTGCAGCCAATTGAGAAAC
NtaAGO1	Forward: CATTTGGCAGCTTTCCGTGCTC
	Reverse: TGCGCTTGTGACTGATCCACTG
NtaPAL1	Forward: ATCACTGCCTCGGGTGATCTTG
	Reverse: GCCTTGGAATTAGGCCTACCAGTG
NtaPAL4	Forward: TGCCATCTAACCTCACCGCATC
	Reverse: AGATGCCATGGCGATTTCAGCTC

Gene	Primers **(5'-3')**
NtaCCR	Forward: AGAACAAGCAGCATGGGACGAG
	Reverse: CACCAACACTGGGTTGATTGCC
NtaCAD	Forward: TGTGGTTGATGGGTGTGAAGGC
	Reverse: TCTGCCTGTGGATCTTTGACTCC
NtaCHS	Forward: CGCTCGAGTCCTTGTTGTTTGTTC
	Reverse: AAGTGGGTGTCATTGGGTCCAC
NtaCAT	Forward: ATGCAAAATCGTTCCCTGACA
	Reverse: TCGAAAAACCAGGCAAAAGTA
NtaAPX	Forward: TCAAGGCTGAGCAAGGACATGG
	Reverse: TCCTTGATGGGCTCCAAGAGTC
NtaFe-SOD	Forward: CCCAGCATTCAACAATGCAGCTC
	Reverse: TCCGTTGGGCTTCATGGACTTC
PolyT adapter	Forward: GCGAGCACAGAATTAATACGACTCACTATAGGTTTTTTTTTTTTAGCATGC
	Reverse: GCGAGCACAGAATTAATACGAC
Nta5.8S rRNA	Forward: ACGTCTGCCTGGGTGTCACA
NtamiR160	Forward: TGCCTGGCTCCCTGTATGCCA
NtamiR164ab	Forward: AGAAGCAGGGCACGTGCA
NtamiR164c	Forward: TGGAGAAGCAGGGCACATGCT
CrPR-1	Forward: TAGTCCGAGCCAGAAAATGG
	Reverse: ACGCTTTTACCGCATCACTC

Gene	Primers **(5'-3')**	
CrPR-5	Forward: TACTCCTCCAGCAACCCTAGC	
	Reverse: CGCCGTTAACTTCAACAATC	
CrRSP9	Forward: GATGGTGCACGTTTCCTTTT	
	Reverse: TGGGTCCTTCTCATCCAAAG	
NbPR-1	Forward: TTCTCAACAAGACTATTTGGATGCC	
	Reverse: GAACCGAGTTACGCCAAACCACCTG	
NbPR-5	Forward: CCTCCTTGCCCTTGTGACTTAC	
	Reverse: GCCAAAGTGTTTGGTGGTTTAC	
NbPR-10-2	Forward: ACAACATCAGCTTCCCCAAC	
	Reverse: CGCCTAAAACATCTCCTTCG	
NbPR-10-4	Forward: CATCAGCTTCCCCAACTAGG	
	Reverse: CCCATCACCCTCAACAATC	
Nb18S	Forward: GCCCGTTGCTGCGATGATTC	
	Reverse: GCTGCCTTCCTTGGATGTGG	
HpGAPDH	Forward: ATGGACCATCAAGCAAGGACTG	Jepson *et al*., 2014
	Reverse: GAAGGCCATTCCAGTCAACTTC	
Hp18SrRNA	Forward: AAACGGCTACCACATCCAAG	
	Reverse: CAACCCAAAGTCCAACTACG	
HpPAL	Forward: TGTGAGGCAACGTGTGAATAG A	Velada *et al*. 2014
	Reverse: TCCCATAGAAGGACCAAGCAA	
HpCHS	Forward: GCGCTGCATCGATCATCA	Velada *et al*., 2016
	Reverse: CAGCTCGAACAAGGGCTTTT	

Gene	Primers **(5'-3')**	
HpBPS	Forward: TGCTCTACAATCAGGGGTGC	This study
	Reverse: CGCATGGAAAGTCATGGCAG	
HpPKS1	Forward: TGTACGTCTCATCCAGTGAGC	Jepson *et al*., 2014
	Reverse: ACACCACCGTAACAGCCTAAG	
HpPKS2	Forward: TACACAAGGAGACACCCAAGC	Karppinen, 2010
	Reverse: GGAACTGGCAACATAGCATCC	
HpOKS	Forward: TGCGAGTTGATGGTGTCGAG	This study
	Reverse: ATATTGGGCGCTCTGTAGGC	
HpPAT	Forward: ACCAGGGTTGGCTTTGAC C	Velada *et al*., 2014
	Reverse: TTCTTCCTCCGTCCTCTCTCC	
HpIGPS	Forward: AACGGGGCCGGATAATTC	
	Reverse: CACCAAAACCGCTCTCACAC	
HpHyp-1	Forward: GAACGCCTGGATTTAGTGGA	This study
	Reverse: AAGCTTGTAGGTGGCCGTAA	
HpPGIP	Forward: CTCAGATTCCTGAGGCTTGACT	This study
	Reverse: ATCGACCCAGATAGCTTGTTGT	
HpAGO5	Forward: ACCAGCAGACCCACCCACTA	This study
	Reverse: GCATAGCTTGTTTGTGAGACTTTG	
HpRDR6	Forward: GGCTTTCTCTTCTCCATTCCA	Galla *et al*., 2015
	Reverse: AGCAATACAATCACCCGTCA	
HpSGS3	Forward: CCAGGGCTCAAGAAATTACCA	
	Reverse: CACGAAGTCCTCCATCTCCTT	

Gene	Primers **(5'-3')**	
HpAOX2	Forward: TCAACGCCTACTTTGTGATCTATCTC	Velada *et al*., 2016
	Reverse: AATGGCCTCTTCTTCCAAATAGC	
HpCAT	Forward: CTTCGTTCGTTCGTTCTCCG	This study
	Reverse: GATCCAACGGTGAGGGAGTG	

2.8 Semiquantitative RT-PCR

2.8.1 Semiquantitative RT-PCR in *C. roseus*

To detect the VIGS silence efficiency in *C. roseus*, silencing of *CrIPR* mRNA was detected from upper, non-inoculated leaf tissue at 21 days post-inoculation (dpi) by semiquantitative RT-PCR, as described (Liscombe and O'Connor, 2011). Primers Cr-IPR-(C)-F2/R2 that anneal outside the region targeted for silencing were used to ensure that the endogenous gene would be tested. The *CrRSP9* was used as internal control (Sheshadri *et al.*, 2018). PCR cycles included denaturation at 98 °C for 30 s, annealing at 58 °C for 20 s, and elongation at 72 °C for 30 s. Aliquots were removed from the thermocycler after 36, 39, and 42 cycles. 10 µl of the PCR products were analyzed on a 1.7% agarose gel stained with ethidium bromide.

2.8.2 Semiquantitative RT-PCR in *N. benthamiana*

To detect the VIGS silence efficiency in *N. benthamiana*, silencing of *PGIP* mRNA was detected from upper, non-inoculated leaf tissue at 15 dpi by semiquantitative RT-PCR, as described (Liu *et al.*, 2002). Primers NbPGIP-F/R that anneal outside the region targeted for silencing were used to ensure that the endogenous gene was tested. The *Actin* gene transcripts were used as the internal control, using primers NbActin-F/R. PCR cycles included denaturation at 98 °C for 30 s, annealing at 60 °C for 20 s, and elongation at 72 °C for 30 s.

Aliquots were removed from the thermocycler after 30, 33, and 36 cycles for mRNA detection. PCR products were analyzed on a 1.7% agarose gel stained with ethidium bromide.
All the primers were given in Table 3.

Table 3 Gene-specific primers used for gene expression analysis by semiquantitative RT-PCR

Gene	Primers **(5'-3')**
Cr-IPR-(C)-2	Forward: GTGTTCAAGGCGTTT GTCC
	Reverse: ACCGAAATGGACCAACTTG
NbPGIP	Forward: TTTCTTTTCCCTCCCCTTCTC
	Reverse: GTGAGATTTGTGATATGATGGCG
NbActin	Forward: GATGGACAAGTCATCACCATT
	Reverse: CTGAGGACAATGTTTCCGTACA

2.9 GUS staining assays

Fresh plant leaves disks were collected by sterile core borer or cut into pieces of rhombus-like shape. To avoid contamination, the disks were sterilized with 70% ethanol for 30 s, 6% NaClO for 90 s, followed by washing with sterilized water. Leaf disks were kept on MSIB medium in the plant culture room for 2 days. The leaf disc transformation method was used to introduce *Agrobacterium* strain EHA105 harboring pCAMBIA2301-GUS into plant tissues. After 5-6 days, the infected leaf disks were incubated in the GUS staining buffer (0.5 mg/μl X-Gluc (5-bromo-4-chloro-3-indolyl β-D-glucuronide cyclohexylammonium salt), 20 mM sodium phosphate buffer (pH 7.0), 10 mM EDTA (pH 8.0), 5 mM K_4FeCN_6 and 5mM K_3FeCN_6) at 37 °C overnight. Next day, the samples were washed by 70% ethanol and the GUS activity was viewed and photographed.

2.10 Subcellular localization

For Hyp-1 subcellular localization assays, *A. tumefaciens* cultures harboring the plasmid GFP-Hyp-1 and the mCherry-labeled-plasma membrane marker PM-RK (Nelson *et al.*, 2007) were co-infiltrated into the leaves of 5-week-old *N. tabacum* plants, follow the method describe above (Hou *et al.*, 2011).

For PGIP subcellular localization assays, *A. tumefaciens* cultures harboring the plasmid GFP-PGIP together with the mCherry-labeled-plasma membrane marker PM-RK or GFP-PGIP together with mRFP were co-infiltrated into the leaves of 5-week-old *N. tabacum* plants, respectively.

Confocal fluorescence of GFP and mCherry were captured with Leica TCS SP2 confocal microscope. Excitation and emission settings in nanometers (nm) were 488 and 500-to-530 respectively for GFP; 561 and 575-to-640 respectively for mCherry. Images were processed with ImageJ (Schindelin *et al.*, 2012) and Adobe Photoshop software (Adobe Systems).

2.11 Virus-induced gene silencing

2.11.1 VIGS in *C. roseus*

For VIGS, TRV vectors pTRV1 and pTRV2:00 were obtained from ABRC (http://www.arabidopsis.org). pTRV2: CrChlhI containing a fragment of *C. roseus Protoporphyrin IX magnesium Chelatase subunit H* (*ChlH*) gene served as marker to evaluate VIGS efficiency. The vector was received kindly from Prof. Mariana Sottomayor from University of Porto (Liscombe and O'Connor, 2011).

Three-four weeks-old *C. roseus* plants having two pairs of fully developed true leaves were used for agroinfiltration. *A. tumefaciens* strains containing recombinant TRV vectors were grown overnight and resuspended in buffer containing 10 mM MgCl2, 10 mM MES and 0.15 mM AS, and the OD_{600} was adjusted to 1.5. *Agrobacterium* strains containing pTRV2: CrIPR, pTRV2: CrChlH and pTRV2:00 were mixed with pTRV1 in a ratio 1:1 and left at room temperature for 3-4 hours before inoculation. A sterile 1.1x25mm needle carrying a drop of

each *A. tumefaciens* mixture was used to prick twice the stem in the apical meristem and just below the insertion of the youngest leaf on the first node.

2.11.2 VIGS in *N. benthamiana*

pTRV2: BoPDS2 carrying a fragment of the *B. oleracea* var. *oleracea Phytoene desaturase* (*PDS*) gene served as a marker to evaluate VIGS efficiency (kindly provided by Prof. Marcel Dicke from Wageningen University (Zheng *et al.*, 2010).
A. tumefaciens cells containing recombinant TRV vectors were prepared as described above and the OD_{600} was adjusted to 0.2. *Agrobacterium* strains containing pTRV2: BoPGIP, pTRV2:BoPDS2 and pTRV2:00 were mixed with pTRV1 in a ratio 1:1 and left at room temperature for 3-4 hours before inoculation. Four-week-old *N. benthamiana* plants were used for agroinfiltration as described (Hou *et al.*, 2011).

2.11.3 VIGS in *H. perforatum* L.

To process the VIGS in *H. perforatum* L., there were three methods used, namely tooth-pick (pinch-wounding method) (Liscombe and O'Connor, 2011), agroinfiltration and sap infection (Hou *et al.*, 2011).

2.12 Plant virus inoculation

To select the plant virus which could infect *H. perforatum* L., the sap infection method was employed. Five-week-old *N. benthamiana* leaves from confirmed infected plants were ground in 5 mM sodium phosphate buffer (pH 7.2) and clarified by filtration. The sap was applied to carborundum-dusted leaves with mechanical rubbing. Buffer-treated plants were used as a negative control (Hou *et al.*, 2011).

2.13 Western blotting

Samples were collected at 3 dpi and 5 dpi and western blot was carried out to measure GFP expression. Total proteins were extracted from 100 mg plant leaves in 400 µl extraction buffer containing 0.1 M Tris-HCl (pH 8.0), 10mM EDTA (pH 8.0), 0.1 M LiCl, 1% SDS and 1% fresh added β-mercaptoethanol. Samples were separated on 15% SDS-PAGE gels and transferred to poly- (vinylidene difluoride) (PVDF) membranes (Amersham, GE Healthcare, Little Chalfont, Buckinghamshire, UK). The membranes were blotted with rabbit anti-GFP, N-terminal antibody (Sigma-Aldrich, St Louis, MO, USA). Blotted proteins were detected by secondary antibody Goat anti-Rabbit IgG HRP (Sigma-Aldrich, USA) and LiteAblot® PLUS Enhanced Chemiluminescent Substrate (Euroclone, Italy). Or blotted proteins were detected by secondary antibody Goat Anti-Rabbit IgG (whole molecule)-Alkaline Phosphatase (Sigma-Aldrich, USA) and SIGMA FAST™ BCIP/NBT (5-Bromo-4-chloro-3-indolyl phosphate/Nitro blue tetrazolium) Tablets (Sigma-Aldrich, USA).

2.14 Statistical analysis

The transcript levels of target genes involved in different plant defense pathways were compared by One-way ANOVA and the relative accumulation of *PR* genes in *C. roseus*, *N. benthamiana* and plant defense gene detection in *H. perforatum* L. glands were analyzed by Student´s t-test using GraphPad Prism 6 (GraphPad Software, Inc., UK). In the figures, the values were marked with asterisks to denote the significance levels compared with control: *, $P \leq 0.05$; **, $P \leq 0.01$; ***, $P \leq 0.001$; and ****, $P \leq 0.0001$ and ns, stands not significant.

2.15 References

Arvidsson, S., Kwasniewski, M., Riaño-Pachón, D.M. and Mueller-Roeber, B. (2008) QuantPrime - A flexible tool for reliable high-throughput primer design for quantitative PCR. *BMC Bioinformatics* **9**, 1–15.

Conley, A.J., Joensuu, J.J., Jevnikar, A.M., Menassa, R. and Brandle, J.E. (2009) Optimization of elastin-like polypeptide fusions for expression and purification of

recombinant proteins in plants. *Biotechnol. Bioeng.* **103**, 562–573.

Dias, A.C.P., Seabra, R.M., Andrade, P.B., Ferreres, F. and Ferreira, M.F. (2001) Xanthone production in calli and suspended cells of Hypericum perforatum. *J. Plant Physiol.* **158**, 821–827.

Franklin, G., Conceição, L.F.R., Kombrink, E. and Dias, A.C.P. (2008) Hypericum perforatum plant cells reduce Agrobacterium viability during co-cultivation. *Planta* **227**, 1401–1408.

Galla, G., Vogel, H., Sharbel, T.F. and Barcaccia, G. (2015) De novo sequencing of the Hypericum perforatum L. flower transcriptome to identify potential genes that are related to plant reproduction sensu lato. *BMC Genomics* **16**, 1–22.

Gasic, K., Hernandez, A. and Korban, S.S. (2004) RNA extraction from different apple tissues rich in polyphenols and polysaccharides for cDNA library construction. *Plant Mol. Biol. Report.* **22**, 437–438.

Horsch, R.B., Fry, J.E., Hoffmann, N.L., Eichholtz, D., Rogers, S.G. and Fraley, R.T. (1985) A simple and general method for hybridization revealed the expected. *Science (80-.).* **227**, 1229–1231.

Hou, W.N., Duan, C.G., Fang, R.X., Zhou, X.Y. and Guo, H.S. (2011) Satellite RNA reduces expression of the 2b suppressor protein resulting in the attenuation of symptoms caused by Cucumber mosaic virus infection. *Mol. Plant Pathol.* **12**, 595–605.

Jepson, C., Karppinen, K., Daku, R.M., Sterenberg, B.T. and Suh, D.Y. (2014) Hypericum perforatum hydroxyalkylpyrone synthase involved in sporopollenin biosynthesis - phylogeny, site-directed mutagenesis, and expression in nonanther tissues. *FEBS J.* **281**, 3855–3868.

Karppinen, K. (2010) Biosynthesis of hypericins and hyperforins in Hypericum perforatum L.(St. John's wort)—precursors and genes involved.

Liscombe, D.K. and O'Connor, S.E. (2011) A virus-induced gene silencing approach to understanding alkaloid metabolism in Catharanthus roseus. *Phytochemistry* **72**, 1969–1977.

Liu, Y., Schiff, M., Marathe, R. and Dinesh-Kumar, S.P. (2002) Tobacco Rar1, EDS1 and NPR1/NIM1 like genes are required for N-mediated resistance to tobacco mosaic virus. *Plant J.* **30**, 415–429.

Nelson, B.K., Cai, X. and Nebenführ, A. (2007) A multicolored set of in vivo organelle markers for co-localization studies in Arabidopsis and other plants. *Plant J.* **51**, 1126–

1136.

Schindelin, J., Arganda-Carreras, I., Frise, E., Kaynig V., Longair M., Pietzsch T., Preibisch S., Rueden C., Saalfeld S., Schmid B., Tinevez JY., White DJ., Hartenstein V., Eliceiri K., Tomancak P., and Cardona A. (2012) Fiji: An open-source platform for biological-image analysis. *Nat. Methods* **9**, 676–682.

Schmidt, G.W. and Delaney, S.K. (2010) Stable internal reference genes for normalization of real-time RT-PCR in tobacco (Nicotiana tabacum) during development and abiotic stress. *Mol. Genet. Genomics* **283**, 233–241.

Sheshadri, S.A., Nishanth, M.J., Yamine, V. and Simon, B. (2018) Effect of Melatonin on the stability and expression of reference genes in Catharanthus roseus. *Sci. Rep.*, 1–11.

Shi, R., Sun, Y., Zhang, X. and Chiang, V.L. (2012) Next-generation microRNA expression profiling technology. **822**.

Shi, R., Yang, C., Lu, S., Sederoff, R. and Chiang, V.L. (2010) Specific down-regulation of PAL genes by artificial microRNAs in populus trichocarpa. *Planta* **232**, 1281–1288.

Singh, R.K., Hou, W. and Franklin, G. (2016) Protocols for in vitro cultures and secondary metabolite analysis of aromatic and medicinal plants, Second Edition. **1391**, 317–334.

Velada, I., Cardoso, H.G., Ragonezi, C., Nogales, A., Ferreira, A., Valadas, V. and Arnholdt-Schmitt, B. (2016) Alternative oxidase gene family in Hypericum perforatum L.: characterization and expression at the post-germinative phase. *Front. Plant Sci.* **7**, 1–16.

Velada, I., Ragonezi, C., Arnholdt-Schmitt, B. and Cardoso, H. (2014) Reference genes selection and normalization of oxidative stress responsive genes upon different temperature stress conditions in hypericum perforatum L. *PLoS One* **9**, 1–24.

Zheng, S.J., Snoeren, T.A., Hogewoning, S.W., van Loon, J.J., and Dicke, M. (2010) Disruption of plant carotenoid biosynthesis through virus-induced gene silencing affects oviposition behaviour of the butterfly Pieris rapae. *New Phytol* 733–745.

Chapter 3

Transgenic expression of *Hyp-1* gene from *H. perforatum* L. alters expression of defense-related genes and modulates recalcitrance to *A. tumefaciens*

Part of the content of this chapter is included in the following publication:

Weina Hou, Rupesh Kumar Singh, Pan Zhao, Viviana Martins, Emmanuel Aguilar, Tomás Canto, Franklin Gregory, Francisco Tenllado, Alberto Carlos Pires Dias. (2018) Transgenic expression of *Hyp-1* gene from *Hypericum perforatum* L. alters expression of defense-related genes and modulates recalcitrance to *Agrobacterium tumefaciens*. *Plant Science* (submitted).

Chapter 3 Transgenic expression of *Hyp-1* gene from *H. perforatum* L. alters expression of defense-related genes and modulates recalcitrance to *A. tumefaciens*

3.1 Summary

H. perforatum L. is a reservoir of high-value secondary metabolites, with a rapidly increasing interest for both researchers and the pharmaceutical industry. Hence, improving their production via genetic manipulation is a challenging task. However, *H. perforatum* L. remains recalcitrant to *A. tumefaciens*-mediated transformation. Here, we aimed to identify genes from *H. perforatum* L. involved in defense responses against *A. tumefaciens. Phenolic oxidative coupling protein* (*Hyp-1*), a pathogenesis-related (PR) class 10 family gene, was selected from a forward subtractive cDNA library from *A. tumefaciens*-treated *H. perforatum* L. suspension cells. The role of *Hyp-1* in defense against *A. tumefaciens* was analyzed in transgenic *N. tabacum* and *L. sativa* plants overexpressing *Hyp-1*, and in *C. roseus* silenced for the homologous *Hyp-1* gene, *CrIPR*. Our results showed that transformation efficiency of *A. tumefaciens* is greatly decreased in tobacco and lettuce overexpressing *Hyp-1*. However, silencing of *CrIPR* in *C. roseus* led to induction of *CrPR-5* and an increased resistance to *Agrobacterium*. Moreover, the expression of core genes regulating several defense pathways was analyzed in *Hyp-1* transgenic tobacco plants. Overall, overexpressing of *Hyp-1* led to an ample down-regulation of key genes involved in auxin signaling (*NtaTIR1*, *NtaAFR8)*, microRNA(miR)-based gene silencing (*NtaAGO1*, *Nta*miR*160*, *NtamiR164ab)*, detoxification of reactive oxygen species (*NtaFe-SOD*), phenylpropanoid pathway (*NtaPAL1*, *NtaPAL4* and *NtaCHS*) and PRs (*NtaPR10* and *NtaPR1)*. Moreover, Hyp-1 was detected in the nucleus, plasma membrane and the cytoplasm of epidermal cells by confocal microscopy. Overall, our findings suggest that *Hyp-1* modulates recalcitrance to *A. tumefaciens*-mediated transformation in *H. perforatum* L.

3.2 Introduction

H. perforatum L., popularly known as St. John's wort, is widely researched medicinal plant with a history of more than 2000 years, possesses pharmacological properties like anti-depressant, anti-inflammatory, anti-viral, anti-cancer, and anti-bacterial (Patočka J, 2003; Tatsis *et al.,* 2007; Saddiqe *et al*., 2010). *H. perforatum* L. contains a wide range of biologically active secondary metabolites, include hypericin, hyperforin, xanthones, essential oils, phenolic acids and a broad array of flavonoids (Butterweck *et al*., 2003; Tatsis *et al.*, 2007; Karppinen, 2010; Saddiqe *et al*., 2010). Hence, metabolic engineering could offer opportunities to maximize the production of *valuable* substances on an industrial scale. Although genetic transformation of *H. perforatum* L. by *A. rhizogenes* and biolistic bombardment has been reported, these protocols cannot achieve the requirements of functional genomic research (Hou *et al*., 2016).

A. tumefaciens is a gram-negative, soil-borne bacterium that causes crown gall disease on a broad range of host plants by integrating a transfer DNA (T-DNA) from a tumor-inducing plasmid from bacterium into the host genome (Pitzschke, 2013; Gohlke and Deeken, 2014). This feature has been widely exploited to introduce foreign genes into the plant to perform functional genomics and genetic engineering purposes. However, as a bacterium pathogen, *A. tumefaciens* activates a number of defense responses in plants that include alterations in 1) phytohormone metabolism (Pitzschke, 2013), 2) pathogenesis-related protein synthesis (Anand *et al.*, 2007; Pruss *et al*., 2008), 3) microRNA-mediated gene silencing (Dunoyer *et al*., 2006), 4) lignin deposition (Singh *et al.*, 2014; Miedes *et al*., 2014), 5) secondary metabolite profiles (Franklin *et al.*, 2009), and 6) production of ROS (Franklin *et al.*, 2008).

Plants grown in natural world are constantly attacked by pathogens, to response the infection, plants have evolved a series of defense mechanisms. In the amount of mechanisms, the phytohormones play an important role in defense against pathogenic microorganisms. Plant produces a wide variety of phytohormones including auxin as a key character in plant-pathogen interaction system which involves two group of protein complexes: the auxin signaling repressor auxin/indole acetic acid (Aux/IAA) and the auxin signaling receptor Transport inhibitor response 1/Auxin signaling F-box proteins (TIR1/AFB). In this pathway, pathogen produced IAA is perceived by TIR1, the core member of the auxin signaling receptor and

activates TIR1/AFB to degrade Aux/IAA which negatively regulates auxin signaling by binding and inhibiting Auxin responsive factor (ARFs), and achieve the final goal to release ARFs, which regulates transcription of auxin-responsive genes. (Fu and Wang, 2011; Nazari *et al.*, 2017). In addition, plant IAA biosynthesis can be up-regulated by some ARFs, and the increased IAA level causes cell wall expansion by inducing the expression of structural proteins like Endo-β-1,4-glucanases (EGases) and Xyloglucan endotransglycosylases (XETs). These activities participate in cell wall loosening that promotes pathogen invasion and disease development. Moreover, auxin is involved in stomata opening that allows some pathogens to gain access to the interior of plant tissues. It has been reported that auxin acts as a key modulator in *Arabidopsis* and *A. tumefaciens* interaction, adjust the ratio of cytokinin to auxin could develop the crown gall, and the crosstalk among IAA, ethylene, and SA balances the host launched pathogen defense and *A. tumefaciens* initiated tumor growth (Lee *et al.*, 2009; Zhang *et al.*, 2015). Phytohormone SA has been certified as the primary phytohormone regulating plant responses to *A. tumefaciens* infection. It has been demonstrated that SA inhibits the *vir* regulon and induces quormone degradation system to directly interfere with *A. tumefaciens* infection (Yuan *et al.*, 2007). In addition, the resistance to *A. tumefaciens* infection is enhanced by exogenous application of SA in *N. benthamiana* and plants hypersusceptible to *A. tumefaciens* infection could be induced by expression of bacterial *NahG* gene which encoding salicylate hydroxylase or silencing the genes involved in SA biosynthesis. Furthermore, *PR-1* is induced in *A. tumefaciens* infiltrated *N. tabacum* leaves and resistance to subsequent infection with *Tobacco mosaic virus* (Anand *et al.*, 2007; Pruss *et al*., 2008). JA, another well-recognized hormone mediates plant defense against pathogens. Exogenous application of JA induces expression of rice *JIOsPR-10* (jasmonate inducible) (Jwa *et al.*, 2001). Lipoxygenases (LOXs; EC 1.13.11.12) are key enzymes in the biosynthesis of oxylipins, catalyze the formation of fatty acid hydroperoxides, present at the first step in synthesis of JA pathway in plant. *PR-10* and *LOX* are considered as the hallmarks in JA pathway (Allmann *et al.*, 2010; Huang and Schwab, 2011; Peng *et al.*, 2012).

Pathogenesis-related (PR) proteins have been described as a class of plant specific proteins that accumulation in response to pathogen infection. Recently, based on the sequence homology, structural differences and biological activities, PR proteins have been classified into 17 families. PR-1 as the first PR family is discovered from *Tobacco mosaic virus* infected *N. tabacum* in 1970s (Loon and Kammen, 1968). PR-1 is characterized as the marker for SA mediated disease

resistance. SA activates the systemic acquired resistance (SAR) which increases the expression of PR-1s to responds to the pathogens infection in plant (Kumar, 2014; Janda and Ruelland, 2015; Breen *et al.*, 2017; Palmer *et al.*, 2017). It has been reported SA regulated PR-1 plays a significant role in defense against *Agrobacterium* infection in tobacco (Anand *et al.*, 2007; Pruss *et al.*, 2008) and tomato (Liu *et al.*, 2012). PR-5 (Thaumatin-like proteins (TLPs)) have a sequence similar with thaumatin, a sweet-tasting protein from *Thaumatococcus daniellii.* PR-5 family distributes throughout plants to resistance the pathogens infection and abiotic stresses (Tachi *et al.*, 2009; Yasmin and Saleem, 2014; Rather *et al.*, 2015; Souza *et al.*, 2017). Together with PR-1 and PR-2 are considered as SA signaling pathways markers (Molinari *et al.*, 2014). PR-10 family is small (154-163 amino acids, 15-18 KDa) and slightly acidic proteins. Unlike other PR proteins, PR-10s are intracellular and cytosolic proteins. Bet v1, known as birch pollen allergen, is the first characterized protein from this family serves as the subclass to contribute PR-10 (Fernandes *et al.*, 2013; Hsu *et al.*, 2014; Xu *et al.*, 2014; Sliwiak *et al.*, 2016). *Hyp-1* belongs to PR-10 family (Sliwiak *et al.*, 2015; Karppinen *et al.*, 2016; Sliwiak *et al.*, 2016).

Plant defense against *Agrobacterium* is very complicated and multifaceted. It includes not only the phytohormone and PR proteins pathways, but also the gene silencing pathway, specially microRNA-mediated gene silencing pathway (Dunoyer *et al.*, 2006). RNA silencing in plants function as a defense mechanism against invading pathogens. Plant microRNAs are 21-24nt small non-coding RNAs processed from primary miRNAs (pri-miRNAs) with stem-loop structures by the RNase III DICER-like 1(DCL1) to generate unstable pre-miRNA (80-200nt) then to miRNA-miRNA* duplex. In plant cytoplasm, one stand of miRNA-miRNA* duplex is recruited into ARGONAUTE 1 protein (AGO1) forming RNA-induced silencing complex (RISC), which targets transcripts for posttranscriptional gene silencing (PTGS) (Duan *et al.*, 2012). MicroRNAs are involved into plant development and immunity systems. MiR393 is the first microRNA discovered to contribute to antibacterial resistance in *Arabidopsis*. Bacteria caused miR393 accumulation negatively regulates transcripts of F-box auxin receptors (TIR1, AFB2, and AFB3) protect from bacterial pathogens by suppression of the auxin signaling pathway (Navarro *et al*., 2006). Recently, miR393 and miR167 have been detected in *Agrobacterium* infected tobacco plants (Dunoyer *et al.*, 2006; Pruss *et al.*, 2008; Nazari *et al.*, 2017).

Plant secondary metabolites have an essential role in defense against pathogens (Mazid *et al.*, 2011; Andersson, 2012; Goyal *et al.*, 2012). Phenylalanine ammonia-lyase (PAL; EC 4.3.1.5) is the first enzyme of phenylpropanoid pathway, which involves the plant lignin and flavonoid biosynthetic pathways (Heldt and Piechulla, 2011; Bagal *et al.*, 2012). Lignin as a critical constituent of plant call wall, plays a major role in plant structure defense mechanism against pathogens. In this pathway, Cinnamoyl CoA reductase (CCR; E.C.1.2.1.44) is one of the key enzymes in lignin synthesis, which is the first enzyme of the monolignol specific part of the lignin biosynthetic pathway. Another key enzyme of this pathway is Cinnamyl alcohol dehydrogenase (CAD; E.C. 1.1.1.195) which catalyzes the last step in monolignol biosynthesis (Raes, 2003; Prasad *et al*., 2011). Flavonoids are a group of polyphenolic compounds from plant secondary metabolites to defense against pathogens. Chalcone synthase (CHS; EC 2.3.1.74) is a key enzyme which catalyzes the first committed step in the flavonoid biosynthesis pathway (El-kereamy *et al.*, 2011; Zhou *et al.*, 2013; Meng *et al.*, 2015; Yahyaa *et al.*, 2017).

Plant defense themselves from pathogens has another hallmark is generation of ROS both pathogenic, as well as symbiotic causes the hypersensitive reaction (HR). ROS comprise of enzymatic and non-enzymatic components: include Superoxide dismutase (SOD; EC 1.15.1.1), Catalase (CAT; EC 1.11.1.6), Ascorbate peroxidase (APX; EC 1.11.1.11), Ascorbic acid (ASC) and Glutathione (GSH) (Oliveira *et al.*, 2012; Peleg-Grossman *et al.*, 2012; Pandey *et al.*, 2014; Maschietto *et al.*, 2016; Pandey *et al.*, 2017).

A. tumefaciens mediated transformation is the most preferred method of gene transfer to plants, which could be useful for metabolic engineering and functional genomic studies in *H. perforatum* L. However, *H. perforatum* L. recalcitrance to *A. tumefaciens*-mediated transformation constitutes a major concern in the field (Hou *et al*., 2016). In our previous study, *H. perforatum* L. suspension cells showed intense oxidative burst upon *A. tumefaciens* interaction, with 99% mortality of *A. tumefaciens* taking place in 12 h while no apoptotic process in plant cells was recorded (Franklin *et al.*, 2008).

Hyp-1 was first cloned and characterized from *H. perforatum* L. cell cultures (Bais *et al.*, 2003). The cDNA sequence of Hyp-1 contains an open reading frame of 480 nucleotides, encoding a protein of 159 amino acids with a molecular weight of 17.8 kDa. Hyp-1 was considered as the solely enzyme that catalyze the conversion of emodin to the key biocompound hypericin in *H. perforatum* L. *in vitro* (Bais *et al.*, 2003), while other reports did not confirm the catalytic

activity of this protein (Košuth *et al*., 2007; Michalska *et al*., 2010; Košuth *et al*., 2011; Karppinen *et al.*, 2016). Moreover, highest expression level of *Hyp-1* was found in *H. perforatum* L. roots where no dark glands (sites of production of compounds of pharmacological value) are present, which left unresolved the function of *Hyp-1* in the biosynthesis of hypericin (Košuth *et al.*, 2007). Furthermore, it was observed that there was no clear correlation between hypericin production and *Hyp-1* expression since the *Hyp-1* gene was expressed in both "hypericin producing" and "hypericin lacking" species. These findings suggest that *Hyp-1* is not a limiting factor in the biosynthesis of hypericin (Košuth *et al.*, 2011).

In silico studies on crystal structure of Hyp-1 evidenced that *Hyp-1* belongs to PR-10 family (Fernandes *et al.*, 2008; Michalska *et al.*, 2010; Sliwiak *et al*., 2016). PR-10 proteins are a family of small (154-163 amino acids, 15-18 KDa) and slightly acidic proteins which, unlike other PR proteins, accumulate in the cytosol. The major birch pollen allergen Bet v1 is considered the prototype for the PR-10 protein family and shares 45.1% homology to Hyp-1 (Fernandes *et al*., 2013; Hsu *et al*., 2014; Xu *et al*., 2014; Sliwiak *et al*., 2016). Some PR-10 proteins have been shown to have antifungal activities. For instance, MtPR-10 identified from *Medicago truncatula* had antifungal activity against *Aphanomyces euteiches* (Colditz *et al.*, 2005). SsPR-10 from *Solanum surattense* inhibited hyphal growth of *Pyricularia oryzae* (Pungartnik *et al.*, 2009). ZmPR-10.1 from *Zea mays* had antifungal activity against *Aspergillus flavus* (Xie *et al.*, 2010). CsPR10 from *Crocus sativus* inhibited the growth of *Fusarium oxysporum* (Gómez-Gómez *et al*., 2011). Besides, some PR-10s also showed antiviral and antibacterial activities. CaPR-10 from *Capsicum annuum* had antiviral activities against *Tobacco mosaic virus* (Park *et al.*, 2004). ZmPR-10 and ZmPR-10.1 conferred antibacterial activities against *Pseudomonas syringae* pv. *tomato* DC3000 (Xie *et al.*, 2010). The increased expression of *Hyp-1* upon wounding and treatments with SA, and ABA suggested its role in plant defense (Košuth *et al*., 2013; Karppinen *et al*., 2016). Furthermore, upon infection by *A. tumefaciens*, *Hyp-1* expression was significant upregulated in all analyzed *Hypericum* species (Košuth *et al.*, 2013).

Gain-of-function approaches constitute useful tools for connecting genes to biological pathways. Among them, overexpression of individual genes by genetic transformation has been used to identify genes that confer stress tolerance to plants (Kondou *et al.*, 2010). There are also abundant reports on studies in plants overexpressing PR genes, resulting in enhanced tolerance

to pathogen infection. In addition, loss-of-function approaches have been exploited by plant pathologists as a parallel or complementary method to overexpression studies. VIGS has been developed as a well-known technique based on RNA silencing to knock-down the expression of endogenous genes by utilizing recombinant viruses. Recently, *Tobacco rattle virus* (TRV)-based VIGS has been successfully used in the genetically non-tractable plant species *C. roseus* to investigate gene function (Liscombe and O'Connor, 2011).

In the present study, *Hyp-1* was selected from a forward subtractive cDNA library from *A. tumefaciens*-treated *H. perforatum* L. suspension cells. Its biological function in defense against *A. tumefaciens* was analyzed in transgenic *N. tabacum* and *L. sativa* plants overexpressing *Hyp-1*, and in *C. roseus* silenced for the *Hyp-1* homologous gene. Moreover, the expression of core genes regulating several defense pathways was analyzed in *Hyp-1* overexpressing lines. Hyp-1 was detected in the nucleus, plasma membrane and the cytoplasm of epidermal cells by confocal microscopy. Overall, our findings suggest that *Hyp-1* from *H. perforatum* L. modulates tolerance to *A. tumefaciens* as part of defense mechanisms against pathogenic infection.

3.3 Results

3.3.1 Overexpression of *Hyp-1* in *N. tabacum* and *L. sativa*

To identify genes from *H. perforatum* L. involved in defense responses against *A. tumefaciens*, a SSH-based cDNA library was performed. RNAs isolated from *H. perforatum* L. suspension cells challenged with *A. tumefaciens* as tester and with RNAs from control cultures as driver were used to construct the forward subtracted cDNA library from which a highly expressed *Hyp-1* gene was selected.

To characterize *Hyp-1* function in defense responses, we established transgenic *N. tabacum* plants expressing Hyp-1 fused at the N-terminus to GFP under the control of 35S promoter in the binary expression vector pBI121 (Fig. 3.1). Four transgenic tobacco plant lines, GFP-Hyp-1-2/-3/-4/-5, were selected by antibiotic resistance, and T-DNA insertion was confirmed by PCR. As control, besides wild type (WT), transgenic tobacco plants expressing GFP were obtained.

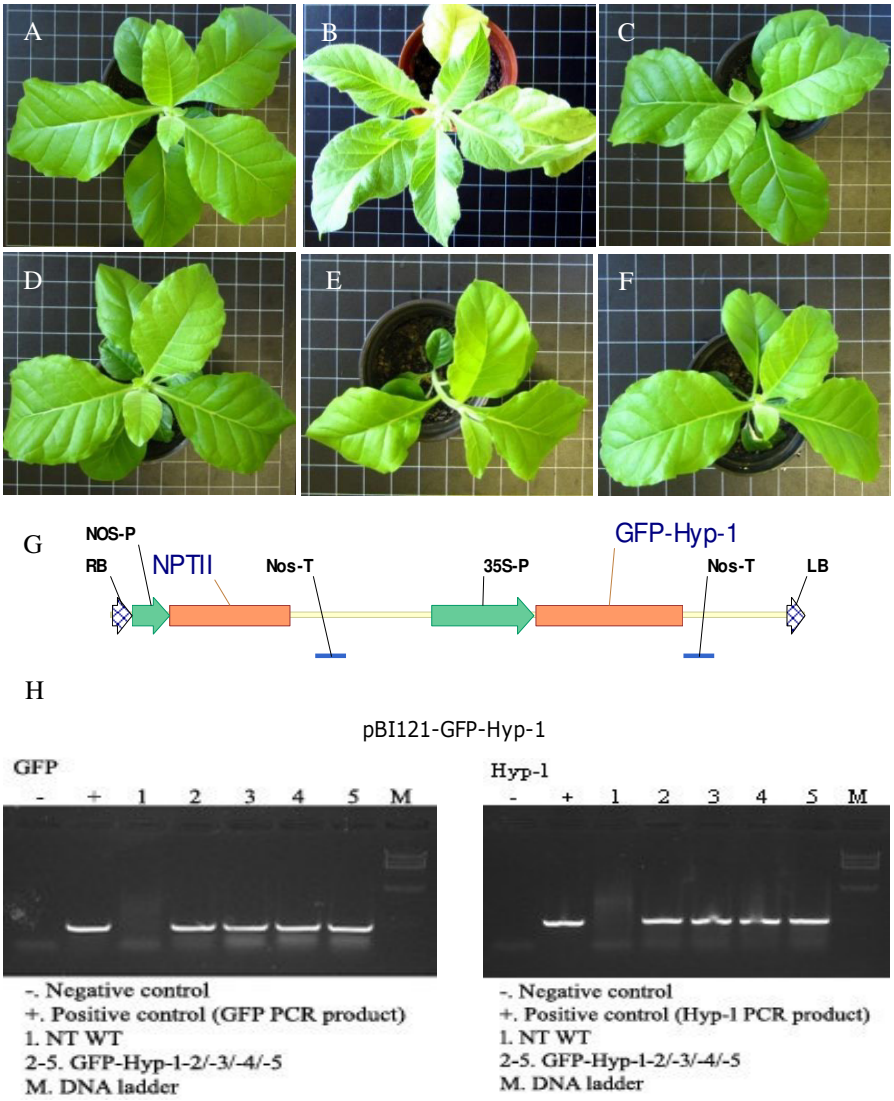


Fig. 3.1 Generation of *N. tabacum* GFP-Hyp-1 overexpressing plants. (A) WT *N. tabacum* control plant. (B) GFP transgenic plant as control. (C-F) GFP-Hyp-1-2/-3/-4/-5 transgenic plant lines. (G) Schematic diagram of pBI121-GFP-Hyp-1 made by software Vector NTI. (H) Confirmation of T-DNA insertion by PCR.

In order to determine whether overexpression of *Hyp-1* influences the efficiency of *Agrobacterium*-mediated expression in tobacco, we inoculated two T2 progenies derived from each of three T1 lines, GFP-Hyp-1-3/-4/-5, with the strain EHA105 harboring a binary plasmid to express GUS. Whereas GFP transgenic control plants showed an intense GUS staining and behaved similarly to WT plants (Fig. 3.2 B, C), GUS staining was absent in either of the six

GFP-Hyp-1 T2 transgenic lines (Fig. 3.2 D-I) or WT plants inoculated with *A. tumefaciens* containing the empty vector (Fig. 3.2 A).

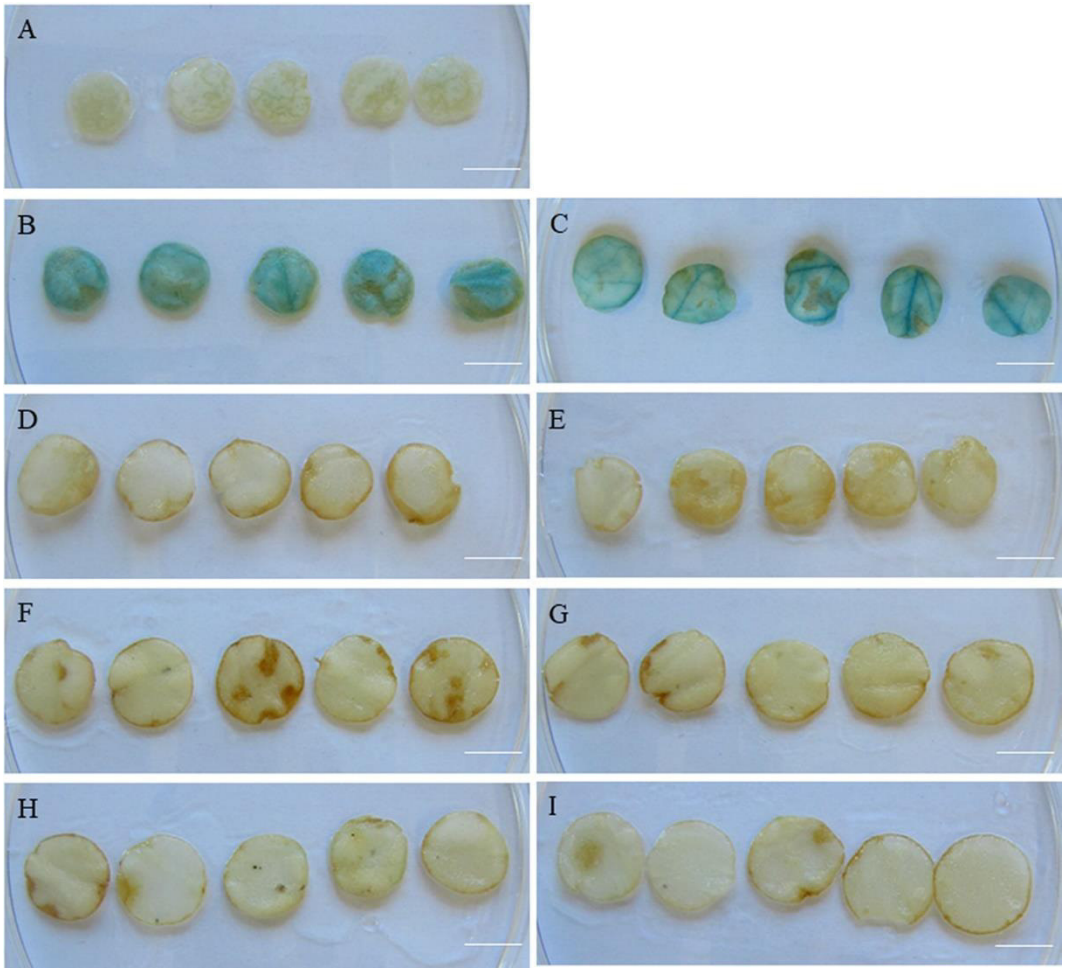


Fig. 3.2 Detection of *Agrobacterium*-mediated expression in GFP-Hyp-1 tobacco T2 lines by GUS staining. (A) WT plant inoculated with *A. tumefaciens* EHA105 containing the empty vector as negative control. (B) WT plant inoculated with *A. tumefaciens* containing pCAMBIA 2301-GUS as positive control. (C) GFP transgenic line inoculated with *A. tumefaciens* containing pCAMBIA 2301-GUS as positive control. (D-E) GFP-Hyp-1-3-2/-3 transgenic lines inoculated with *A. tumefaciens* containing pCAMBIA 2301-GUS. (F-G) GFP-Hyp-1-4-1/-3 transgenic lines inoculated with *A. tumefaciens* containing pCAMBIA 2301-GUS. (H-I) GFP-Hyp-1-5-2/-3 transgenic lines inoculated with *A. tumefaciens* containing pCAMBIA 2301-GUS. Bars in each panel represent 10 mm.

Next, we assessed *Agrobacterium*-mediated expression in two varieties of *L. sativa*, BL and SBR, overexpressing *GFP-Hyp-1* and *Hyp-1* respectively (Fig. 3.3 and 3.4), by inoculation with

Agrobacterium harboring the GUS gene. T1 transgenic plants expressing either *GFP-Hyp-1* or *Hyp-1* showed no staining at all (Fig. 3.5 D, F, and Fig. 3.6 C) or a clear decrease in GUS staining (Fig. 3.5 C, E) compared to WT plants (Fig. 3.5 B and 3.6 B). Our results indicate that expression efficiencies by *A. tumefaciens* greatly decrease in tobacco and lettuce plants constitutively overexpressing *Hyp-1*, suggesting the involvement of *Hyp-1* in defense response against *A. tumefaciens*.

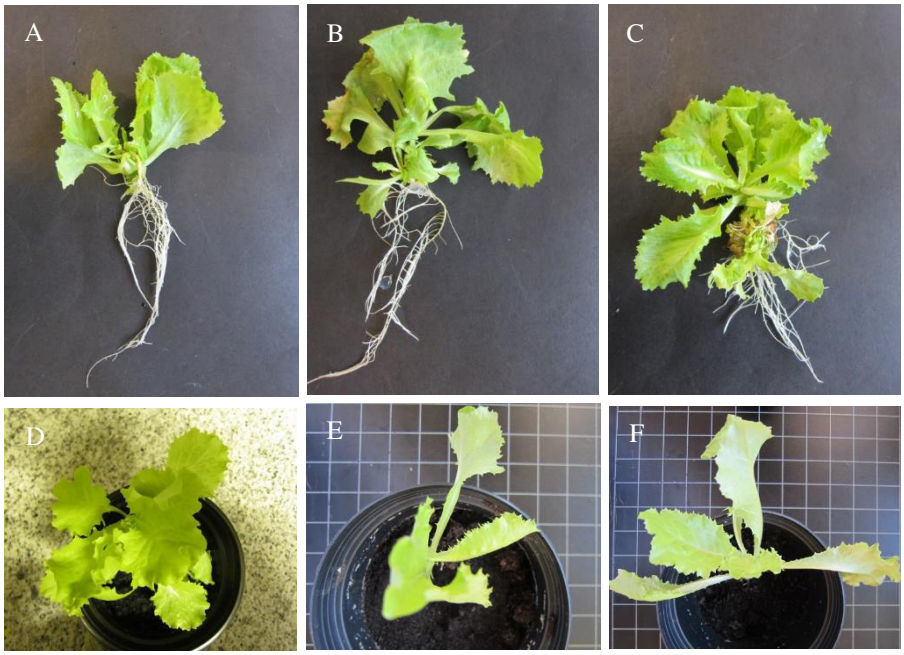


Fig. 3.3 Generation of *L. sativa* BL *Hyp-1* overexpression plants. (A, D) *L. sativa* BL control plant. (B, E) BL GFP-Hyp-1 plant. (C, F) BL Hyp-1 plant.



Fig. 3.4 Generation of *L. sativa* SBR *Hyp-1* overexpression plants. (A, C) *L. sativa* SBR control plant. (B, D) SBR Hyp-1 plant.

To study the contribution of the N-terminal part of Hyp-1 to the defense response against *A. tumefaciens*, we generated transgenic tobacco plants expressing the N-terminal 80 amino acids of Hyp-1 fused to GFP (GFP-Hyp-1-N plants). Three T2 progenies derived from each of two T1 lines, GFP-Hyp-1-N-2/-3, were inoculated with the *A. tumefaciens* strain harboring the GUS gene. Interestingly, T2 transgenic plants expressing GFP-Hyp-1-N showed an intense GUS staining comparable to that in WT control plants (Fig. 3.7 B vs 3.7 C-H). This suggests that the N-terminal region of Hyp-1 is not sufficient to function as a defense protein against *A. tumefaciens.*

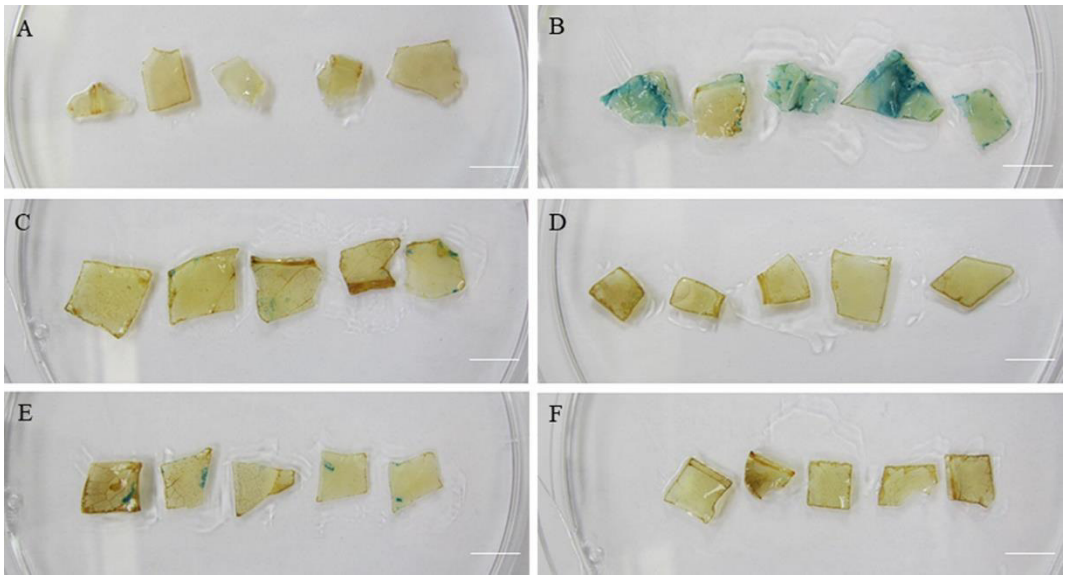


Fig. 3.5 Detection of *Agrobacterium*-mediated expression in Hyp-1 *L. sativa* BL T1 lines by GUS staining. (A) WT plant inoculated with *A. tumefaciens* EHA105 containing the empty vector as negative control. (B) WT plant inoculated with *A. tumefaciens* containing pCAMBIA 2301-GUS as positive control. (C, D) GFP-Hyp-1-1/-3 transgenic lines inoculated with *A. tumefaciens* containing GUS vector. (E, F) Hyp-1-6/-8 transgenic lines inoculated with *A. tumefaciens* containing GUS vector. Bars in each panel represent 10 mm.

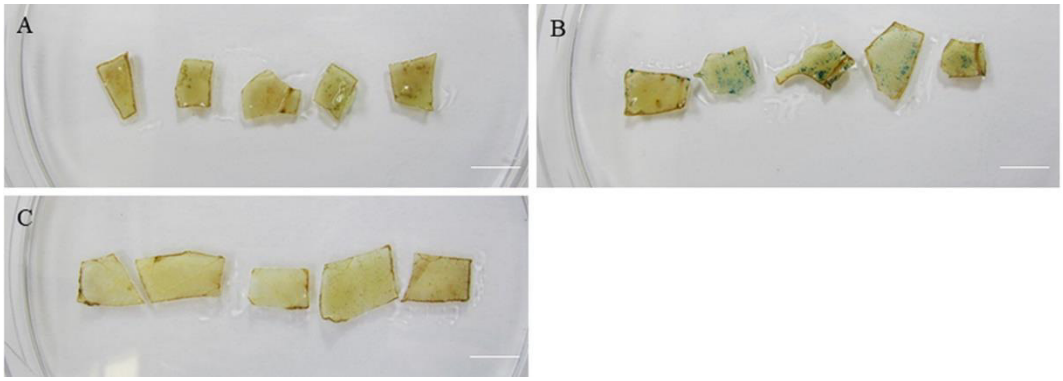


Fig. 3.6 Detection of *Agrobacterium*-mediated expression in Hyp-1 *L. sativa* SBR T1 lines by GUS staining. (A) WT plant inoculated with *A. tumefaciens* EHA105 containing the empty vector as negative control (B) WT plant inoculated with *A. tumefaciens* containing pCAMBIA 2301-GUS as positive control. (C) Hyp-1-12 transgenic line inoculated with *A. tumefaciens* containing GUS vector. Bars in each panel represent 10 mm.

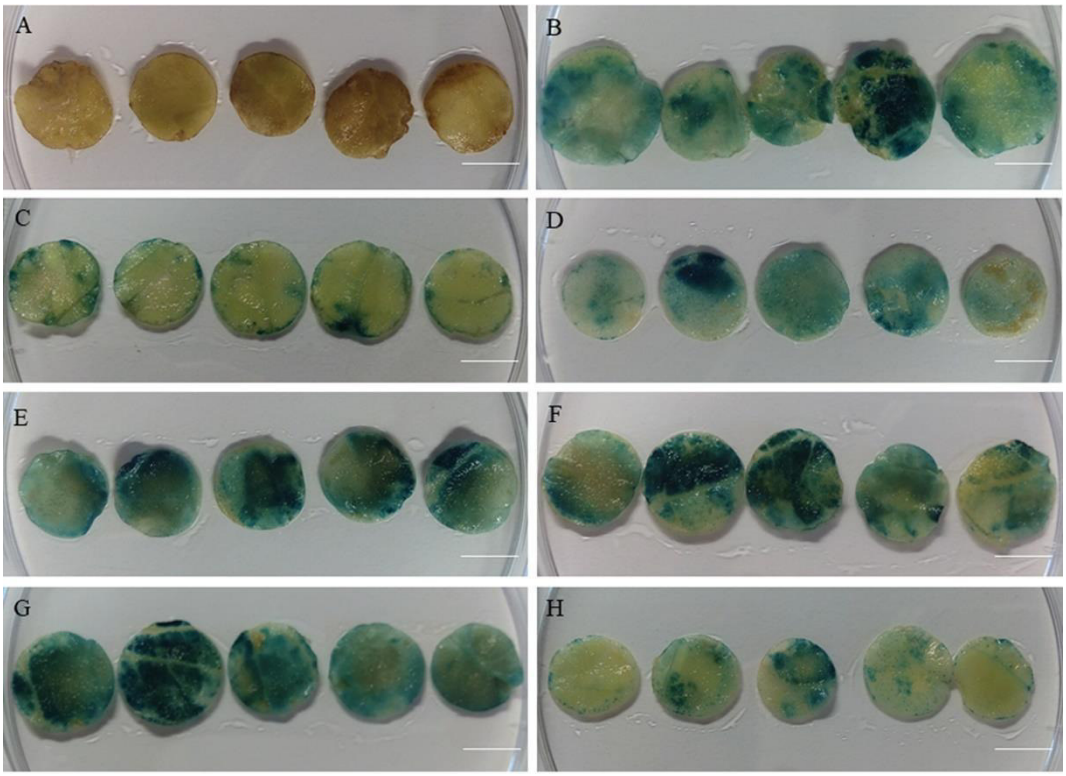


Fig. 3.7 Detection of *Agrobacterium*-mediated expression in GFP-Hyp-N tobacco T2 lines by GUS staining. (A) WT plant inoculated with *A. tumefaciens* containing the empty vector as negative control. (B) WT plant inoculated with *A. tumefaciens* containing pCAMBIA 2301-GUS as positive control. (C-E) GFP-Hyp-N-2 (1/-2/-3) transgenic lines inoculated with *A. tumefaciens* containing GUS vector. (F-H) GFP-Hyp-N-3 (1/-2/-3) transgenic lines inoculated with *A. tumefaciens* containing GUS vector. Bars in each panel represent 10 mm.

3.3.2 Subcellular localization studies

To examine the subcellular localization of Hyp-1, *Agrobacterium* strains carrying either GFP-Hyp-1 or the plasma membrane marker PM-RK were co-expressed transiently in leaf epidermal cells of WT *N. tabacum* by agroinfiltration. Two days after agroinfiltration, the fluorescence of

both proteins was observed by confocal fluorescence microscopy to compare their localization. The fluorescence of GFP-Hyp-1 coincided with that of PM-RK in the plasma membrane (Fig. 3.8). Besides, GFP-Hyp-1 was also detected in the nucleus, but not in nucleolus, and the cytoplasm of leaf epidermal cells of *N. tabacum*. The antibacterial defense activity of the Hyp-1 protein was retained with the N-terminal GFP fusion (Figs. 3.2,5,6), suggesting the biological relevance of the subcellular localization of GFP-Hyp-1.

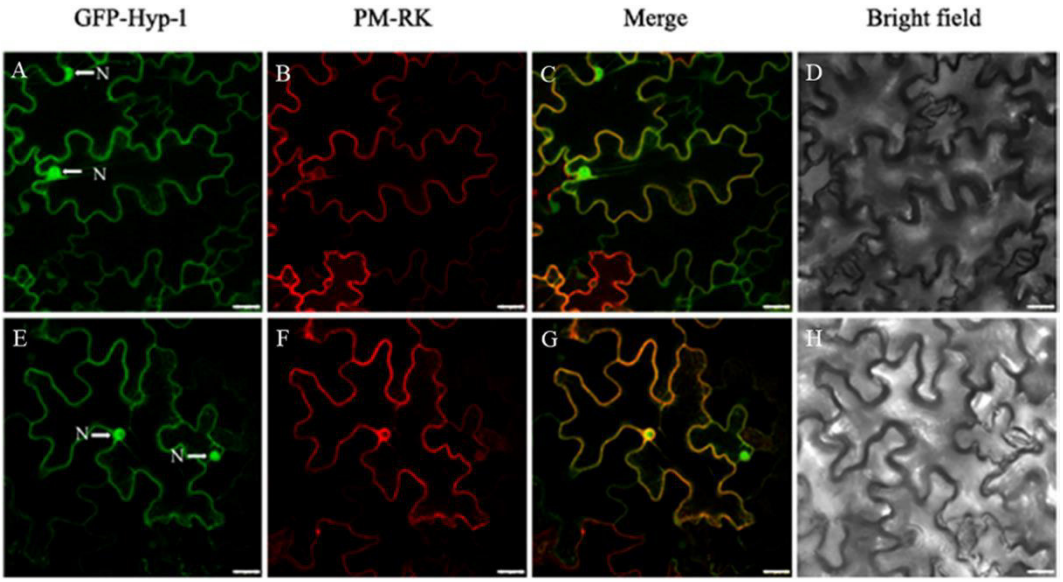


Fig. 3.8 Subcellular localization of GFP-Hyp-1 at the plasma membrane, nucleus and cytoplasm. Leaves of *N. tabacum* were co-infiltrated with GFP-Hyp-1 and plasma membrane marker PM-RK. Panels show either monochrome green (from GFP) (A and E) or red (from mCherry) (B and F) fluorescence, overlays for colocalization studies (C and G), or bright field (D and H). Arrows indicate nucleus (N). Scale bars all images are 25μm.

We next investigated the subcellular localization of GFP-Hyp-1 in the GFP-Hyp-1-4/-5 transgenic tobacco lines. Green fluorescence was localized in the cytoplasm and nucleus of GFP-Hyp-1 expressing plants (Fig. 3.9 B-D), similar to the localization of transiently-expressed free GFP (Fig. 3.9 A). The integrity of the GFP-Hyp-1 fusion in the GFP-Hyp-1 transgenic plants was confirmed by western blot using antibodies against GFP (Fig. 3.9 E).

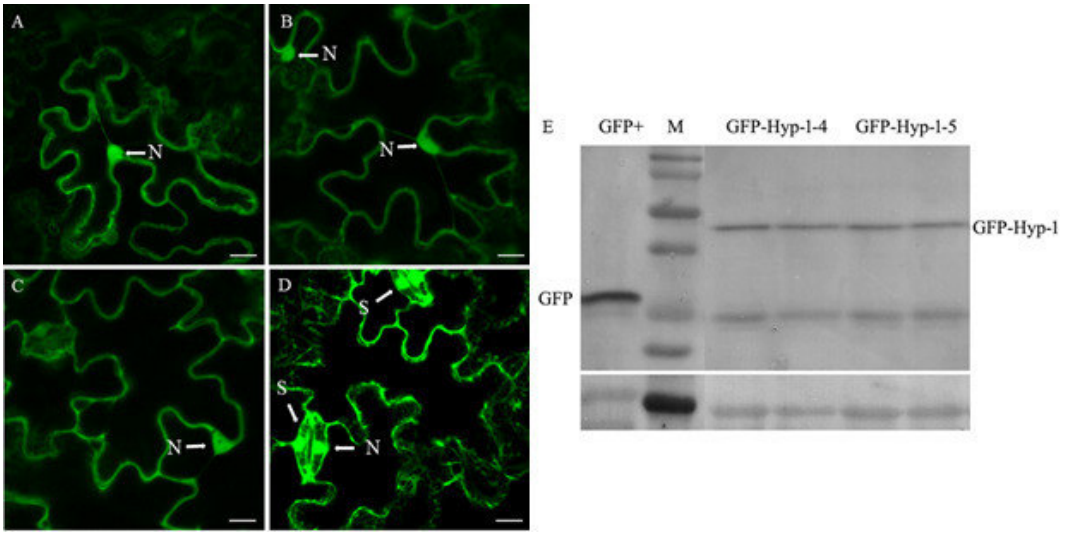


Fig. 3.9 Fluorescence microscopy and western blot analysis in GFP-Hyp-1 transgenic lines. (A) GFP transient expression in leaf epidermal cells of *N. benthamiana.* (B) Leaf epidermal cells of *N. tabacum* GFP-Hyp-1-4 transgenic line. (C-D) Leaf epidermal cells of *N. tabacum* GFP-Hyp-1-5 transgenic line. Contrary to the transient expression of free GFP, constitutive fluorescence in GFP-Hyp-1 transgenic plants were also detected in stomata guard cells (D). (E) Western blot to detect GFP-Hyp-1 expression by using antibodies against GFP. GFP+ was free GFP agroinfiltrated into *N. benthamiana* as positive control. Lane M shows the molecular weight markers in kilodalton (kDa). The panel below the western blot shows the membrane stained with Ponceau-S after blotting as control of loading. Arrows indicate nucleus (N) and stomata (S). Scale bars in all images are 25μm.

3.3.3 Overexpression of *Hyp-1* alters expression of multiple defense-related genes

To survey plant defense pathways involved in *Hyp-1*-mediated defense against *A. tumefaciens*, the expression levels of core genes implicated in different microbial defense pathways were determined in GFP-Hyp-1 transgenic tobacco plants by qRT-PCR. T2 GFP-Hyp-1-3, GFP-Hyp-1-4 and GFP-Hyp-1-5 transgenic lines were selected for subsequent experiments since they exhibited higher levels of *Hyp-1* mRNA than GFP-Hyp-1-2 (Fig. 3.10 A).

Phytohormones such as auxin and JA play an important role in plant defense against pathogenic microorganisms. We focused on the auxin-responsive genes *NtaTIR1* and *NtaAFR8*, and the JA biosynthesis gene *NtaLOX*. The transcript levels of *NtaTIR1* and *NtaARF8* were significantly

reduced in *Hyp-1* overexpression plants whereas *NtaLOX* did not show significant differences in two out of three transgenic lines tested, compared to WT control plants (Fig. 3.10 B-D).

PR proteins have been described as plant specific proteins that accumulate in response to pathogen interaction. To assess the involvement of PR proteins in *Hyp-1*-mediated antibacterial defense, the transcript levels of *NtaPR-10* and *NtaPR-1* were monitored by qRT-PCR (Fig. 3.10 E-F). Both *NtaPR-1* and *NtaPR-10* mRNAs were decreased in most of the GFP-Hyp-1 lines, especially *NtaPR-1*.

The microRNA-mediated gene silencing pathway is also involved in plant defense responses against pathogens. The key component in the miRNA pathway *NtaAGO1*, as well as NtamiR*160*, *NtamiR164ab* and *NtamiR164c* were analyzed by qRT-PCR in *Hyp-1* overexpressing plants (Fig. 3.10 G-J). Results indicate that *NtaAGO1* and *Nta164ab* were significantly reduced in all transgenic lines analyzed, whereas *NtamiR160* was reduced in GFP-Hyp-1-4 and GFP-Hyp-1-5 lines which displayed the higher expression level of Hyp-1 (Fig. 3.10 A). There were no significant differences in *NtamiR164c* expression between transgenic and control plants.

Production of secondary metabolites via the phenylpropanoid pathway serves in plants as a defense mechanism to protect themselves from pathogens. The lignin biosynthesis genes *NtaPAL1*, *NtaPAL4, NtaCCR* and *NtaCAD* were analyzed in *Hyp-1* overexpressing plants by qRT-PCR. Transcripts of *NtaPAL1,4* genes were downregulated in the *Hyp-1* transgenic lines, while the expression levels of *NtaCCR* and *NtaCAD* were not significantly different to those in control plants (Fig. 3.10 K-N). The transcripts of *NtaCHS,* a key enzyme which catalyzes the first committed step in the flavonoid biosynthesis pathway, was drastically reduced in *Hyp-1* overexpressing plants (Fig. 3.10 O).

Lastly, transcripts of core enzymes involved in ROS homeostasis, i.e., *NtaAPX*, *NtaCAT* and *NtaFe-SOD*, were also monitored in *Hyp-1* overexpressing plants by qRT-PCR. Results showed no significant differences in *NtaAPX* and *NtaCAT* expression between transgenic and control plants (Fig. 3.10 P, Q), whereas the levels of *NtaFe-SOD* mRNA were downregulated in two out of three transgenic plants compared to control plants (Fig. 3.10 R).

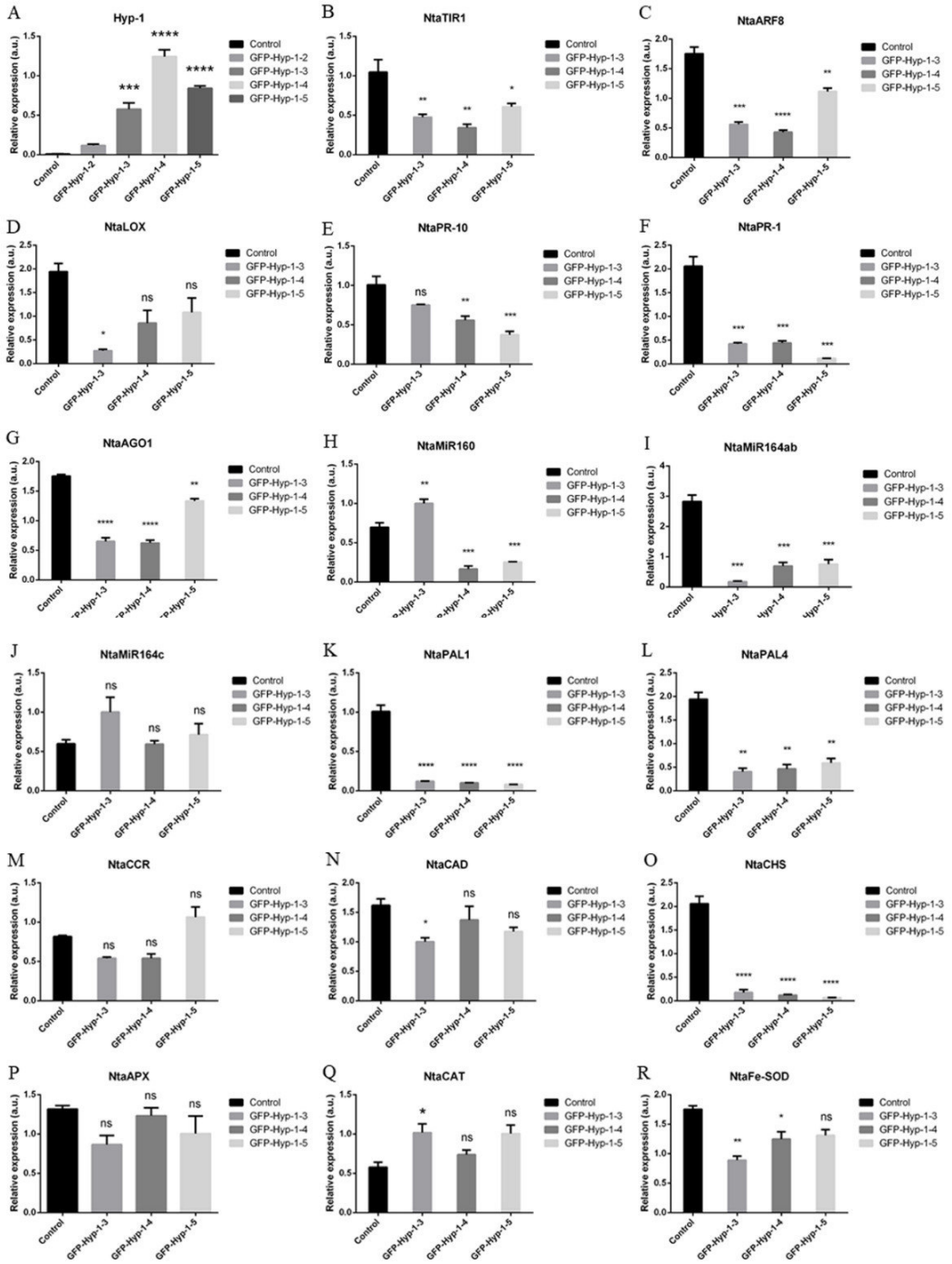


Fig. 3.10 Quantitative real time PCR to assess core genes involved in different plant defense pathways in GFP-Hyp-1 transgenic tobacco plants. (A) Relative transcript levels of *Hyp-1*. (B-C) Relative transcript levels of *TIR1* and *ARF8*. (D) Relative transcript levels of *LOX*. (E-F) Relative transcript levels of *PR-10* and *PR-1*. (G-J) Relative transcript levels of *AGO1*, MiR160, MiR164ab and MiR164c. (K-N) Relative transcript levels of *PAL1*, *PAL4*, *CCD* and *CAD*. (K, L- O) Relative transcript levels of *PAL1*, *PAL4*, and *CHS*. (P-R) Relative transcript levels of *APX*, *CAT*, and *Fe-SOD*. Asterisks denote the

significance levels compared with control: *, $P \leq 0.05$; **, $P \leq 0.01$; ***, $P \leq 0.001$; ****, $P \leq 0.0001$ and ns denotes not significant.

3.3.4 Virus-induced gene silencing in *C. roseus*

To investigate the loss-of function phenotype of *Hyp-1*, we used the VIGS technique to knock-down the expression of the *Hyp-1* homolog in *C. roseus.* We choose *C. roseus* because is a genetically non-tractable plant species that resembles the recalcitrance of *H. perforatum* L. to *Agrobacterium* infection (Di Fiore *et al*., 2004). The *Hyp-1* homolog in *C. roseus* is *Intracellular pathogenesis related protein* (*CrIPR*), as revealed by phylogenetic analysis of *Hyp-1*-related genes (Fig. 3.11). 3-4 weeks-old *C. roseus* plants were agroinfiltrated with a TRV-based VIGS vector carrying a 318-bp fragment of *CrIPR* (pTRV2: CrIPR) or the empty TRV vector (pTRV2:00) as a control. Silencing of the *Magnesium Chelatase subunit H* (*ChlH*) gene, which provides a visual bleached leaf phenotype, was also used to monitor VIGS in *C. roseus.* At 21 dpi, photobleaching occurred in the third and fourth pairs of leaves in all pTRV2: CrChlH treated plants, whereas there was no visible phenotype in control and pTRV2: CrIPR infected plants (Fig. 3.12 A). Silencing efficiency of *CrIPR* was examined by semiquantitative RT-PCR in upper leaves equivalent to those showing the bleached phenotype in pTRV2: CrChlH infected plants. Transcripts of *CrIPR* was reduced substantially in pTRV2: CrIPR infected plants compared to pTRV2:00 infected, control plants (Fig. 3.12 B).

In order to determine whether the knock-down of *CrIPR* influences the efficiency of *Agrobacterium*-mediated expression in *C. roseus*, *CrIPR*-silenced and control plants were inoculated in the third pairs of leaves with an *A. tumefaciens* strain expressing GFP at 21 dpi. GFP expression was monitored in duplicated samples at 3 and 5 dpi by western blot, using GFP agroinfiltrated into *N. benthamiana* as positive control (Fig. 3.12 C). Intriguingly, GFP accumulated at lower levels in *CrIPR*-silenced plants than in controls at both time points. Our result indicates that expression efficiency by *A. tumefaciens* is decreased in *CrIPR*-knocked-down plants.

It has been reported that silencing of PR-10-like proteins in *M. truncatula* led to induction of other PR proteins and increased tolerance to the oomycete *A. euteiches* (Colditz *et al.*, 2007).

Thus, the relative accumulation of another set of PR protein genes from *C. roseus*, *CrPR-1* and *CrPR-5*, were monitored in *CrIPR*-silenced and control plants by qRT-PCR. Interestingly, no significant difference in the expression of *CrPR-1* mRNA was found between *CrIPR*-knock-down and control plants, whereas a 40% increase of *CrPR-5* expression was measured in *CrIPR*-silenced plants compared with control plants (Fig. 3.12 D). These findings suggest that the enhanced tolerance to *A. tumefaciens* in *CrIPR*-silenced *C. roseus* was associated with the increase expression of *CrPR-5*.

3.3.5 Virus-induced gene silencing in *H. perforatum* L.

To knock-out the *Hyp-1* gene in *H. perforatum* L., VIGS was processed in *H. perforatum* L. also. Comparatively few information regarding the occurrence of viruses on *H. perforatum* L. is found in literature. H. Kegler *et al*. (1999) evidenced and characterized a hitherto unknown virus in *H. perforatum* L. However, there is no report that known plant virus infects *H. perforatum* L. successfully so far since the antiviral potential of this medicinal plant. So, the first step of this task is to identify the workable plant virus. Five plant viruses which could be utilized for VIGS were selected as the candidates, including TRV tagged with GFP (TRV-GFP), *Plum pox virus* tagged with GFP (PPV-GFP), *Potato virus X* tagged with GFP (PVX-GFP), *Turnip mosaic virus* tagged with GFP (TuMV-GFP) and *Cucumber mosaic virus* (CMV). The symptoms of *N. benthamiana* plants infected with viruses showed in Fig. 3.13.

The system leaves of infected plant were collected and utilized as the virus sources, to infect *H. perforatum* L. with two-three pairs of true leaves by pinch-wounding method, agroinfiltration and sap infection, respectively. After 10 days, the system leaves of *H. perforatum* L. were observed, fluorescent of GFP was checked under UV lap and collected to confirm the virus infection by using western blot to detect the expression of GFP of TRV, PPV, PVX, TuMV and CP of CMV expression. Unfortunately, there were no visible symptoms neither GFP expression observed in any of *H. perforatum* L groups. Western blot didn't detect any expression of GFP neither CP. Our results indicated that the five plant viruses TRV, PPV, PVX, TuMV and CMV are not able to infect *H. perforatum* L.

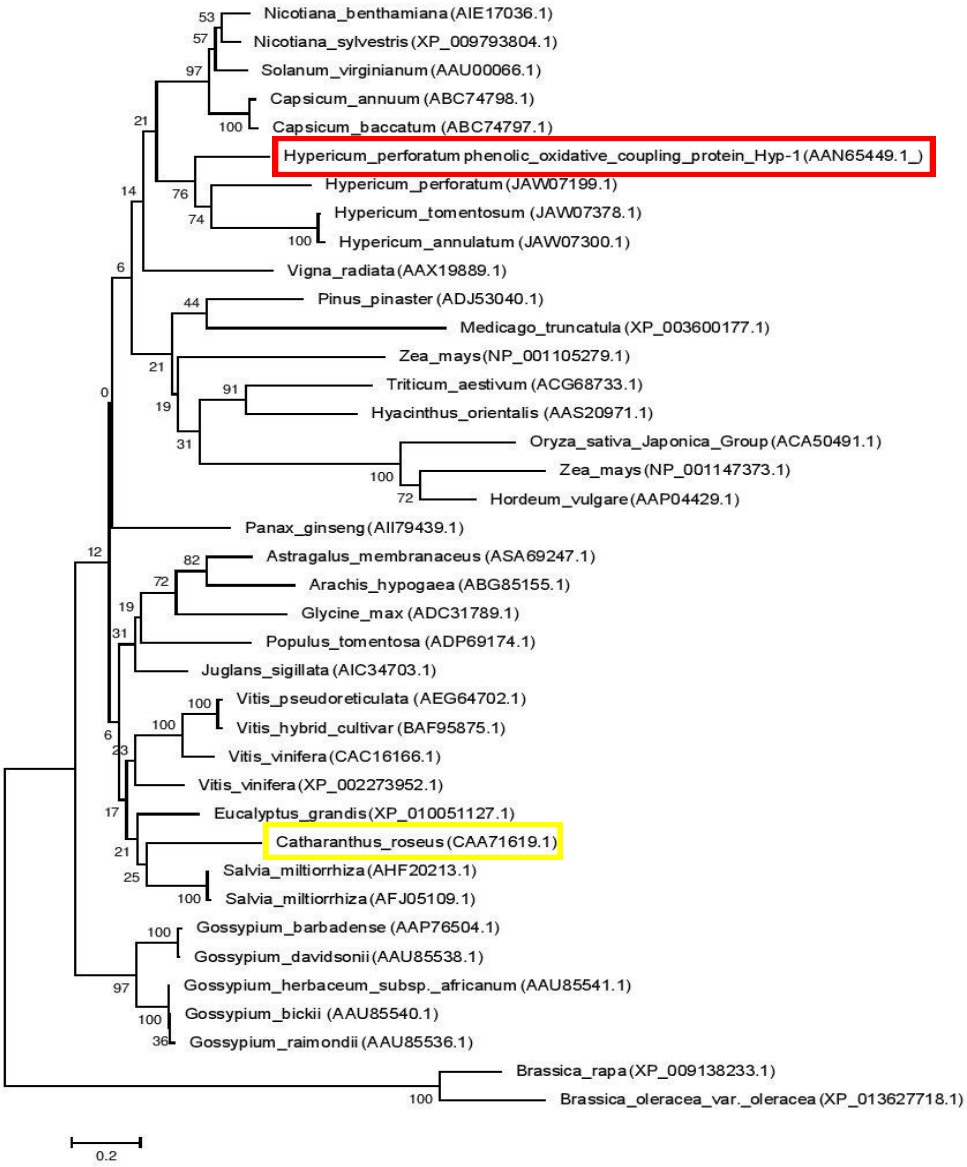


Fig. 3.11 Phylogenetic relationships of Hyp-1 homologs in plants, constructed using the program MEGA 6. The amino acid sequences were obtained from GenBank. Plant Latin names and GenBank accession numbers were used to marker the phylogenetic tree. *Hyp-1* was framed in red box and the VIGS candidate from *C. roseus* was framed in yellow box. The scale was shown in units of number of amino acid substitutions per site.

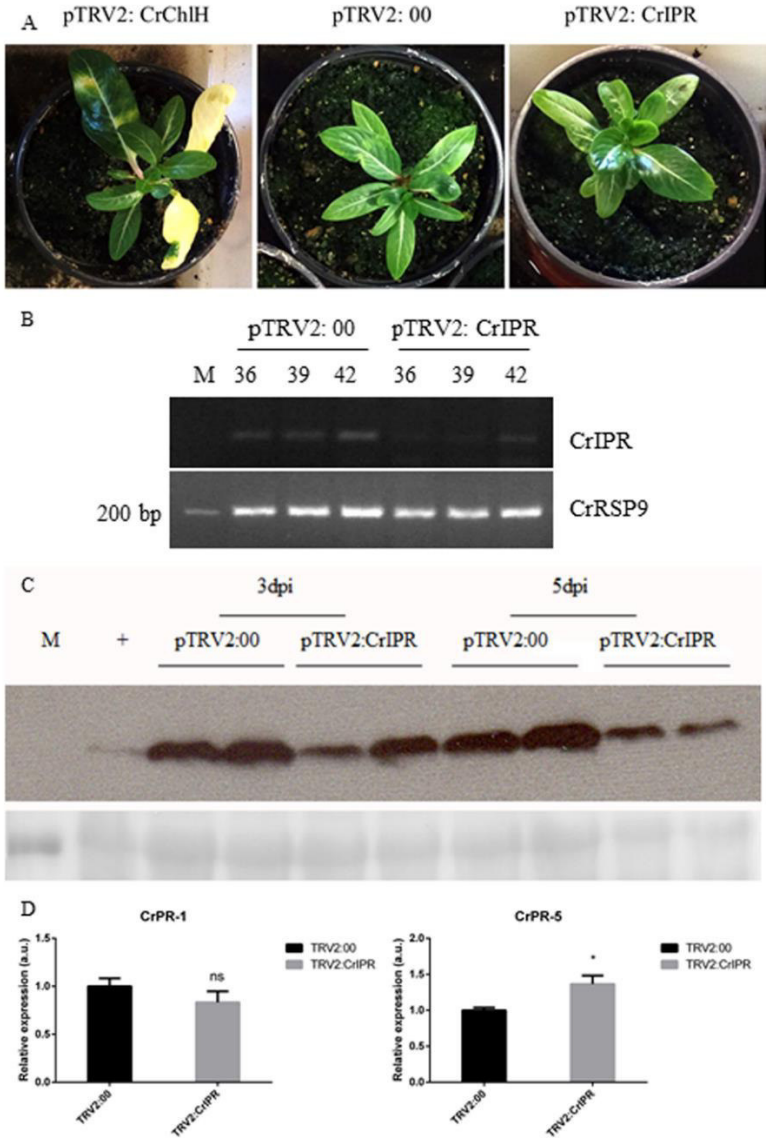


Fig. 3.12 Silencing of *CrIPR* in *C. roseus* results in enhanced tolerance to *A. tumefaciens*. (A) Representative *C. roseus* plants inoculated with *Agrobacterium* strains containing pTRV2: CrChlH, pTRV2:00 and pTRV2: CrIPR at 21 days after inoculation (dpi). (B) Silencing of *CrIPR* transcripts was analyzed by semiquantitative RT-PCR at 21 dpi. The same RT reactions were used to amplify *CrRPS9* gene transcripts as a control. (C) Western blot analysis of GFP accumulation in *CrIPR*-silenced and control *C. roseus* leaves at 3 and 5 days after infiltration with an *Agrobacterium* strain expressing GFP. The panel below the western blot shows the membrane stained with Ponceau-S after blotting as control of loading. +, sample from *N. benthamiana* leaf agroinfiltrated with GFP as positive control. Lane M, molecular weight markers. (D) Expression analysis of *CrPR-1* and *CrPR-5* in *CrIPR*-silenced and control *C. roseus* leaves at 21 dpi. *CrRPS9* was used as reference gene. *, $P \leq 0.05$; ns, not significant.

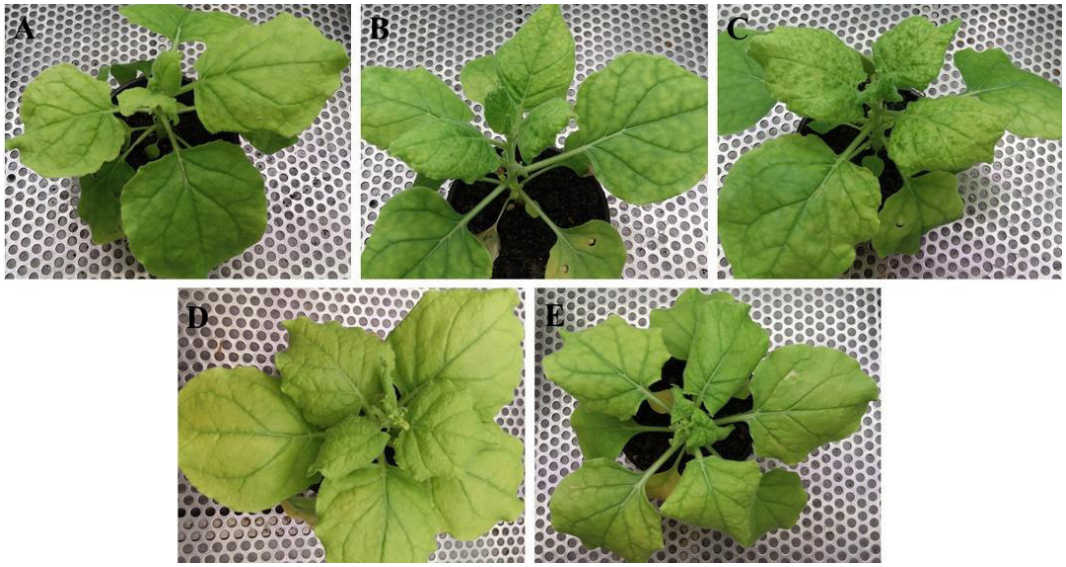


Fig. 3.13 Symptoms of *N. benthamiana* plants infected with viruses. (A) TRV-GFP. (B) PPV-GFP. (C) PVX-GFP. (D) TuMV-GFP. (E) CMV.

3.4 Discussion

Hyp-1 was selected from a forward subtracted cDNA library of *H. perforatum* L. suspension cells, treated with *A. tumefaciens.* The function of *Hyp-1* as a member of the PR-10 gene family has been barely studied (Košuth *et al.*, 2013). *Hyp-1* overexpression was carried out in tobacco as well as in two varieties of lettuce to unveil its participation in defense against *A. tumefaciens*. Expression efficiencies of disarmed *A. tumefaciens* greatly decreased in all transgenic plants as assayed by GUS staining, indicating that *Hyp-1* participates in defense responses against *A. tumefaciens*. In addition, transgenic tobacco plants expressing a C-terminal truncated version of the protein were used to study the contribution of the first 80 aa to the antibacterial activity of Hyp-1. Defense activities towards *A. tumefaciens* were highly reduced in GFP-Hyp-1-N transgenic plants, suggesting that the N terminal part of Hyp-1 is not enough to contribute to the biological function of the Hyp-1 protein. The importance of maintaining Hyp-1 protein integrity could be interpreted in the light of studies on the crystal structure of Hyp-1 (Michalska *et al.*, 2010). The Hyp-1 molecule exhibits a typical PR-10-like protein structure, whose fold consists of seven-stranded antiparallel β-sheet wrapped around the C-terminal helix α3. Together with another two α-helixes, those main structural elements form a huge cavity within the protein interior to bound various hydrophobic ligands, like plant hormone cytokinin.

Besides, the characteristic of Bet.v.1 domain is positioned at 89-120 aa residues in Hyp-1 (Bais *et al.*, 2003). Therefore, several of those structural motifs are lacking in the Hyp-1mutant, which results in the loss of biological activity.

Hyp-1 protein was localized at the plasma membrane, nucleus and cytoplasm, as judged by the subcellular distribution of fluorescence derived from the transient expression of GFP-Hyp-1 in *N. tabacum* leaves. Moreover, confirmation of the integrity of the full-length fusion protein in GFP-Hyp-1 transgenic plants by Western blot confirmed that the nuclear visualization of GFP fluorescence was due to Hyp-1 accumulation in nucleus rather than the import of free GFP cleaved from the fusion protein. This study demonstrates for the first time the subcellular localization of Hyp-1 in nucleus, as had been reported for the PR-10 proteins from *Tamarix hispida* and *Vitis vinifera* (Zhang *et al.*, 2010; He *et al.*, 2013). The nuclear localization of Hyp-1 might play an important role in defense responses against invading pathogens, especially in pathogens like *A. tumefaciens*, whose virulence depends on integration of T-DNA into the nucleus.

To further corroborate the role of *Hyp-1* in defense responses against *A. tumefaciens*, *we used* a TRV-based *VIGS* approach to study the loss-of-*function* phenotype of the *Hyp-1* homologous *CrIPR* in the recalcitrant plant *C. roseus*. Contrary to what could be expected, *CrIPR*-silenced plants showed increased resistance to *A. tumefaciens*, which correlated with the up-regulation of *CrPR-5* but not *CrPR-1*. It was reported that *M. truncatula* transgenic lines silenced for *PR-10* showed a reduced colonization of the oomycete *A. euteiches,* and a suppressed infection in the roots of transgenic plants (Colditz *et al.*, 2007). Interestingly, *MtPr-10* silencing led to the *de novo* induction of two isoforms of Thaumatin-like proteins (PR-5b). Thus, antagonistic induction of PR-5 proteins, which are normally repressed due to PR-10 expression, is not an unprecedented phenomenon in plant-microbe interactions. A similar antagonistic crosstalk was observed in our *Hyp-1* overexpressing tobacco lines, where overexpression of *PR-10* from *H. perforatum* L. led to reduced expression of endogenous PR genes, *PR-1* and *PR-10*. These findings illustrate the complex crosstalk regulating plant-pathogen interactions. Moreover, the trial of VIGS in *H. perforatum* L. clearly indicated that TRV, PPV, PVX, TuMV and CMV are not able to infect *H. perforatum* L.

A. tumefaciens as a microbial pathogen provokes a series of plant defense responses, but understanding how these responses affect pathogen infection is still unclear (Pitzschke, 2013). To survey which plant defense responses could be involved in *Hyp-1*-mediated defense against

A. tumefaciens, the expression levels of core genes from different pathways including auxin metabolism, microRNA-mediated gene silencing, lignin deposition, secondary metabolites, ROS signaling, and pathogenesis-related proteins, were determined in GFP-Hyp-1 tobacco plants. Auxin as a phytohormone is a critical contributor in plant-pathogen interaction (Fu and Wang, 2011). In the present study, transcripts of auxin-responsive genes *NtaTIR1* and *NtaAFR8* were remarkably reduced when *Hyp-1* was overexpressed, which suggests that *Hyp-1* overexpression could contribute to antibacterial defenses by reducing auxin signaling. Besides, overexpression of *Hyp-1* in transgenic plants led to a decrease in the transcriptional levels of *NtaAGO1* and two microRNAs, *NtamiR160* and *NtamiR164ab*. In *A. thaliana*, miR164 has been reported to target the transcripts of NAM/ATAF/CUC (NAC) domain protein *NAC1*, which acts downstream of *TIR1* to transmit auxin signals for lateral root emergence (Guo *et al.*, 2005). A recent report suggested that miR164 and target gene *NAC4* regulate cell death during plant-pathogen interactions, possibly by repressing GDSL lipase 1 which is an important regulator of plant immune responses (Lee *et al.*, 2017). MiR164 is also involved in plant response to abiotic stresses in *Brassica*, rice and potato (Bhardwaj *et al.*, 2014; Fang *et al.*, 2014; Zhang *et al.*, 2018). MiR160 targets *ARF10*, *ARF16* and *ARF17* to down regulate auxin signaling, which in turn protect plants against bacteria and fungi (Pinweha *et al.*, 2015; Wójcik *et al.*, 2017). Our results offer preliminary evidence for the involvement of those two microRNAs in the regulation of plant defense against *A. tumefaciens* that need to be further investigated.

Several key genes involved in the lignin and flavonoids biosynthesis pathways, *NtaPAL1,4, NtaCCR*, *NtaCAD* and *NtaCHS,* were monitored in *Hyp-1* overexpressing plants. PAL is the first enzyme of phenylpropanoid pathway, which comprises the synthesis of lignin and flavonoids (Heldt and Piechulla, 2011; Bagal *et al.*, 2012). Lignin, as a critical constituent of cell wall, plays a major role in structural defense against pathogens. Flavonoids are small molecular secondary metabolites acting as antimicrobial compounds in defense against pathogens (Mazid *et al*., 2011; Andersson, 2012; Goyal *et al*., 2012). Our findings showed that *Hyp-1* overexpression in transgenic plants downregulated the expression of genes involved in the phenylpropanoid pathway (*NtaPAL1,4* and *NtaCHS*), whereas *NtaCCR* and *NtaCAD* were not changed, suggesting that overexpressing of *Hyp-1* increased the tolerance to *A. tumefaciens* independently from synthesis of lignin and flavonoids. Similarly, ROS signaling did not seem to play a significant role in *Hyp-1*-mediated defense against *A. tumefaciens* since the transcript

levels of core enzymes were unaltered (*NtaAPX*, *NtaCAT)* or repressed (*NtaFe-SOD)* in *Hyp-1* overexpressing plants. Nevertheless, although *Hyp-1* overexpression could induce wide changes in the *gene expression* pattern of defense genes, not all of these changes are necessarily involved in the molecular mechanisms underlying *Hyp-1*-mediated antibacterial defense.

Several PR-10 proteins have shown *in vitro* and *in vivo* to have DNase and RNase activities, which could help to explain the role of *Hyp-1* in antibacterial defense (Chen *et al.*, 2006; Kim *et al.*, 2008; Xie *et al.*, 2010; Kim *et al.*, 2011; Krishnaswamy *et al.*, 2011; He *et al.*, 2013). Chadha and Das (2006) reported that an RNase activity-competent version of PR-10 from peanut was internalized by hyphae of *Fusarium oxysporum* and inhibited fungal growth. Moreover, DNA fragmentation was detected in rice suspension-cultured cells treated with PBZ1, a rice PR-10 family protein (Kim *et al.*, 2011). Therefore, the putative DNase and RNase activities of *Hyp-1* might also play an important role in the death of *A. tumefaciens* cells observed upon co-cultivation with *H. perforatum* L. (Franklin *et al.*, 2008). In addition, our subcellular localization data suggest that Hyp-1 localized to the plasma membrane. The plasma membrane is important during plant-microbe interactions, because it acts as a barrier between the host and the pathogen and many pathogen-associated molecular pattern recognition receptors are localized at the plasma membrane (Boller and Felix, 2009). Other PR proteins with associated RNase activities have been localized in the cell plasma membrane (Jiang *et al.*, 2015).

Future research on the characterization of RNase and DNase activities of Hyp-1 might shed light on its protective role in degrading DNA or RNA of invading pathogens in *H. perforatum* L. *Agrobacterium*-mediated genetic transformation approaches that reduce *Hyp-1* expression in *H. perforatum* L. could give a better chance at efforts aimed at the genetic manipulation of this recalcitrant and medicinal plant spp. However, antagonistic regulation of PR proteins and that of other inducible defense-related proteins that result in enhanced resistance to *A. tumefaciens* should be taken into consideration. In summary, the present study provides a better understanding regarding the functional characterization of *Hyp-1* gene from *H. perforatum* L., and adds significant knowledge about the molecular mechanism of the *H. perforatum* L.-*A. tumefaciens* interaction.

3.5 Acknowledgements

The author acknowledges the financial support provided by the FCT-Portuguese Foundation for Science and Technology (SFRH/BD/52561/2014), under the Doctoral Programme "Agricultural Production Chains – from fork to farm" (PD/00122/2012) and the *Ministry of Economy and Competitiveness* of Spain (grant BIO2016-75619-R [AEI/FEDER, UE]) to T.C. and F.T.

We gratefully acknowledge the advice of Prof. Vincent L. Chiang and Dr. Rui Shi (North Carolina State University) for the MicroRNA detection. We gratefully thank Prof. Mariana Sottomayor and Dr Joana Guedes (University of Porto) for kindly providing pTRV2: CrChlh and advice.

3.6 References

Allmann, S., Halitschke, R., Schuurink, R.C. and Baldwin, I.T. (2010) Oxylipin channelling in Nicotiana attenuata: Lipoxygenase 2 supplies substrates for green leaf volatile production. *Plant, Cell Environ.* **33**, 2028–2040.

Anand, A., Uppalapati, S.R., Ryu, C.-M., Allen, S.N., Kang, L., Tang, Y. and Mysore, K.S. (2007) Salicylic acid and systemic acquired resistance play a role in attenuating crown gall disease caused by Agrobacterium tumefaciens. *Plant Physiol.* **146**, 703–715.

Andersson, P. (2012) Secondary metabolites associated with plant disease, plant defense and biocontrol.

Bagal, U.R., Leebens-Mack, J.H., Lorenz, W.W. and Dean, J.F.D. (2012) The phenylalanine ammonia lyase (PAL) gene family shows a gymnosperm-specific lineage. *BMC Genomics* **13**, S1.

Bais, H.P., Vepachedu, R., Lawrence, C.B., Stermitz, F.R. and Vivanco, J.M. (2003) Molecular and biochemical characterization of an enzyme responsible for the formation of hypericin in St. John's wort (Hypericum perforatum L.). *J. Biol. Chem.* **278**, 32413–32422.

Bhardwaj, A.R., Joshi, G., Pandey, R., Kukreja, B., Goel, S., Jagannath, A., Kumar, A., Katiyar-Agarwal, S. and Agarwal, M. (2014) A genome-wide perspective of miRNAome in response to high temperature, salinity and drought stresses in Brassica juncea (Czern) L. *PLoS One* **9**.

Boller, T. and Felix, G. (2009) A renaissance of elicitors: perception of microbe-associated molecular patterns and danger signals by pattern-recognition receptors. *Annu. Rev. Plant Biol.* **60**, 379–406.

Breen, S., Williams, S.J., Outram, M., Kobe, B. and Solomon, P.S. (2017) Emerging insights into the functions of pathogenesis-related protein 1. *Trends Biotechnol.* **xx**, 1–9.

Butterweck, V., Christoffel, V., Nahrstedt, A., Petereit, F., Spengler, B. and Winterhoff, H. (2003) Step by step removal of hyperforin and hypericin: Activity profile of different Hypericum preparations in behavioral models. *Life Sci.* **73**, 627–639.

Chadha, P. and Das, R.H. (2006) A pathogenesis related protein, AhPR10 from peanut: An insight of its mode of antifungal activity. *Planta* **225**, 213–222.

Chen, Z.Y., Brown, R.L., Rajasekaran, K., Damann, K.E. and Cleveland, T.E. (2006) Identification of a maize kernel pathogenesis-related protein and evidence for its involvement in resistance to Aspergillus flavus infection and aflatoxin production. *Phytopathology* **96**, 87–95.

Colditz, F., Braun, H.P., Jacquet, C., Niehaus, K. and Krajinski, F. (2005) Proteomic profiling unravels insights into the molecular background underlying increased Aphanomyces euteiches-tolerance of Medicago truncatula. *Plant Mol. Biol.* **59**, 387–406.

Colditz, F., Niehaus, K. and Krajinski, F. (2007) Silencing of PR-10-like proteins in Medicago truncatula results in an antagonistic induction of other PR proteins and in an increased tolerance upon infection with the oomycete Aphanomyces euteiches. *Planta* **226**, 57–71.

Duan, C.G., Fang, Y.Y., Zhou, B.J., Zhao, J.H., Hou, W.N., Zhu, H., Ding, S.W. and Guo, H.S. (2012) Suppression of Arabidopsis ARGONAUTE1-mediated slicing, transgene-induced RNA silencing, and DNA methylation by distinct domains of the Cucumber mosaic virus 2b Protein. *Plant Cell* **24**, 259–274.

Dunoyer, P., Himber, C. and Voinnet, O. (2006) Induction, suppression and requirement of RNA silencing pathways in virulent Agrobacterium tumefaciens infections. *Nat. Genet.* **38**, 258–263.

El-kereamy, A., El-sharkawy, I., Ramamoorthy, R., Taheri, A., Errampalli, D., Kumar, P. and Jayasankar, S. (2011) Prunus domestica pathogenesis-related protein-5 activates the defense response pathway and enhances the resistance to fungal infection. *PLoS One* **6**, 1–11.

Fang, Y., Xie, K. and Xiong, L. (2014) Conserved miR164-targeted NAC genes negatively regulate drought resistance in rice. *J. Exp. Bot.* **65**, 2119–2135.

Fernandes, H., Konieczna, M., Kolodziejczyk, R., Bujacz, G., Sikorski, M. and Jaskolski, M. (2008) Crystallization and preliminary crystallographic studies of Hyp-1, a St John's wort protein implicated in the biosynthesis of hypericin. *Acta Crystallogr. Sect. F Struct. Biol. Cryst. Commun.* **64**, 405–408.

Fernandes, H., Michalska, K., Sikorski, M. and Jaskolski, M. (2013) Structural and functional aspects of PR-10 proteins. *FEBS J.* **280**, 1169–1199.

Fiore, S. Di, Hoppmann, V., Fischer, R. and Schillberg, S. (2004) Transient gene expression of recombinant terpenoid indole alkaloid enzymes in Catharanthus roseus leaves. *Plant Mol. Biol. Report.* **22**, 15–22.

Franklin, G., Conceição, L.F.R., Kombrink, E. and Dias, A.C.P. (2008) Hypericum perforatum plant cells reduce Agrobacterium viability during co-cultivation. *Planta* **227**, 1401–1408.

Franklin, G., Conceição, L.F.R., Kombrink, E. and Dias, A.C.P. (2009) Xanthone biosynthesis in Hypericum perforatum cells provides antioxidant and antimicrobial protection upon biotic stress. *Phytochemistry* **70**, 60–68.

Fu, J. and Wang, S. (2011) Insights into auxin signaling in plant-pathogen interactions. *Front. Plant Sci.* **2**, 1–7.

Gohlke, J. and Deeken, R. (2014) Plant responses to Agrobacterium tumefaciens and crown gall development. *Front. Plant Sci.* **5**, 1–11.

Gómez-Gómez, L., Rubio-Moraga, A. and Ahrazem, O. (2011) Molecular cloning and characterisation of a pathogenesis-related protein CsPR10 from Crocus sativus. *Plant Biol.* **13**, 297–303.

Goyal, S., Merillon, J. and Ramawat, K.G. (2012) Plant Defence: Biological Control.

Guo, H., Xie, Q., Fei, J. and Chua, N. (2005) microRNA164 Directs NAC1 mRNA Cleavage to Downregulate Auxin Signals for Lateral Root Development. *Plant Cell*, 1–12.

He, M., Xu, Y., Cao, J., Zhu Z, Jiao Y, Wang Y, Guan X, Yang Y, Xu W and Fu Z. (2013) Subcellular localization and functional analyses of a PR10 protein gene from Vitis pseudoreticulata in response to Plasmopara viticola infection. *Protoplasma* **250**, 129–140.

Heldt, H.-W. and Piechulla, B. (2011) Phenylpropanoids comprise a multitude of plant secondary metabolites and cell wall components. *Plant Biochem.*, 431–449.

Hou, W., Shakya, P. and Franklin, G. (2016) A perspective on Hypericum perforatum genetic transformation. *Front. Plant Sci.* **7**, 1–12.

Hsu, S.W., Liu, M.C., Zen, K.C. and Wang, C.S. (2014) Identification of the tapetum/microspore-specific promoter of the pathogenesis-related 10 gene and its regulation in the anther of Lilium longiflorum. *Plant Sci.* **215**–**216**, 124–133.

Huang, F.C. and Schwab, W. (2011) Cloning and characterization of a 9-lipoxygenase gene induced by pathogen attack from Nicotiana benthamiana for biotechnological application. *BMC Biotechnol.* **11**, 30.

Janda, M. and Ruelland, E. (2015) Magical mystery tour: Salicylic acid signalling. *Environ. Exp. Bot.* **114**, 117–128.

Jiang, L., Wu, J., Fan, S., Li, W., Dong, L., Cheng, Q., Xu, P. and Zhang, S. (2015) Isolation and characterization of a novel pathogenesis-related protein gene (GmPRP) with induced expression in soybean (*Glycine max*) during infection with *Phytophthora sojae*. *PLoS One* **10**, e0129932.

Jwa, N.S., Kumar Agrawal, G., Rakwal, R., Park, C.H. and Prasad Agrawal, V. (2001) Molecular cloning and characterization of a novel jasmonate inducible pathogenesis-related class 10 protein gene, JIOsPR10, from rice (Oryza sativa L.) seedling leaves.

Biochem. Biophys. Res. Commun. **286**, 973–983.

Karppinen, K. (2010) Biosynthesis of hypericins and hyperforins in Hypericum perforatum L.(St. John's wort)—precursors and genes involved.

Karppinen, K., Derzsó, E., Jaakola, L. and Hohtola, A. (2016) Molecular cloning and expression analysis of hyp-1 type PR-10 family genes in Hypericum perforatum. *Front. Plant Sci.* **7**, 526.

Kegler, H., Fuchs, E., Plescher, A., Ehrig, F., Schliephake, E. and Grüntzig, M. (1999) Evidence and characterization of a virus of St John's Wort *(Hypericum perfora tum* L.). *Arch. Phytopathol. Plant Prot.* **32**, 205–221.

Kim, S.G., Kim, S.T., Wang, Y.M., Yu, S., Choi, S.I., Kim, Y.C., Kim,W.T., Agrawal,G.K., Rakwal, R., and Kang, K.Y,. (2011) The RNase activity of rice probenazole-induced protein1 (PBZ1) Plays a key role in cell death in plants. *Mol. Cells* **31**, 25–31.

Kim, S.T., Yu, S., Kang, Y.H., Kim, S.G., Kim, J.Y., Kim, S.H. and Kang, K.Y. (2008) The rice pathogen-related protein 10 (JIOsPR10) is induced by abiotic and biotic stresses and exhibits ribonuclease activity. *Plant Cell Rep.* **27**, 593–603.

Kondou, Y., Higuchi, M. and Matsui, M. (2010) High-throughput characterization of plant gene functions by using gain-of-function technology. *Annu. Rev. Plant Biol.* **61**, 373–393.

Košuth, J., Hrehorová, D., Jaskolski, M. and Čellárová, E. (2013) Stress-induced expression and structure of the putative gene hyp-1 for hypericin biosynthesis. *Plant Cell. Tissue Organ Cult.* **114**, 207–216.

Košuth, J., Katkovčinová, Z., Olexová, P. and Čellárová, E. (2007) Expression of the hyp-1 gene in early stages of development of Hypericum perforatum L. *Plant Cell Rep.* **26**, 211–217.

Košuth, J., Smelcerovic, A., Borsch, T., Zuehlke, S., Karppinen, K., Spiteller, M., Hohtola, A. and Čellárová, E. (2011) The hyp-1 gene is not a limiting factor for hypericin biosynthesis in the genus Hypericum. *Funct. Plant Biol.* **38**, 35–43.

Krishnaswamy, S., Baral, P.K., James, M.N.G. and Kav, N.N.V. (2011) Site-directed mutagenesis of histidine 69 and glutamic acid 148 alters the ribonuclease activity of pea

ABR17 (PR10.4). *Plant Physiol. Biochem.* **49**, 958–962.

Kumar, D. (2014) Salicylic acid signaling in disease resistance. *Plant Sci.* **228**, 127–134.

Lee, C.W., Efetova, M., Engelmann, J.C., Kramell, R., Wasternack, C., Ludwig-Muller, J., Hedrich, R. and Deeken, R. (2009) Agrobacterium tumefaciens promotes tumor induction by modulating pathogen defense in Arabidopsis thaliana. *Plant Cell Online* **21**, 2948–2962.

Lee, M.H., Jeon, H.S., Kim, H.G. and Park, O.K. (2017) An Arabidopsis NAC transcription factor NAC4 promotes pathogen-induced cell death under negative regulation by microRNA164. *New Phytol.* **214**, 343–360.

Liscombe, D.K. and O'Connor, S.E. (2011) A virus-induced gene silencing approach to understanding alkaloid metabolism in Catharanthus roseus. *Phytochemistry* **72**, 1969–1977.

Liu, J., Li, H., Miao, M., Tang, X., Giovannoni, J., Xiao, F. and Liu, Y. (2012) The tomato UV-damaged DNA-binding protein-1 (DDB1) is implicated in pathogenesis-related (PR) gene expression and resistance to Agrobacterium tumefaciens. *Mol. Plant Pathol.* **13**, 123–134.

Loon, L.C. van and Kammen, A. van (1968) Polyacrylamide disc electrophoresis of the soluble leaf proteins from Nicotiana tabacumvar. "Samsun" and "Samsun NN"-I. *Phytochemistry* **7**, 1727–1735.

Maschietto, V., Lanubile, A., Leonardis, S. De, Marocco, A. and Paciolla, C. (2016) Constitutive expression of pathogenesis-related proteins and antioxydant enzyme activities triggers maize resistance towards Fusarium verticillioides. *J. Plant Physiol.* **200**, 53–61.

Mazid, M., Khan, T.A. and Mohammad, F. (2011) Role of secondary metabolites in defense mechanisms of plants. *Biol. Med.* **3**, 232–249.

Meng, C., Zhang, S., Deng, Y.S., Wang, G.D. and Kong, F.Y. (2015) Overexpression of a tomato flavanone 3-hydroxylase-like protein gene improves chilling tolerance in tobacco. *Plant Physiol. Biochem.* **96**, 388–400.

Michalska, K., Fernandes, H., Sikorski, M. and Jaskolski, M. (2010) Crystal structure of Hyp-1, a St. John's wort protein implicated in the biosynthesis of hypericin. *J. Struct. Biol.* **169**, 161–171.

Miedes, E., Vanholme, R., Boerjan, W. and Molina, A. (2014) The role of the secondary cell wall in plant resistance to pathogens. *Front. Plant Sci.* **5**, 1–13.

Molinari, S., Fanelli, E. and Leonetti, P. (2014) Expression of tomato salicylic acid (SA)-responsive pathogenesis-related genes in Mi-1-mediated and SA-induced resistance to root-knot nematodes. *Mol. Plant Pathol.* **15**, 255–264.

Nazari, F., Safaie, N., Soltani, B.M., Shams-Bakhsh, M. and Sharifi, M. (2017) Bacillus subtilis affects miRNAs and flavanoids production in Agrobacterium-Tobacco interaction. *Plant Physiol. Biochem.* **118**, 98–106.

Navarro, L., Dunoyer, P., Jay, F., Arnold, B., Dharmasiri, N., Estelle, M., Voinnet, O., and Jones, J.D. (2006) A plant miRNA contributes to antibacterial resistance by repressing auxin signaling. *Science*. **312**(5772):436-9.

Oliveira, J.T.A., Andrade, N.C., Martins-Miranda, A.S., Soares, A.A., Gondim, D.M.F., Araújo-Filho, J.H., Freire-Filho, F.R. and Vasconcelos, I.M. (2012) Differential expression of antioxidant enzymes and PR-proteins in compatible and incompatible interactions of cowpea (Vigna unguiculata) and the root-knot nematode Meloidogyne incognita. *Plant Physiol. Biochem.* **51**, 145–152.

Palmer, I.A., Shang, Z. and Fu, Z.Q. (2017) Salicylic acid-mediated plant defense: Recent developments, missing links, and future outlook. *Front. Biol. (Beijing).* **12**, 258–270.

Pandey, S., Fartyal, D., Agarwal, A., Shukla, T., James, D., Kaul, T., Negi, Y.K., Arora, S. and Reddy, M.K. (2017) Abiotic stress tolerance in plants: Myriad roles of Ascorbate peroxidase. *Front. Plant Sci.* **8**, 1–13.

Pandey, S., Negi, Y.K., Chinreddy, S., Sathelly, K., Arora, S. and Kaul, T. (2014) Modeling and phylogenetic analysis of cytosolic ascorbate peroxidase (OsAPX1) from rice reveal signature motifs that may play a role in stress tolerance. *Bioinformation* **10**, 973–2063.

Park, C.J., Kim, K.J., Shin, R., Park, J.M., Shin, Y.C. and Paek, K.H. (2004) Pathogenesis-related protein 10 isolated from hot pepper functions as a ribonuclease in an antiviral

pathway. *Plant J.* **37**, 186–198.

Patočka J (2003) The chemistry, pharmacology, and toxicology of the biologically active constituents of the herb Hypericum perforatum L. *J. Appl. Biomed.* **1**, 61–70.

Peleg-Grossman, S., Melamed-Book, N. and Levine, A. (2012) ROS production during symbiotic infection suppresses pathogenesis-related gene expression. *Plant Signal. Behav.* **7**, 409–415.

Peng, X., Hu, Y., Tang, X., Zhou, P., Deng, X., Wang, H. and Guo, Z. (2012) Constitutive expression of rice WRKY30 gene increases the endogenous jasmonic acid accumulation, PR gene expression and resistance to fungal pathogens in rice. *Planta* **236**, 1485–1498.

Pinweha, N., Asvarak, T., Viboonjun, U. and Narangajavana, J. (2015) Involvement of miR160/miR393 and their targets in cassava responses to anthracnose disease. *J. Plant Physiol.* **174**, 26–35.

Pitzschke, A. (2013) Agrobacterium infection and plant defense—transformation success hangs by a thread. *Front. Plant Sci.* **4**, 1–12.

Prasad, N.K., Vindal, V., Kumar, V., Kabra, A., Phogat, N. and Kumar, M. (2011) Structural and docking studies of Leucaena leucocephala Cinnamoyl CoA reductase. *J. Mol. Model.* **17**, 533–541.

Pruss, G.J., Nester, E.W. and Vance, V. (2008) Infiltration with Agrobacterium tumefaciens induces host defense and development-dependent responses in the infiltrated zone. *Mol. Plant. Microbe. Interact.* **21**, 1528–1538.

Pungartnik, C., Silva, A.C. da, Melo, S.A. de, Gramacho, K.P., Mattos Cascardo, J.C. de, Brendel, M., Micheli, F. and Silva Gesteira, A. da (2009) High-affinity copper transport and Snq2 export permease of *saccharomyces cerevisiae* modulate cytotoxicity of PR-10 from *Theobroma cacao*. *Mol. Plant-Microbe Interact.* **22**, 39–51.

Raes, J. (2003) Genome-wide characterization of the lignification toolbox in Arabidopsis. *Plant Physiol.* **133**, 1051–1071.

Rather, I.A., Awasthi, P., Mahajan, V., Bedi, Y.S., Vishwakarma, R.A. and Gandhi, S.G. (2015) Molecular cloning and functional characterization of an antifungal PR-5 protein

from Ocimum basilicum. *Gene* **558**, 143–151.

Saddiqe, Z., Naeem, I. and Maimoona, A. (2010) A review of the antibacterial activity of Hypericum perforatum L. *J. Ethnopharmacol.* **131**, 511–521.

Singh, R.K., Hou, W. and Franklin, G. (2016) Protocols for in vitro cultures and secondary metabolite analysis of aromatic and medicinal plants, Second Edition. **1391**, 317–334.

Sliwiak, J., Dauter, Z. and Jaskolski, M. (2016) Crystal structure of Hyp-1, a Hypericum perforatum PR-10 Protein, in complex with melatonin. *Front. Plant Sci.* **7**, 1–10.

Sliwiak, J., Dauter, Z., Kowiel, M., Mccoy, A.J., Read, R.J. and Jaskolski, M. (2015) ANS complex of St John's wort PR-10 protein with 28 copies in the asymmetric unit: A fiendish combination of pseudosymmetry with tetartohedral twinning. *Acta Crystallogr. Sect. D Biol. Crystallogr.* **71**, 829–843.

Souza, T.P., Dias, R.O. and Silva-Filho, M.C. (2017) Defense-related proteins involved in sugarcane responses to biotic stress. *Genet. Mol. Biol.* **40**, 360–372.

Tachi, H., Fukuda-Yamada, K., Kojima, T., Shiraiwa, M. and Takahara, H. (2009) Molecular characterization of a novel soybean gene encoding a neutral PR-5 protein induced by high-salt stress. *Plant Physiol. Biochem.* **47**, 73–79.

Tatsis, E.C., Boeren, S., Exarchou, V., Troganis, A.N., Vervoort, J. and Gerothanassis, I.P. (2007) Identification of the major constituents of Hypericum perforatum by LC/SPE/NMR and/or LC/MS. *Phytochemistry* **68**, 383–393.

Wójcik, A.M., Nodine, M.D. and Gaj, M.D. (2017) miR160 and miR166/165 contribute to the LEC2-mediated auxin response involved in the somatic embryogenesis induction in Arabidopsis. *Front. Plant Sci.* **8**, 1–17.

Xie, Y.R., Chen, Z.Y., Brown, R.L. and Bhatnagar, D. (2010) Expression and functional characterization of two pathogenesis-related protein 10 genes from Zea mays. *J. Plant Physiol.* **167**, 121–130.

Xu, P., Jiang, L., Wu, J., Li, W., Fan, S. and Zhang, S. (2014) Isolation and characterization of a pathogenesis-related protein 10 gene (GmPR10) with induced expression in soybean (Glycine max) during infection with Phytophthora sojae. *Mol. Biol. Rep.* **41**, 4899–4909.

Yahyaa, M., Ali, S., Davidovich-Rikanati, R., Ibdah, M., Shachtier, A., Eyal, Y., Lewinsohn, E. and Ibdah, M. (2017) Characterization of three chalcone synthase-like genes from apple (Malus x domestica Borkh.). *Phytochemistry* **140**, 125–133.

Yasmin, N. and Saleem, M. (2014) Biochemical characterization of fruit-specific pathogenesis-related antifungal protein from basrai banana. *Microbiol. Res.* **169**, 369–377.

Yuan, Z.-C., Edlind, M.P., Liu, P., et al. (2007) The plant signal salicylic acid shuts down expression of the vir regulon and activates quormone-quenching genes in Agrobacterium. *Proc. Natl. Acad. Sci.* **104**, 11790–11795.

Zhang, L., Yao, L., Zhang, N., Yang, J., Zhu, X., Tang, X., Calderón-Urrea, A. and Si, H. (2018) Lateral root development in potato is mediated by Stu-mi164 regulation of NAC transcription factor. *Front. Plant Sci.* **9**, 383.

Zhang, R., Wang, Y., Liu, G. and Li, H. (2010) Cloning and characterization of a pathogenesis-related gene (ThPR10) from Tamarix hispida. *Acta Biol. Cracoviensia Ser. Bot.* **52**, 17–25.

Zhang, Y., Lee, C.W., Wehner, N., Imdahl, F., Svetlana, V., Weiste, C., Dröge-Laser, W. and Deeken, R. (2015) Regulation of oncogene expression in T-DNA-transformed host plant cells. *PLoS Pathog.* **11**, 1–27.

Zhou, B., Wang, Y., Zhan, Y., Li, Y. and Kawabata, S. (2013) Chalcone synthase family genes have redundant roles in anthocyanin biosynthesis and in response to blue/UV-A light in turnip (Brassica rapa; Brassicaceae). *Am. J. Bot.* **100**, 2458–2467.

Chapter 4

Evidence for the involvement of a *Polygalacturonase-inhibiting protein* from *H. perforatum* L. in its recalcitrance to *A. tumefaciens*-mediated transformation

This chapter is included in the following publication:

Weina Hou, Rupesh Kumar Singh, Viviana Martins, Emmanuel Aguilar, Tomás Canto, Franklin Gregory, Francisco Tenllado, Alberto Carlos Pires Dias. (2018) Evidence for the involvement of a *Polygalacturonase-inhibiting protein* from *Hypericum perforatum* L. in its recalcitrance to *Agrobacterium tumefaciens*-mediated transformation. *Planta* (submitted).

Chapter 4 Evidence for the involvement of a *Polygalacturonase-inhibiting protein* from *H. perforatum* L. in its recalcitrance to *A. tumefaciens*-mediated transformation

4.1 Summary

H. perforatum L., a reservoir of high-value secondary metabolites of increasing interest to researchers and the pharmaceutical industry. However, improving their production via genetic manipulation is a challenging task as *H. perforatum* L. is recalcitrant to *A. tumefaciens*-mediated transformation. In the present study, a *Polygalacturonase-inhibiting protein* (*PGIP*) gene was identified from a subtractive cDNA library from *A. tumefaciens*-treated *H. perforatum* L. suspension cells. The role of *HpPGIP* in defense against *A. tumefaciens* was analyzed in transgenic *N. tabacum* overexpressing *HpPGIP* alone or fused at the N-terminus to *Hyp-1*, a gene that positively modulates resistance to *A. tumefaciens*. Furthermore, virus-induced gene silencing was employed to knock down the expression of the *PGIP* homologous in *N. benthamiana.* Results showed that *Agrobacterium*-mediated expression efficiency greatly decreased in both HpPGIP and Hyp-1-PGIP transgenic plants, as assessed by GUS staining assays. However, silencing of *PGIP* in *N. benthamiana* increased the resistance to *A. tumefaciens* rather than susceptibility, which correlated with induction of pathogenesis-related proteins (PRs). The expression of core genes involved in several defense pathways was also analyzed in transgenic tobacco plants. Overexpression of *HpPGIP* led to up-regulation of key genes involved in hormone signaling, microRNA-based gene silencing, homeostasis of reactive oxygen species, and the phenylpropanoid pathway. Overexpression of *Hyp-1-PGIP* enhanced the effect of *PGIP* on the expression of most genes analyzed. Moreover, HpPGIP was detected in the plasma membrane, cytoplasm and the nucleus of cells by confocal microscopy. Overall, our findings suggest *HpPGIP* modulates recalcitrance to *A. tumefaciens*-mediated transformation in *H. perforatum* L.

4.2 Introduction

H. perforatum. L., commonly known as St. John's wort, is perennial herb from *Hypericaceae* (Guttiferae) family, with 450 known species of the genus *Hypericum* in Europe, North America, Australia, New Zealand, Eastern Asia and South America (Saddiqe *et al*., 2010; Raak *et al*. , 2012; Klejdus *et al.* , 2013; Tocci, 2013). *H. perforatum* L. attracts the interest of scientists due to its pharmacological properties like anti-depressant, anti-inflammatory, anti-viral, anti-cancer, and anti-bacterial (Butterweck *et al*., 2003; Tatsis *et al*., 2007; Saddiqe *et al.*, 2010; Shrivastava and Dwivedi, 2015). A wide range of biologically active secondary metabolites, include hypericin, hyperforin, xanthones, essential oils, phenolic acids and a broad array of flavonoids has been detected in *H. perforatum* L. (Butterweck *et al*., 2003; Tatsis *et al*., 2007; Karppinen, 2010; Saddiqe *et al*., 2010).

A. tumefaciens is a gram-negative, soil-borne bacterium that causes crown gall disease in a wide range of plant species by integrating a transfer DNA into the host genomic DNA (Pitzschke, 2013; Gohlke and Deeken, 2014). This feature makes *A. tumefaciens* as a popular molecular technique to introduce foreign genes into plants for functional genomics and genetic engineering purposes. *A. tumefaciens* mediated transformation could be useful for metabolic engineering and functional genomic studies in *H. perforatum* L. However, plant recalcitrance against *A. tumefaciens* mediated transformation is a major concern (Hou *et al.*, 2016). In our previous study, *A. tumefaciens* rapidly evoked plant defense responses by triggering an intense oxidative burst when co-cultivated with *H. perforatum* L. cell suspensions followed by the death of bacterial cells (Franklin *et al.*, 2008). The molecular mechanism behind is still unknown which may be due to the complex interplay between the host and the pathogen.

Plant grown in natural environment is exposed to multiple pathogens. To defend themselves against pathogenic microorganisms, plants have developed a battery of defense mechanisms. *A. tumefaciens* evokes a number of defense responses in plants that include alteration of 1) phytohormone metabolism (Pitzschke, 2013), 2) PRs (Anand *et al.*, 2007; Pruss *et al.*, 2008), 3) MicroRNA-mediated gene silencing (Dunoyer *et al.*, 2006), 4) lignin deposition *(Singh et al*., 2014; Miedes *et al*., 2014), 5) Secondary metabolites (Franklin *et al.*, 2009), and 6) ROS (Franklin *et al.*, 2008).

Suppression subtractive hybridization (SSH) is a technique that has been developed for the generation of subtracted cDNA libraries from two mRNA populations, with the aim to select

cDNAs that are specifically expressed in one population but not in the other (Diatchenko *et al.*, 1996). A subtractive cDNA library was constructed from *A. tumefaciens*-treated *H. perforatum* L. suspension cells, from which the *Hyp-1* gene was cloned and characterized in terms of its biological function in defense against *Agrobacterium* (Hou *et al*., unpublished results*)*. In the present study, an additional highly expressed cDNA sequence was isolated from *H. perforatum* L. suspension cells and identified as *PGIP* gene.

Polygalacturonase-inhibiting protein (*PGIP*) belongs to a group of plant defense proteins against pathogens and are widespread in the plant kingdom. Plant grown in natural environment is exposed to risk multiple pathogens, the cell wall is the first barrier that plant utilize to defend themselves against pathogenic microorganisms. PG is the first cell wall degrading enzyme secreted by fungi and bacteria such as *A. tumefaciens* (Rodriguez-Palenzuela *et al.*, 1991). PGIP is from the LRR superfamily and produced by plant could specially recognize and inhibit those PGs. The PG-PGIP interaction limits the destructive potential of PGs and leads to the accumulation of OGs, which have been reported as elicitors of immunity. OGs activate a wide range of defense responses, including the accumulation of phytoalexins and lignin, the expression of defense-related genes, and the production of ROS (Srivastava, 2013). Later on the evidence showed that OGs could be generated in planta and activate plant innate immunity by functioning as damage-associated molecular patterns (DAMPs) (Benedetti *et al.*, 2015). Recently, the importance of PGIP in plant defense has been studied from molecular biological level as introduced specially in chapter 1. Overall, overexpression of *PGIP* gene from bean, Chinese cabbage, paper enhanced the resistance to fungi, and the transcripts of *PGIP* gene were up-regulated under abiotic stresses including SA, ABA, MeJA, H_2O_2, etc. treatments. *GhPGIP1* overexpressed transgenic *Arabidopsis* conferred the defense by accumulation of the expression of *PRs* and *GhPGIP1* knock out cotton was highly susceptible to the pathogen's infection (Janni *et al.*, 2008; Hwang *et al.*, 2010; Wang *et al.*, 2013; Zhang *et al.*, 2016; Liu *et al.*, 2017). In this present study, after challenged with *A. tumefaciens* the *HpPGIP* is significantly expressed in *H. perforatum* L. suspension cells. So far, there is no any report about *HpPGIP* from *H. perforatum* L., so our present work makes the first contribution toward to *HpPGIP* defense activities in plants.

The biological function of *HpPGIP* in defense against *A. tumefaciens* was analyzed in transgenic *N. tabacum* plants overexpressing either *PGIP* or *PGIP* fused to *Hyp-1 (*Hyp-1-PGIP), and in *N. benthamiana* plants silenced for the *PGIP* homologous gene. Moreover, the expression of core genes regulating several defense pathways was analyzed in both *PGIP* and *Hyp-1-PGIP* overexpressing lines. In addition, HpPGIP was detected in the nucleus and the

cytoplasm of epidermal cells by confocal microscopy. Overall, our findings suggest that *HpPGIP* from *H. perforatum* L. modulates recalcitrance to *A. tumefaciens* as part of defense mechanisms against pathogenic infection.

4.3 Results

4.3.1 Cloning and characterization of *HpPGIP*

To identify genes from *H. perforatum* L. involved in defense responses against *A. tumefaciens*, a SSH-based cDNA library was performed. RNAs isolated from *H. perforatum* L. suspension cells challenged with *A. tumefaciens* as tester and RNAs from control cultures as driver were used to construct the forward subtracted cDNA library from which a highly expressed *HpPGIP* gene was selected.

The cDNA of *HpPGIP* (GenBank Accession No. MK290240) sequence with an open reading frame of 945bp including stop codon, is predicted to encode a protein of 314 aa with molecular mass of 34.54KDa and pI of 8.04 (Fig. 4.1 A). The predicted protein HpPGIP showed a high degree of similarity with previously reported PGIPs in NCBI, and possessed the features of the other PGIPs. Phylogenetic tree showing the close relationship of *HpPGIP* with others known plant PGIPs (Fig. 4.2). Structural analysis revealed that HpPGIP contains four LRR motifs (LRR CC:100-125aa, LRR BAC: 149-169aa, LRR TYP: 149-173aa and LRR SD22: 200-218aa, respectively) (Fig. 4.1 B).

4.3.2 Overexpression of *HpPGIP* in *N. tabacum*

To characterize *HpPGIP* function in defense responses against *Agrobacterium*, we established transgenic *N. tabacum* plants expressing *HpPGIP* alone or fused at the N-terminus to *Hyp-1* or *GFP* under the control of 35S promotor in the binary expression vector pBI121 (Fig. 4.3). Three transgenic tobacco plant lines per construct, PGIP-1/-12/-13, GFP-PGIP-3/-7/-8 and Hyp-1-PGIP-1/-5/-8 were selected by antibiotic resistance, and T-DNA insertion was confirmed by PCR. As control, besides wild type, transgenic tobacco plants expressing GFP were obtained.

In order to determine whether overexpression of *HpPGIP* alone or fused to *Hyp-1* influences the efficiency of *Agrobacterium*-mediated gene expression in tobacco leaves, we inoculated T2 progenies derived from each of two T1 lines, PGIP-1/-13 (Fig. 4.4 D, E), GFP-PGIP-3/-7 (Fig. 4.4 F, G) and Hyp-1-PGIP-1/-5 (Fig. 4.4 H, I), with the strain EHA105 harboring a binary plasmid to express GUS. Whereas GFP transgenic control plants showed an intense GUS staining and behaved similarly to wild-type (WT) plants (Fig. 4.4 B, C), GUS staining was absent in transgenic lines expressing either PGIP, GFP-PGIP or Hyp-1-PGIP fusion gene (Fig. 4.4 D-I), or in WT plants inoculated with *A. tumefaciens* containing the empty vector (Fig. 4.4 A). Our results suggest that transformation efficiency of *A. tumefaciens* is greatly decreased in tobacco plants overexpressing *HpPGIP*, suggesting the involvement of *HpPGIP* in defense response against *A. tumefaciens*.

A

```
atg aga gcc cat ttc ctc tcc ctt gta gca att tca act tgc ctc ctc atc tcc att tcc
 M   R   A   H   F   L   S   L   V   A   I   S   T   C   L   L   I   S   I   S

caa gca gaa gac tgc aat cct gat gac aaa aaa gtt ctc ttc cag att aaa aag tca ctt
 Q   A   E   D   C   N   P   D   D   K   K   V   L   F   Q   I   K   K   S   L

ggc gac cct gct ctc tta gcc tcg tgg gaa aac acc acg gat tgc tgt acc aaa tgg gac
 G   D   P   A   L   L   A   S   W   E   N   T   T   D   C   C   T   K   W   D

ggc ata agg tgt ctc cgg aaa acc cac cgc atc atc tcc ctt act gtg ttc aac gac gac
 G   I   R   C   L   R   K   T   H   R   I   I   S   L   T   V   F   N   D   D

gta ctc cca gtt tcc ggg atc cag cct tcc ggc aaa ttc cca ccc gct gtc ggg gat ttg
 V   L   P   V   S   G   I   Q   P   S   G   K   F   P   P   A   V   G   D   L

cct tac ctc cgg gag ctt tac ttc cac aat cta tca cag gtc aca ggc ccg atc cca caa
 P   Y   L   R   E   L   Y   F   H   N   L   S   Q   V   T   G   P   I   P   Q

gaa ctc gcc aag ctc agg cgt ctc aga ttc ctg agg ctt gac ttg cta aac ctt act ggg
 E   L   A   K   L   R   R   L   R   F   L   R   L   D   L   L   N   L   T   G

cca atc cct cca atc ttt ggc cag ctc aag aga ctc tat ttc ata aat tta gcc aac aac
 P   I   P   P   I   F   G   Q   L   K   R   L   Y   F   I   N   L   A   N   N

aag cta tct ggg tcg atc cca tcg tcc cta ggc gag tta cca gga aac ttc ggg gcg ctt
 K   L   S   G   S   I   P   S   S   L   G   E   L   P   G   N   F   G   A   L

tcc att atc ctc tcc aat aac caa ctt aca ggc atg att ctc acc tcg ttt agc aac aac
 S   I   I   L   S   N   N   Q   L   T   G   M   I   L   T   S   F   S   N   N

ctt aac ctg acc ggc atc gac cta tct gga aac aag ctc gaa gga gac gct tcg atg ctg
 L   N   L   T   G   I   D   L   S   G   N   K   L   E   G   D   A   S   M   L

ttc gga tcc aac aag ata gtt gga tct att gtc ctg agc agg aac cag ctg gag ttc aac
 F   G   S   N   K   I   V   G   S   I   V   L   S   R   N   Q   L   E   F   N

ttg tcc ttg gtt gtc ttg ccc gat gac ttc att tat tta gac att agc cat aat aag atc
 L   S   L   V   V   L   P   D   D   F   I   Y   L   D   I   S   H   N   K   I

tat ggt tcg att cct cct cag atg ggc gac att ggt att cat tac ttc aac gtc agc tac
 Y   G   S   I   P   P   Q   M   G   D   I   G   I   H   Y   F   N   V   S   Y

aat aga ctg tgt ggt gag att cct gtc ggg ctt caa agc ttt gat acc tcc aat tac gtc
 N   R   L   C   G   E   I   P   V   G   L   Q   S   F   D   T   S   N   Y   V

cat aac aag tgc ttg tgt ggg gct cca ctt cca gct tgc aag taa
 H   N   K   C   L   C   G   A   P   L   P   A   C   K   -
```

B

MRAHFLSLVAISTCLLISISQAEDCNPDDKKVLFQIKKSLGDPALLASWENTTDCCTKWD
GIRCLRKTHRIISLTVFNDDVLPVSGIQPSGKFPPAVGDLPYLRELYFHNLSQVTGPIPQ
ELAKLRRLRFLRLDLLNLTGPIPPIFGQ***LKRLYFINLANNKLSGSIPSS******LGEL***PGNFGAL
SIILSNNQLTGMILTSFSNNLNLTGIDLSGNKLEGDASMLFGSNKIVGSIVLSRNQLEFN
LSLVVLPDDFIYLDISHNKIYGSIPPQMGDIGIHYFNVSYNRLCGEIPVGLQSFDTSNYV
HNKCLCGAPLPACK

Fig. 4.1 cDNA and amino acid sequence of *HpPGIP* from *H. perforatum* L. (A) Nucleotide sequence and amino acid sequence of *HpPGIP*. (B) LRR motifs were showed in amino acid sequence of *HpPGIP* with different colors or font. LRR_CC, in red, LRR_BAC, in yellow, LRR_TYP, in black with italic and bold, and LRR_SD22, in green.

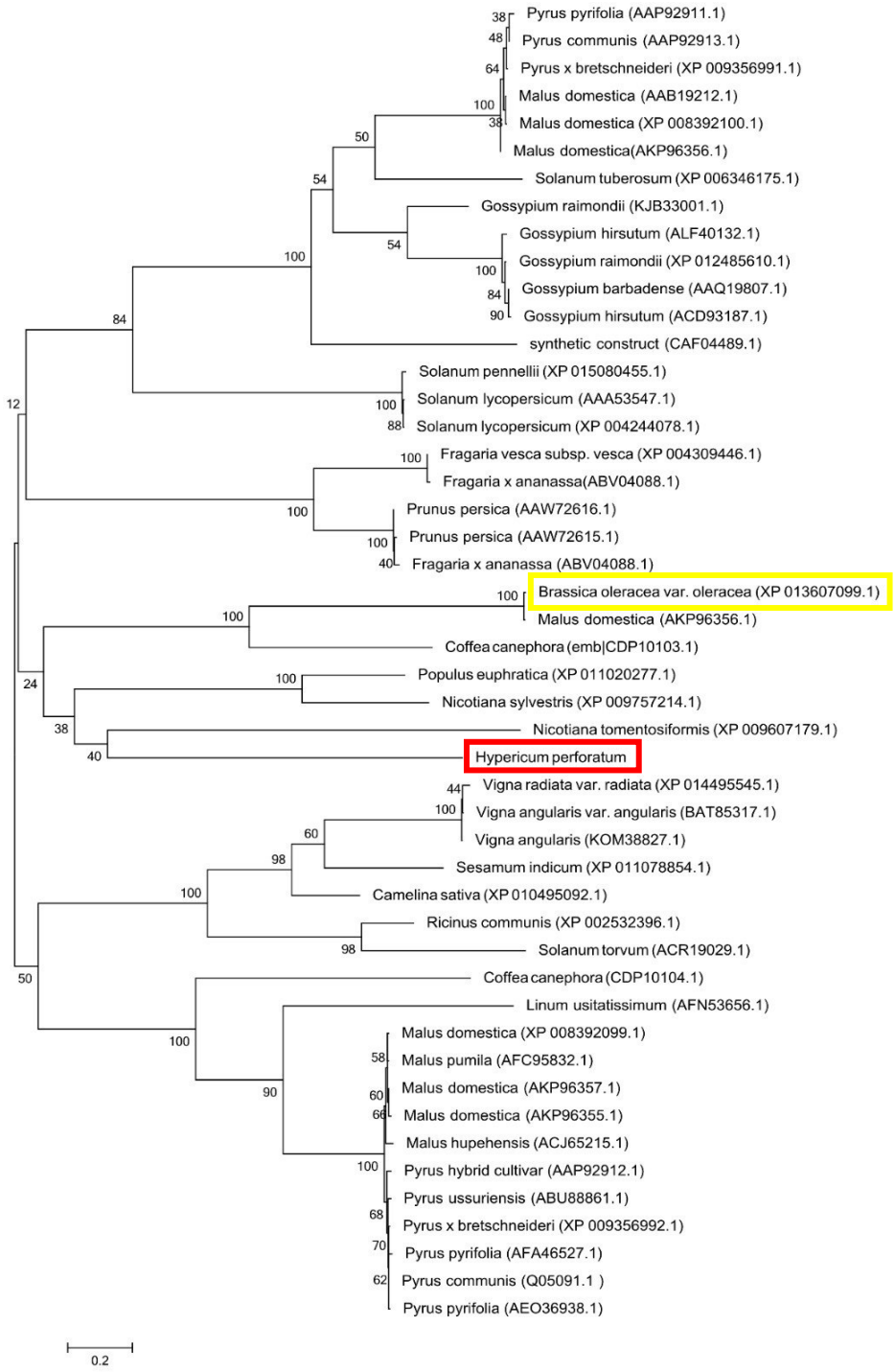


Fig. 4.2 Phylogenetic analysis of *HpPGIP* and other homologous genes. The amino acid sequences were obtained from GenBank. Plant Latin names and GenBank accession numbers were used to marker the phylogenetic tree. The phylogenetic tree was generated by MEGA 6. *H. perforatum* L. *HpPGIP* was framed in red box and the *B. oleracea* candidate was framed in yellow box. The scale was shown in units of number of amino acid substitutions per site.

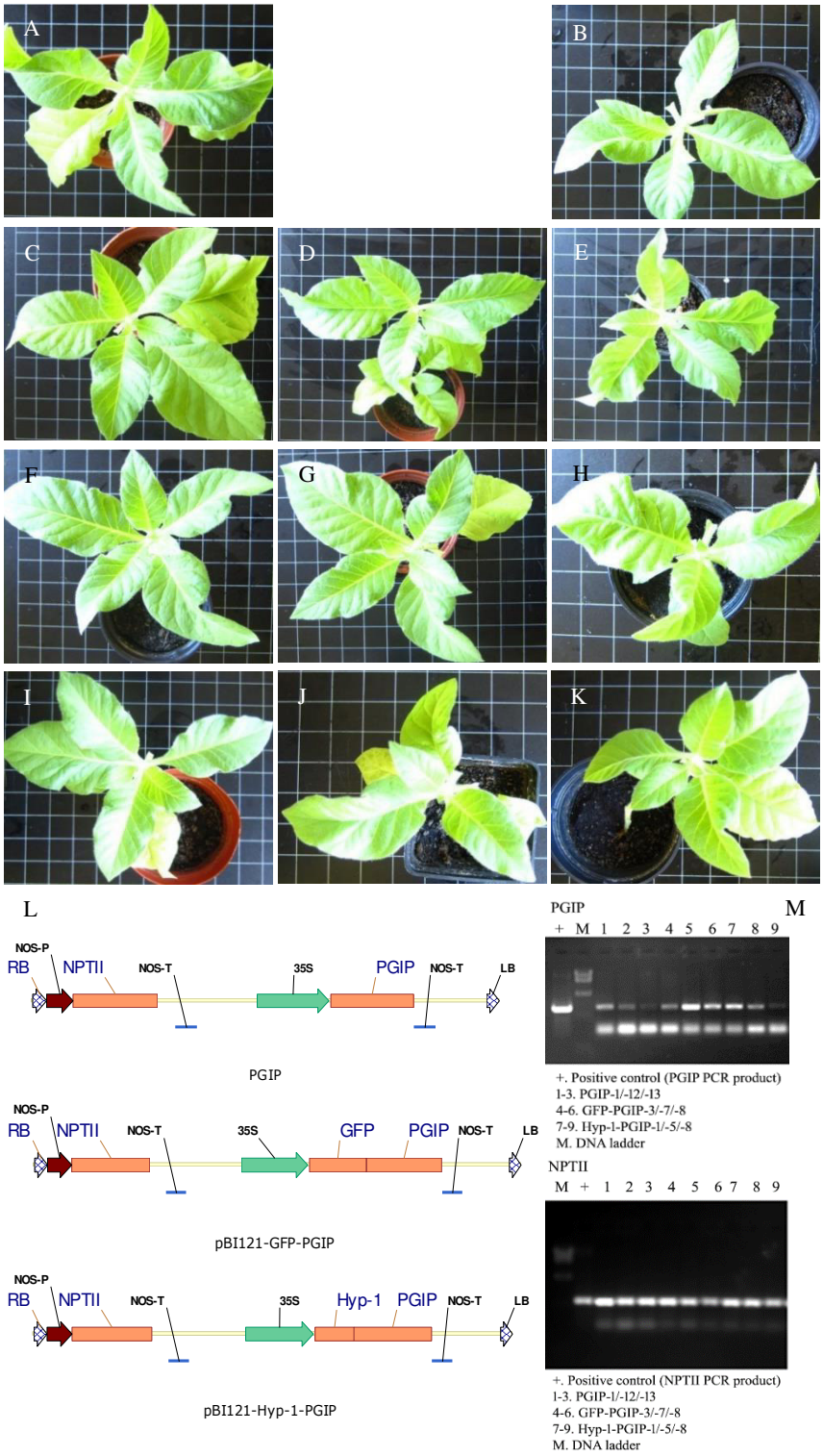


Fig. 4.3 Generation of *HpPGIP* overexpressed tobacco T2 plant lines. (A) *N. tabacum* control plant. (B) Transgenic plant GFP. (C-E) Transgenic plant PGIP-1/-12/-13 lines. (F-H) Transgenic plant GFP-PGIP-3/-7/-8. (I-K) Transgenic plant Hyp-1-PGIP-1/-5/-8 lines. (L) Schematic diagram of PGIP, GFP-PGIP and Hyp-1-PGIP, which were made by software Vector NTI; m Confirmation of T-DNA insertion by PCR.

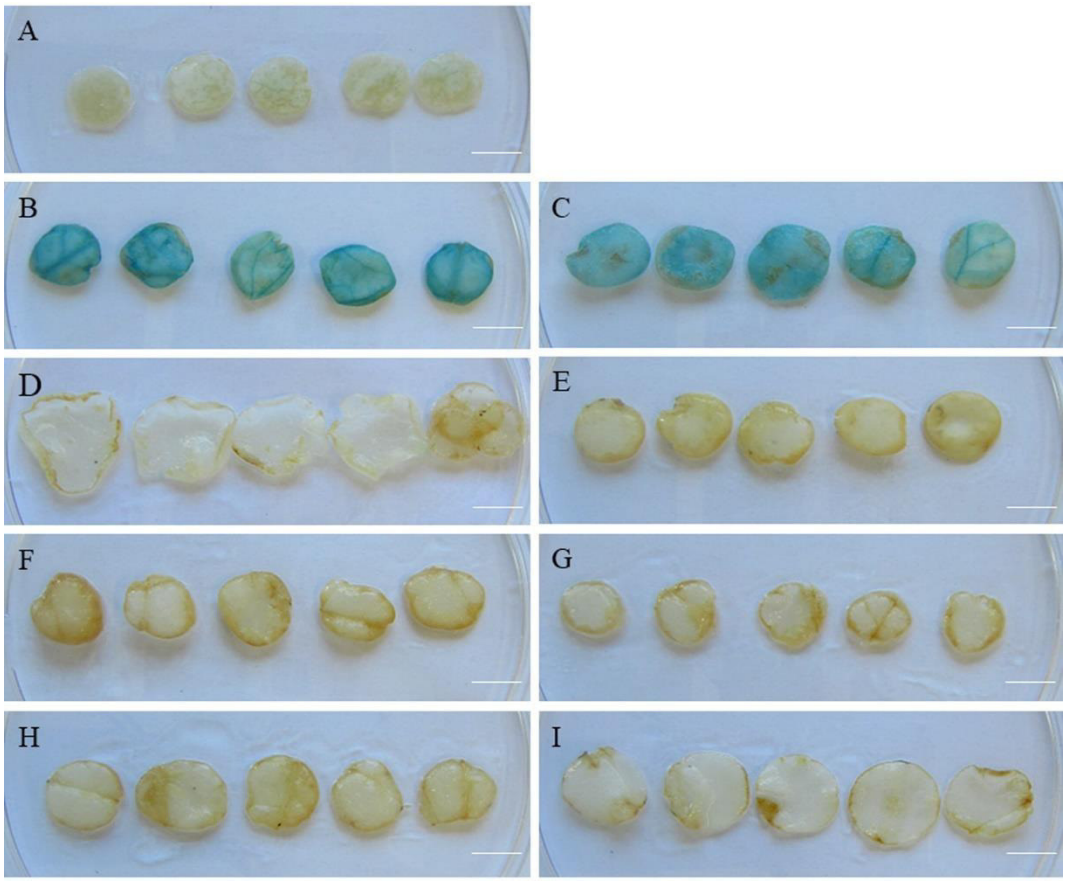


Fig. 4.4 Detection of *Agrobacterium*-mediated gene expression in T2 HpPGIP tobacco lines by GUS staining. (A) *N. tabacum* WT inoculated with *A. tumefaciens* containing the empty vector as negative control. (B) *N. tabacum* WT inoculated with *A. tumefaciens* containing pCAMBIA 2301-GUS as positive control. (C) GFP transgenic plant inoculated with *A. tumefaciens* containing pCAMBIA 2301-GUS as positive control. (D-E) PGIP-1/-13 transgenic plants inoculated with *A. tumefaciens* containing GUS vector. (F-G) GFP-PGIP-3/-7 transgenic plants inoculated with *A. tumefaciens* containing GUS vector. (H-I) Hyp-1-PGIP-1/-5 transgenic plants inoculated with *A. tumefaciens* containing GUS vector. Bars in each panel represent 10 mm.

4.3.3 Subcellular localization assays

To examine the subcellular localization of HpPGIP, *Agrobacterium* strains carrying mRFP or the mCherry-labeled-plasma membrane marker PM-RK were mixed with the *Agrobacterium* strain carrying GFP-PGIP and co-expressed transiently in leaves of *N. tabacum* plants. Three days after agroinfiltration, the fluorescence in green and red channels was observed by confocal fluorescence microscopy to compare their localization. The fluorescence of GFP-PGIP coincided with that of mRFP in the nucleus and cytoplasm (Fig. 4.5 G) as well as with PM-RK

in the plasma membrane (Fig. 4.5 C). Besides, GFP-PGIP was clearly present in nucleus of epidermal cells (Fig. 4.5 A and E).

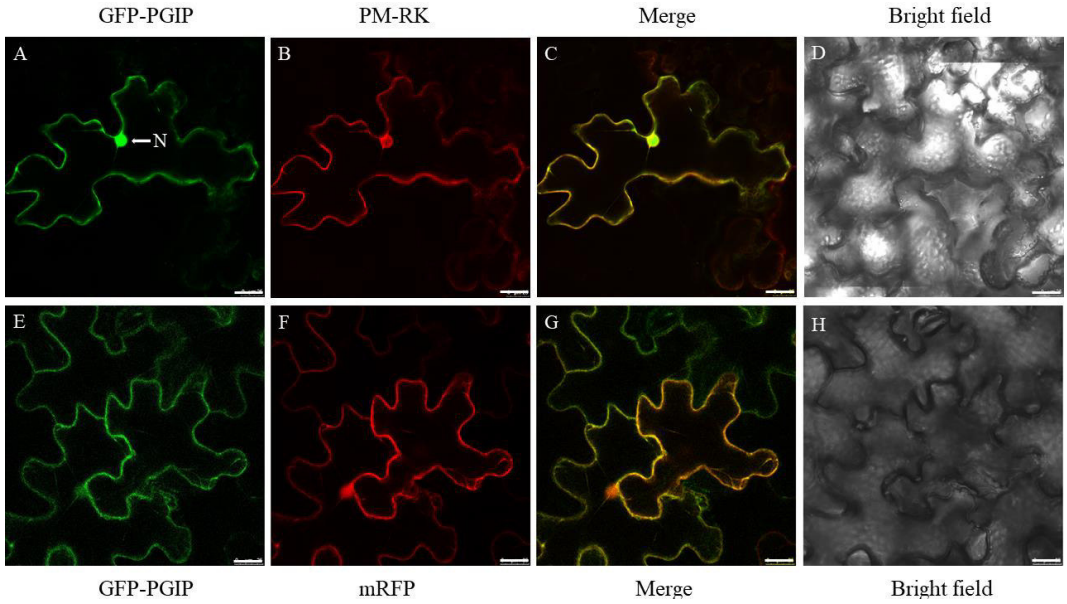


Fig. 4.5 Subcellular localization of GFP-PGIP in the nucleus, plasma membrane and cytoplasm. Leaves of *N. tabacum* were co-infiltrated with GFP-PGIP plus either mRFP or the plasma membrane marker PM-RK. Panels show either monochrome green (from GFP) (A and E) or red (from mCherry) (B and F) fluorescence, overlays for colocalization studies (C and G), or bright fields (D and H). N, nucleus. Scale bars all images are 25µm.

4.3.4 *HpPGIP* alters gene expression of multiple defense pathways

To survey plant defense pathways involved in *HpPGIP*-mediated defense against *A. tumefaciens*, the expression levels of key genes implicated in different microbial defense pathways were evaluated in PGIP and Hyp-1-PGIP transgenic tobacco plants by quantitative real time PCR. T2 PGIP-1 and PGIP-13 (Fig. 4.6 A) transgenic lines, and Hyp-1-PGIP-1 and Hyp-1-PGIP-5 (Fig. 4.7 A) transgenic lines were selected for subsequent experiments since they exhibited higher levels of *HpPGIP* mRNA.

Phytohormones such as auxin and JA play an important role in plant defense against pathogenic microorganisms. We focused on auxin-responsive genes *NtaTIR1, NtaAFR8* and the JA-biosynthesis gene *NtaLOX*. The transcript levels of *NtaTIR1* were not significantly different in transgenic plants compared with control plants while *NtaARF8* mRNA was significantly

increased in *HpPGIP* overexpressing plants (Fig. 4.6 B, C). The transcript level of *NtaLOX* was increased in the high overexpression line PGIP-13 (Fig. 4.6 D).

PR proteins have been described as plant specific proteins induced in response to pathogen infection. To assess the involvement of PR proteins in *HpPGIP*-mediated antibacterial defense, the transcripts of *NtaPR-1* and *NtaPR-10* were monitored by qRT-PCR. The results showed that *NtaPR-10* was decreased in both transgenic lines and *NtaPR1* was decreased in PGIP-13 line (Fig. 4.6 F, G).

MicroRNA-mediated gene silencing pathway is involved in plant defense against pathogens. *NtaAGO1*, *NtamiR160*, *NtamiR164ab* and *NtamiR164c* were analyzed by qRT-PCR in *HpPGIP* overexpressing plants (Fig. 4.6 H-J). There were no significant differences in *NtamiR160* expression (Fig. 4.6 H), whereas *NtaAGO1* and *Nta164ab* were increased in PGIP-13 line, and the expression levels of *NtamiR164c* was increased in both transgenic lines.

Production of secondary metabolites via the phenylpropanoid pathway has been developed by plants as an important defense mechanism to protect themselves from pathogens. The lignin synthesis pathway genes *NtaPAL1*, *NtaPAL4*, *NtaCCR* and *NtaCAD* were analyzed by qRT-PCR (Fig. 4.6 K-N). The expression of the three genes *NtaPAL1,4* and *NtaCCR*, but not *NtaCAD* were significantly increased in *HpPGIP* overexpressing plants. Flavonoids are polyphenolic compounds and play a major role in defense against pathogens. The transcripts of *NtaCHS*, the first enzyme in the flavonoid biosynthesis pathway, were increased in PGIP transgenic plants compared to controls (Fig. 4.6 O). Lastly, the transcripts of core enzymes involved in ROS homeostasis were also monitored in *HpPGIP* overexpressing plants by RT-qPCR. *NtaAPX* and *NtaFe-SOD* but not *NtaCAT*, were highly increased in *HpPGIP* overexpressing plants (Fig. 4.6 P-R).

To reveal possible additive effects of *Hyp-1* and *HpPGIP* in defense responses against *A. tumefaciens*, the expression levels of the same genes implicated in defense pathways were evaluated in Hyp-1-PGIP transgenic plants by qRT-PCR. In the auxin signaling pathway, not only *NtaARF8* but also *NtaTIR1* was increased significantly in *Hyp-1-HpPGIP* overexpression lines (Fig. 4.7 B, C) compared with *HpPGIP* overexpression lines (Fig. 4.6 B, C). The JA-biosynthesis gene *NaLOX* was induced at greater levels in Hyp-1-PGIP transgenic plants relative to controls than in *HpPGIP* overexpressing lines (Fig. 4.6 D). Similarly, *NtaAGO1* was increased at much higher levels in Hyp-1-PGIP lines compared to PGIP lines (Fig. 4.7 G). *NtamiR164ab* was not significantly alerted in the Hyp-1-PGIP transgenic lines, while

transcripts of *NtamiR160* and *NtamiR164c* were increased in Hyp-1-PGIP-5 (Fig. 4.7 H-G). The expression of four genes involved in the lignin synthesis pathway, including *NtaCAD* (Fig. 4.7 K-N), were induced significantly in Hyp-1-PGIP transgenic lines. *NtaCHS* (Fig. 4.7 O) was expressed differently expressed in Hyp-1-PGIP plants at greater levels than in PGIP transgenic plants (Fig. 4.6 O). In addition, *NtaCAT* was specifically increased in Hyp-1-PGIP lines compared to PGIP lines (Fig. 4.7 Q). Thus, overexpression of the fusion protein Hyp-1-PGIP enhanced the effect of PGIP on the expression of most genes implicated in defense responses.

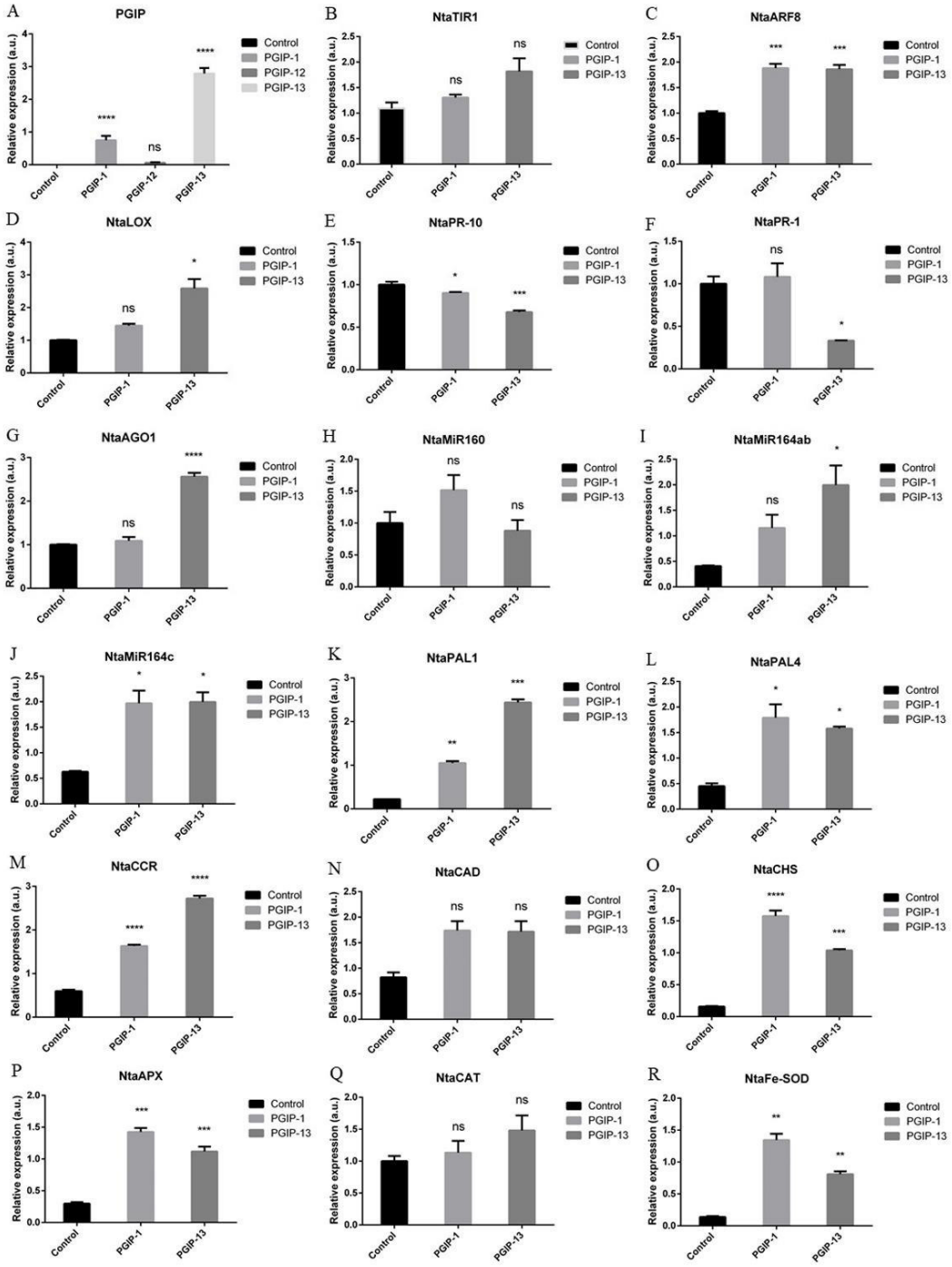


Fig. 4.6 Quantitative real time RT-PCR to assess core genes involved in different plant defense pathways in PGIP transgenic tobacco plants. (A) Relative transcript levels of *PGIP* in transgenic lines. (B-C) Relative transcript levels of *TIR1* and *ARF8*. (D) Relative transcript levels of *LOX*. (E-F) Relative transcript levels of *PR-10* and *PR-1*. (G-J) Relative transcript levels of *AGO1*, *MiR160*, *MiR164ab* and *MiR164c*. (K-N) Relative transcript levels of *PAL1*, *PAL4*, *CCD* and *CAD*. (O) Relative transcript levels of *CHS*. (P-R) Relative transcript levels of *APX*, *CAT*, and *Fe-SOD*. Asterisks denote the significance levels compared with control: *, $P \leq 0.05$; **, $P \leq 0.01$; ***, $P \leq 0.001$; and ****, $P \leq 0.0001$ and ns denotes not significate.

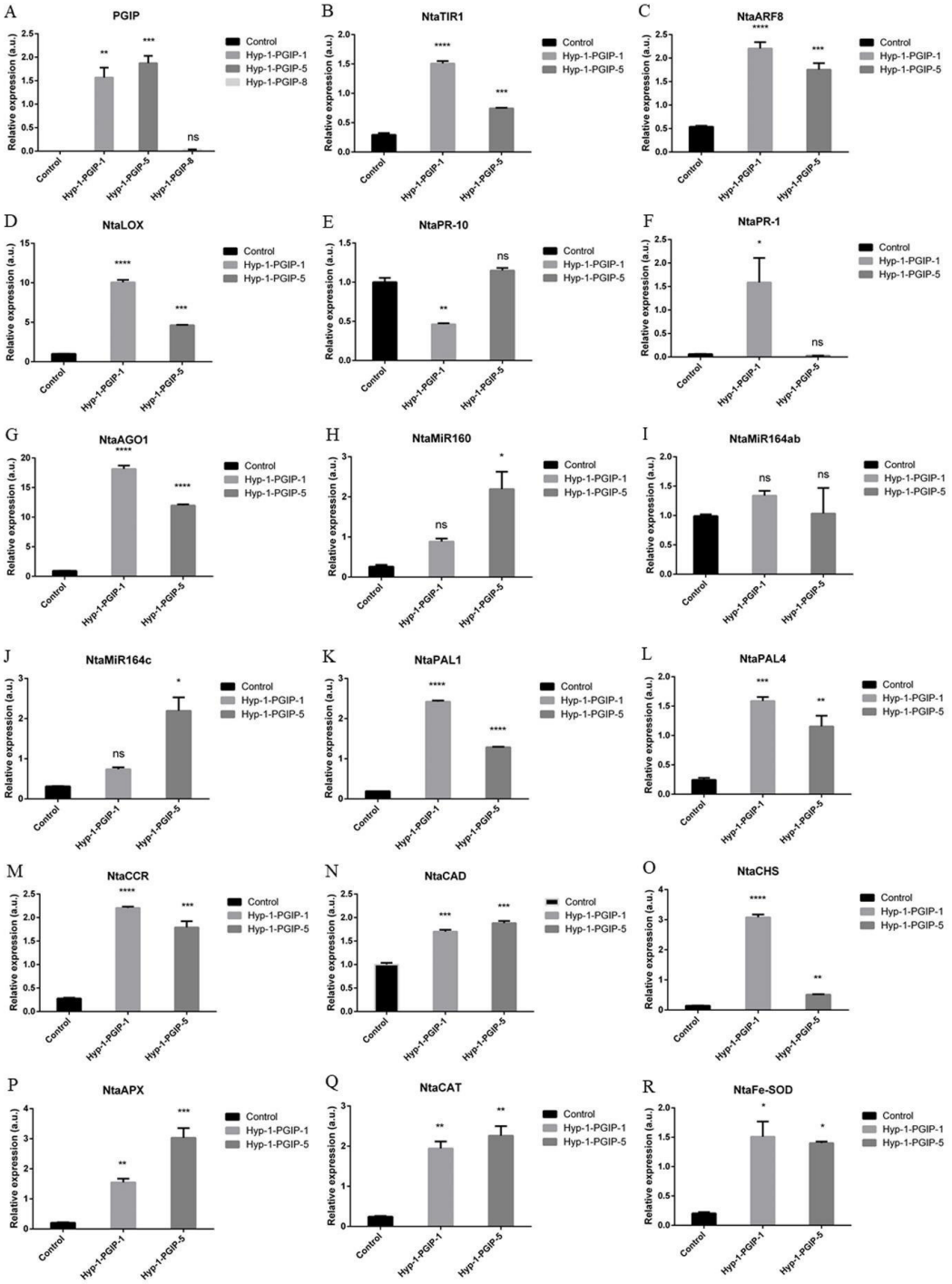


Fig. 4.7 Quantitative real time RT-PCR to assess core genes involved in different plant defense pathways in Hyp-1-PGIP transgenic tobacco plants. (A) Relative transcript levels of *PGIP* in Hyp-1-PGIP transgenic lines. (B-C) Relative transcript levels of *TIR1* and *ARF8*. (D) Relative transcript levels of *LOX*. (E-F) Relative transcript levels of *PR-10* and *PR-1*. (G-J) Relative transcript levels of *AGO1*, *MiR160*, *MiR164ab* and *MiR164c*. (K-N) Relative transcript levels of *PAL1*, *PAL4*, *CCD* and *CAD*. (O) Relative transcript levels of *CHS*. (P-R) Relative transcript levels of *APX*, *CAT*, and *Fe-SOD*. Asterisks denote the significance levels compared with control: *, $P \leq 0.05$; **, $P \leq 0.01$; ***, $P \leq 0.001$; and ****, $P \leq 0.0001$ and ns denote not significate.

4.3.5 Virus-induced gene silencing in *N. benthamiana*

To investigate the loss-of function phenotype of *PGIP*, we used the VIGS technique to knock down the expression of the *HpPGIP* homolog in *Brassica oleracea.* The *PGIP* homolog in *B. oleracea* is *Polygalacturonase inhibitor 1-like* (*BoPGIP*), as revealed by phylogenetic analysis of *HpPGIP*-related genes (Fig. 4.2). It has been reported that overexpression of *PGIP2* in *Brassica* increased resistance to the bacterial pathogen *P. carotovorum* (Hwang *et al.*, 2010). However, several attempts to induce VIGS in *B. oleracea* even with a TRV vector carrying a fragment of the *B. oleracea PDS* gene were unsuccessful. To circumvent this limitation, we performed a heterologous VIGS assay using *BoPGIP* to silence *PGIP* in *N. benthamiana*. The use of heterologous gene sequences to silence their respective homologs in *N. benthamiana* has been previously reported (Senthil-Kumar *et al*., 2007).

Four weeks-old *N. benthamiana* plants were infiltrated with a TRV vector carrying a 507-bp fragment of BoPGIP (pTRV2: BoPGIP) or the empty TRV vector (pTRV2:00) as a control. Silencing of the *PDS* gene by TRV2: BoPDS2, which provides a visual bleached leaf phenotype, was also used to monitor VIGS in *N. benthamiana.* At 7 days post-inoculation (dpi), photobleaching occurred in upper leaves of all pTRV2: PDS2 treated plants, whereas there was no such phenotype in control and pTRV2: BoPGIP infected plants. However, silencing of *PGIP* caused retarded plant growth (Fig. 4.8 A). Silencing efficiency of *PGIP* was examined by RT-PCR in upper leaves equivalent to those showing the bleached phenotype in pTRV2: PDS2 infected plants. Transcripts of *PGIP* were reduced substantially in pTRV2: BoPGIP infected plants compared to pTRV2:00, control plants (Fig. 4.8 B), indicating that heterologous VIGS was induced by *Brassica PGIP* sequences in *N. benthamiana*. In order to determine whether knock down of *PGIP* influences the efficiency of *Agrobacterium*-mediated gene expression, *PGIP*-silenced and control *N. benthamiana* plants were inoculated in the upper leaves with an *Agrobacterium* strain expressing GFP at a concentration of either OD_{600} = 0.1 or 0.01. The plants were photographed after 3 days under UV lamp (Fig. 4.8 C), and GFP expression was monitored in duplicated samples at 3 and 5 days after challenge with GFP by western blot. Intriguingly, GFP accumulated at lower levels in *PGIP*-silenced plants than in controls at both OD_{600} values (Fig. 4.8 D). Our result indicates that transformation efficiency of *A. tumefaciens* was decreased in *PGIP*-knock down plants compared to controls.

It has been shown that silencing of the homologous *Hyp-1* gene in *C. roseus* led to induction of *PR* genes overexpression and increased defense to *Agrobacterium* (Hou *et al*., unpublished results). Thus, the relative accumulation of a set of *PR* genes, *NbPR-1*, *NbPR-5* and *NbPR-10*, were monitored in *PGIP*-silenced and control *N. benthamiana* plants by qRT-PCR. Interestingly, a 5 to 10-fold increase in the expression of *NbPR-1*, *NbPR-5* and *NbPR-10* was detected in *PGIP*-silenced plants compared with control plants (Fig. 4.8 E). These findings suggest that the enhanced resistance to *A. tumefaciens* in *PGIP*-silenced plants was associated with the increase expression of endogenous *PR* genes.

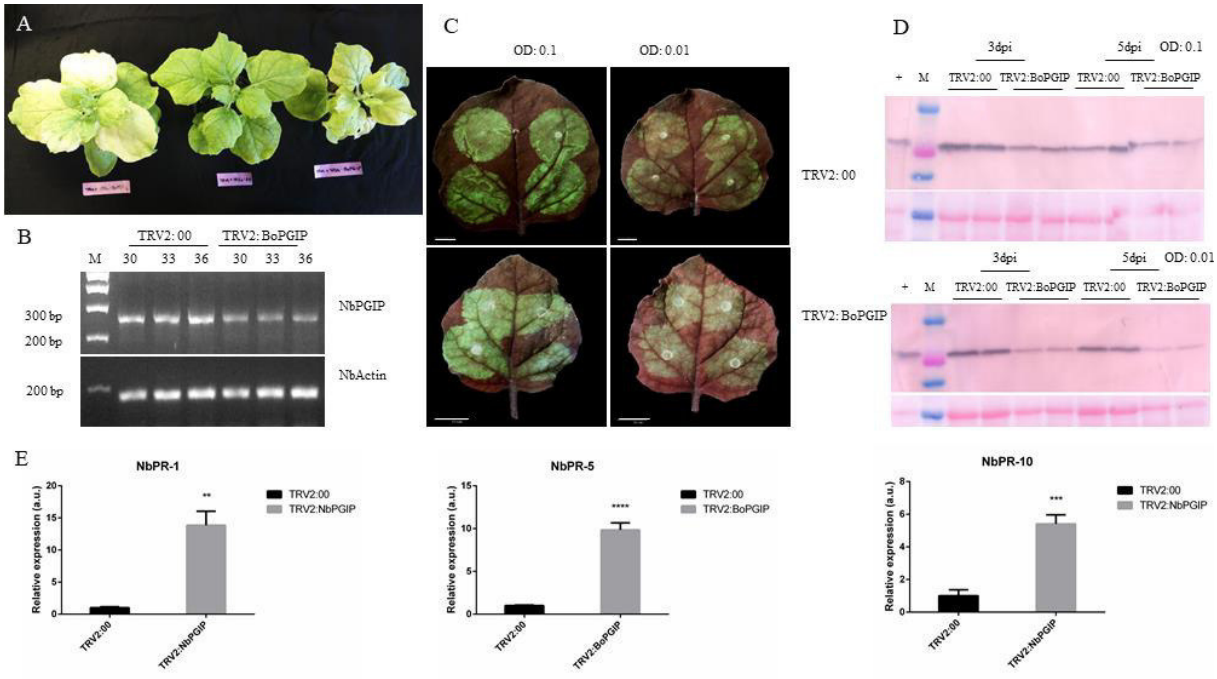


Fig. 4.8 TRV-mediated silencing of *PGIP* in *N. benthamiana*. (A) Representative *N. benthamiana* plants at 15 days post-inoculation (dpi) with a 1:1 mixture of pTRV1 plus pTRV2: BoPDS2 (pTRV2: BoPDS2) as marker, pTRV1 plus pTRV2: 00 (pTRV2: 00) as control, and pTRV1 plus pTRV2: BoPGIP (pTRV2: BoPGIP), from left to right. (B) Silencing of *PGIP* transcripts was analyzed in pTRV2: 00 and pTRV2: BoPGIP infected plants by semiquantitative RT-PCR. PCR products were analyzed at cycles 30, 33 and 36 on a 1.7% agarose gel. Delete the two lanes at the right from the two panels. (C) Visualization of GFP fluorescence under a UV lamp in pTRV2: 00 and pTRV2: BoPGIP infected plants at 3 days after infiltration (dai) with an *Agrobaterium* strain expressing GFP at OD_{600} = 0.1 or 0.01, as indicated. Scales were 10 mm. (D) Western blots analysis of GFP accumulation in pTRV2: 00 and pTRV2: BoPGIP infected plants at 3 and 5 dai. Lane M in the blots showed the molecular weight markers in kilodalton (kDa). The panels below the western blots show the membrane stained with Ponceau-S after blotting as control of loading. (E) Expression analysis of *NbPR-1*, *NbPR-5* and *NbPR-10* in pTRV2: 00 and pTRV2:

BoPGIP infected plants at 21 dai by qRT-PCR. *Nb18S* was used as reference gene. **, $P \leq 0.01$; ***, $P \leq 0.001$; and ****, $P \leq 0.0001$ indicated the significant difference.

4.4 Discussion

PGIP, a cell wall banding protein, from LRR superfamily, specifically inhibits PGs produced by pathogens like *A. tumefaciens* and fungus. *PGIP* is not classified as *PR*, but the expression of *PGIP* could be induced by both biotic and abiotic stimuli, and plays an indispensable role in plant defense. Overexpression of *PGIP* genes from bean, Chinese cabbage, pepper and cotton increased the tolerance to the fungi, like *B. sorokiniana, A.alternate* and *C. nicotianae, V. dahliae* and *F. oxysporum* f. sp. *vasinfectum* and the bacterium *P. carotovorum ssp. carotovorum* (Janni *et al*., 2008; Hwang *et al*., 2010; Wang *et al*., 2013; Liu *et al*., 2017). In this present study, the *HpPGIP* gene was identified and characterized from a forward subtracted cDNA library of *H. perforatum* L. suspension cells treated with *A. tumefaciens*. Overexpression of *HpPGIP* in *N. tabacum* led to greatly decreased expression efficiency of *A. tumefaciens* as assayed by GUS staining, indicating that *HpPGIP* participates in defense responses against *A. tumefaciens*. assays. Although it was reported that PG behaves as a virulence factor in the interaction of *A. tumefaciens* with grape (*Vitis vinifera*) (Rodriguez-Palenzuela, 1991), there was no report so far about the role of *PGIP* in defense against *A. tumefaciens*.

The HpPGIP protein was localized at the plasma membrane, cytoplasm and nucleus, as judged by the subcellular distribution of fluorescence derived from the transient expression of GFP-PGIP in *N. tabacum* leaves. Subcellular localization studies in rice and *Cynanchum komarovii* showed that PGIP is a non-transmembrane protein targeted to the plasma membrane (Wang *et al.*, 2015; Liu *et al*., 2016). The subcellular localization of HpPGIP at the plasma membrane might play an important role in defense responses as cell surface receptors that detect pathogens like *A. tumefaciens*, whose virulence depends on expression of PG (Rodriguez-Palenzuela, 1991). Our study demonstrates for the first time the subcellular localization of HpPGIP in nucleus, as had been reported for Hyp-1 from *H. perforatum* L. and PR-10 proteins from *Tamarix hispida* and *V. vinifera* (Zhang *et al*., 2010; He *et al*., 2013; Hou *et al*., unpublished).

To reveal *PGIP* evokes *A. tumefaciens* defense pathways in plant, the critical genes from the defense pathways described above were detected by qRT-PCR. As it is reported that the exogenous application of ABA, SA, JA increased the *PGIP* expression in plant, indicates that

the phytohormones may take a part in the *PGIP* defense function. Our qRT-PCR result suggests the fact of *HpPGIP* overexpression increases the *A. tumefaciens* defense has the possibility to involve into JA pathway by increasing the expression of *NtaLOX*, but not in auxin pathway since *HpPGIP* overexpression increased *NtaARF8* expression. JA, well-studied hormone mediates plant defense responses to pathogens. Exogenous application of JA induces rice *JIOsPR10* expression (Jwa *et al.*, 2001). As introduced in chapter 3, in auxin signaling pathway, high levels of *TIR* and *ARF* could increase IAA synthesis lead to cell wall expansion and stomatal opening to assist pathogen infection (Fu and Wang, 2011). Specifically, there are two groups of protein complexes in this signaling pathway, namely, Aux/IAA and TIR1/AFB. Pathogen produced IAA is recognized by TIR1 and activates TIR1/AFB to degrade Aux/IAA, which negatively regulates auxin signaling by binding and inhibiting ARFs, and release ARFs, which regulates transcription of auxin-responsive genes. While, plant IAA biosynthesis is induced by some ARFs and the increased IAA level causes plant cell wall expansion by inducing the expression of cell wall structural proteins EGases and XETs, which have the function in cell wall loosening to promote pathogens caused disease development. Moreover, auxin is involved into stomata open to allow some pathogens go through as gateways to colonize the interior of plant tissues. In the present study, transcripts of auxin-responsive gene *NtaAFR8* was remarkable induced when *HpPGIP* was overexpressed, which suggests that *HpPGIP* overexpression increases antibacterial defenses independent from auxin signaling pathway.

PR proteins have been defined as a group of plant specific-proteins accumulate to response pathogen infection. Overexpression of *HpPGIP* affects the expression levels of a series of PR genes, specially, *NtaPR1* and *NtaPR10* genes expression. In our present study, both expression of PRs was reduced, while overexpression cotton *PGIP* gene *GhPGIP1* in *Arabidopsis* increased *AthPR1* and *AthPR5* expression after inoculation with *V. dahliae* (Liu *et al.*, 2017).

Plant microRNAs as one of non-coding small RNAs present in gene silencing pathway to play a critical role in many aspects of plant development and immunity systems. *Arabidopsis* miR393 is the first microRNA discovered to participate antibacterial resistance (Navarro *et al*., 2006). Recently, miR393 and miR167 have been detected in *A. tumefaciens* infected tobacco plants (Dunoyer *et al.*, 2006; Pruss *et al.*, 2008; Nazari *et al.*, 2017). In our present study, microRNA-mediated gene silencing pathway involves into *HpPGIP* defense against *A. tumefaciens* since *NtaAGO1* expression was induced also first time reveals that *NtamiR164*, especially *NtamiR164c* also involved into this pathway. *MiR164* have been recognized into plant response to abiotic stresses in *Arabidopsis*, *Brassica*, rice and potato (Bhardwaj *et al*.,

2014; Fang *et al*., 2014; Park *et al*., 2017; Zhang *et al*., 2018). In biotic stress, transcriptional activity of miR164a promoter was induced during plant virus infection (Bazzini *et al.*, 2009). To best of our knowledge, this is first report that miR164c accumulated in *A. tumefaciens* defense gene overexpression transgenic tobacco plants.

Secondary metabolites found in plants have a significant role in defense against pathogens (Mazid *et al.*, 2011; Andersson, 2012; Goyal *et al.*, 2012). PAL is the core enzyme of phenylpropanoid pathway, which involves in the plant lignin and flavonoid biosynthetic pathways (Heldt and Piechulla, 2011; Dean *et al*., 2012). Lignin as a key constituent of plant call wall, plays a major role in plant structure defense mechanism against pathogens. In lignin biosynthetic pathway, there are important enzymes CCR and CAD have been characterized, which have been considered as the first and last enzymes of monolignol biosynthesis, respectively (Raes, 2003; Prasad *et al*., 2011). Flavonoid as the polyphenolic compound from plant secondary metabolites processes the function to defense against pathogens and CHS is a key enzyme which catalyzes the first committed step in the flavonoid biosynthesis pathway (El-kereamy *et al.*, 2011; Zhou *et al.*, 2013; Meng *et al.*, 2015; Yahyaa *et al.*, 2017). Most importantly, *HpPGIP* increases accumulation of lignin synthesis pathways genes *NtaPAL1,4*, *NtaCCR* and flavonoid pathway gene *NtaCHS* indicate that structure defense and flavonoid pathways are involved into *HpPGIP* overexpression plants against *A. tumefaciens*.

Plant defense mechanisms have another hallmark is synthesis and accumulation of ROS causes the hypersensitive reaction (HR). The increased expression of *NtaAPX* and *NtaFe-SOD*, demonstrates ROS pathway also participate into *A. tumefaciens* defense pathway.

To further discover and expand the knowledge about plant response to the infection of *A. tumefaciens*, *Hyp-1* another *A. tumefaciens* gene selected from the same subtractive cDNA library was fused with *HpPGIP* and the overexpressed in tobacco. Similarly, secondary metabolites and ROS pathways were confirmed to involve into *A. tumefaciens* defense pathway, differently, those two defense pathways were enriched in Hyp-1-PGIP plants by specially increasing the *NtaCAD* and *NtaCAT* expression respectively, besides the increasing expression of *NtaPAL1,4*, *NtaCCR* and *NtaCHS* and *NtaAPX* and *NtaFe-SOD.* It is very interesting that this phenomenon is not the simple superposition of *Hyp-1* and *HpPGIP*, since lignin synthesis and ROS pathway were not involved into *Hyp-1* overexpression plant defense against *A. tumefaciens*, not to mention the flavonoids synthesis pathway is even suppressed in those plants in another of our work (Hou *et al*., unpublished results). To further discover the molecular

mechanism how *Hyp-1* and *HpPGIP* interact to enrich the *A. tumefaciens* defense activities, there should be more researches carried out in the coming future. Our present study makes the preliminary contribution towards the defense activities. Moreover, the increased expression of *NtaLOX* and *NtaAGO1* indicate that JA signaling pathway and miroRNA-mediated gene silencing pathway were employed by *Hyp-1-PGIP* overexpressed plants to defense against *A. tumefaciens*. Furthermore, *NtaARF8* and *NtaTIR1* were particularly induced by the fusion genes in transgenic plants indicates that auxin signaling pathway is not recruited into *A. tumefaciens* defense pathway, conversely, which is employed by *Hyp-1*overexpression plant lines (Hou *et al*., unpublished results). Overexpression of *Hyp-1-PGIP* also interferes with the PR proteins and microRNA expression compared with *PGIP* single expressed plant samples.

To further investigate the functional characterization of *HpPGIP*, VIGS has been performed to knock down the *PGIP* expression. To silence the homologous gene of *HpPGIP*, the phylogenetic analysis has been carried out to select the candidate gene *BoPGIP*. Unfortunately, as the marker of gene silencing, the bleach symptom carried out by silencing of *BoPDS2* was not able to observe in *Brassica nigra* unlike described previously (Zhang *et al*., 2010). So, in our study, the candidate plant was changed into *N. benthamiana* to process the heterologous VIGS. Interestingly, our data presented that silencing of *HpPGIP* homologous gene of *BoPGIP* in *N. benthamiana* result in improved tolerance to *A. tumefaciens* rather than reducing the resistance. The data of qRT-PCR shown that knocking down *PGIP* expression lends to the increasing of *NbPRs* expression as the reason of enhanced resistance to *A. tumefaciens*. Our data agrees with that silencing of PR-10-like proteins in *M. truncatula* results in *MtPR5* accumulation in order to tolerate upon with *A. euteiches* infection (Colditz *et al.*, 2007). Besides, this result is consistent with our other data of silencing *Hyp-1* in *C. roseus* (Hou *et al*., unpublished results).

There are numerous studies about *PGIP* have been done in plant so far, especially in the interaction between plant and fungus, but it is few researches has been carried out to discover the function of PGIP-PGs between pant and bacterium even *A. tumefaciens* produce PGs to infect plants has been reported in 1991 (Rodriguez-Palenzuela, 1991). Here, there are the hypothetical roles of *PGIP* in antibacterial defense. PGIPs belong to the superfamily of LRR protein, a group of proteins are belived to be specialized for recognition of non-self-molecules and protein-protein interaction. LRR motif has been found in the proteins with the functions of resistance and defense against microbial pathogens in plant. The crystal structure of a PGIP from *Phaseolus vulgaris* reveals a negative charge on the surface of the LRR concave face,

which probably participates the function of binding PGs (Di Matteo *et al.*, 2003). Besides, PGIP as the cell wall banding proteins, well-know their fucntions in limiting cell wall degradation and pathogens invasion. In particular, PGIP specifilly regonize and inhibit PGs which are produced by bacteria and fungus to limit the destructive of PGs and accumulate OGs, which activate a wide range of defense responses. In our present study, those defense responses have been confirmed as the biosynthesis of lignin by inducing the expression of *PALs* and *CCR,* and the production of ROS by inducing *APX* and *Fe-SOD* expression. In addition, the increased expression of *CHS* from flavonoid synthesis pathway, provides the first report that the secondary metabolites like flavonoid make the contribution to response *Agrobacterium* defense in *HpPGIP* overexpression transgenic plants, besides the lignin. Moreover, HpPGIP protein was localized at nucleus by GFP-PGIP transient expression in *N. tabacum* leaves in our study, where is defense genes expression, to contribute the defense activity of *HpPGIP*. In our present work, it is first time provide the evidence that *HpPGIP* isolated from *H. perforatum* L. enhanced the *A. tumefaciens* tolerance infection in *HpPGIP* overexpression transgenic tobacco plants and reveals the possible defense pathways. The more detailed studies should be carried out in the coming future to knock the door of how the *HpPGIP* defense against *A. tumefaciens.*

In summary, *Agrobacterium*-mediated genetic transformation approaches that reduce *HpPGIP* expression in *H. perforatum* L. could give a better chance at efforts aimed at the genetic manipulation of this recalcitrant and medicinal plant spp. However, antagonistic regulation of PR proteins and that of other inducible defense-related proteins that result in enhanced resistance to *A. tumefaciens* should be taken into consideration. The present study provides a better understanding regarding the functional characterization of *PGIP* gene from *H. perforatum* L., and adds significant knowledge about the molecular mechanism of the *H. perforatum* L.-*A. tumefaciens* interaction.

4.5 Acknowledgments

The author acknowledges the financial support provided by the FCT-Portuguese Foundation for Science and Technology (SFRH/BD/52561/2014), under the Doctoral Programme "Agricultural Production Chains – from fork to farm" (PD/00122/2012), and by *Ministry of Economy and Competitiveness* of Spain (grant BIO2016-75619-R [AEI/FEDER, UE]) to T.C. and F.T.

We gratefully acknowledge Prof. Vincent L. Chiang and Dr. Rui Shi (North Carolina State University) kindly advised for the MicroRNA detection. We gratefully acknowledge Prof. Marcel Dicke (Wageningen University) kindly provided the maker vectors pTRV2: BoPDS2.

4.6 References

Anand, A., Uppalapati, S.R., Ryu, C.-M., Allen, S.N., Kang, L., Tang, Y. and Mysore, K.S. (2007) Salicylic acid and systemic acquired resistance play a role in attenuating crown gall disease caused by Agrobacterium tumefaciens. *Plant Physiol.* **146**, 703–715.

Andersson, P. (2012) Secondary metabolites associated with plant disease, plant defense and biocontrol.

Bagal, U.R., Leebens-Mack, J.H., Lorenz, W.W. and Dean, J.F.D. (2012) The phenylalanine ammonia lyase (PAL) gene family shows a gymnosperm-specific lineage. *BMC Genomics* **13**, S1.

Bashi, Z.D., Rimmer, S.R., Khachatourians, G.G. and Hegedus, D.D. (2013) Brassica napus polygalacturonase inhibitor proteins inhibit Sclerotinia sclerotiorum polygalacturonase enzymatic and necrotizing activities and delay symptoms in transgenic plants. *Can. J. Microbiol.* **59**, 79–86.

Bazzini, A.A., Almasia, N.I., Manacorda, C.A., Mongelli, V.C., Conti, G., Maroniche, G.A., Rodriguez, M. C., Distéfano, A. J., Hopp, H.E., Vas, M., and Asurmendi, S. (2009) Virus infection elevates transcriptional activity of miR164a promoter in plants. *BMC Plant Biol.* **9**.

Benedetti, M., Pontiggia, D., Raggi, S., Cheng, Z., Scaloni, F., Ferrari, S., Ausubel, F.M., Cervone, F. and Lorenzo, G. De (2015) Plant immunity triggered by engineered in vivo release of oligogalacturonides, damage-associated molecular patterns. *Proc. Natl. Acad. Sci.* **112**, 5533–5538.

Bhardwaj, A.R., Joshi, G., Pandey, R., Kukreja, B., Goel, S., Jagannath, A., Kumar, A., Katiyar-Agarwal, S. and Agarwal, M. (2014) A genome-wide perspective of miRNAome in response to high temperature, salinity and drought stresses in Brassica juncea (Czern) L. *PLoS One* **9**.

Butterweck, V., Christoffel, V., Nahrstedt, A., Petereit, F., Spengler, B. and Winterhoff, H. (2003) Step by step removal of hyperforin and hypericin: Activity profile of different Hypericum preparations in behavioral models. *Life Sci.* **73**, 627–639.

Colditz, F., Niehaus, K. and Krajinski, F. (2007) Silencing of PR-10-like proteins in Medicago truncatula results in an antagonistic induction of other PR proteins and in an increased tolerance upon infection with the oomycete Aphanomyces euteiches. *Planta* **226**, 57–71.

Diatchenko, L., Laut, Y.C., Campbellt, Chenchik, A., Moqadam, F., Huang, B., Lukyanov, S., Lukyanov, K., Gurskaya, N., Sverdlov, E. D., and Siebert, P. D. (1996) Suppression of subtractive hybridization: A method for generating differentially regulated or tissue-specific cDNA probes and libraries. *Proc. Natl. Acad. Sci.* **93**, 6025–6030.

Dunoyer, P., Himber, C. and Voinnet, O. (2006) Induction, suppression and requirement of RNA silencing pathways in virulent Agrobacterium tumefaciens infections. *Nat. Genet.* **38**, 258–263.

El-kereamy, A., El-sharkawy, I., Ramamoorthy, R., Taheri, A., Errampalli, D., Kumar, P. and Jayasankar, S. (2011) Prunus domestica pathogenesis-related protein-5 activates the defense response pathway and enhances the resistance to fungal infection. *PLoS One* **6**, 1–11.

Fang, Y., Xie, K. and Xiong, L. (2014) Conserved miR164-targeted NAC genes negatively regulate drought resistance in rice. *J. Exp. Bot.* **65**, 2119–2135.

Franklin, G., Conceição, L.F.R., Kombrink, E. and Dias, A.C.P. (2008) Hypericum perforatum plant cells reduce Agrobacterium viability during co-cultivation. *Planta* **227**, 1401–1408.

Franklin, G., Conceição, L.F.R., Kombrink, E. and Dias, A.C.P. (2009) Xanthone biosynthesis in Hypericum perforatum cells provides antioxidant and antimicrobial protection upon biotic stress. *Phytochemistry* **70**, 60–68.

Fu, J. and Wang, S. (2011) Insights into auxin signaling in plant-pathogen interactions. *Front. Plant Sci.* **2**, 1–7.

Gohlke, J. and Deeken, R. (2014) Plant responses to Agrobacterium tumefaciens and crown gall development. *Front. Plant Sci.* **5**, 1–11.

Goyal, S., Merillon, J. and Ramawat, K.G. (2012) Plant Defence: Biological Control,.

Heldt, H.-W. and Piechulla, B. (2011) Phenylpropanoids comprise a multitude of plant secondary metabolites and cell wall components. *Plant Biochem.*, 431–449.

He, M., Xu, Y., Cao, J., Zhu, Z., Jiao, Y., Wang, Y., Guan, X., Yang, Y., Xu, W., and Fu, Z. (2013) Subcellular localization and functional analyses of a PR10 protein gene from Vitis pseudoreticulata in response to Plasmopara viticola infection. *Protoplasma* 250, 129–140.

Hou, W., Shakya, P. and Franklin, G. (2016) A perspective on Hypericum perforatum genetic transformation. *Front. Plant Sci.* **7**, 1–12.

Hwang, B.H., Bae, H., Lim, H.S., Kim, K.B., Kim, S.J., Im, M.H., Park, B.S., Kim, D.S. and Kim, J. (2010) Overexpression of polygalacturonase-inhibiting protein 2 (PGIP2) of Chinese cabbage (Brassica rapa ssp. pekinensis) increased resistance to the bacterial pathogen Pectobacterium carotovorum ssp. carotovorum. *Plant Cell. Tissue Organ Cult.* **103**, 293–305.

Janni, M., Sella, L., Favaron, F., Blechl, A.E., Lorenzo, G. De and D'Ovidio, R. (2008) The expression of a bean PGIP in transgenic wheat confers increased resistance to the fungal pathogen *Bipolaris sorokiniana*. *Mol. Plant-Microbe Interact.* **21**, 171–177.

Jwa, N.S., Kumar Agrawal, G., Rakwal, R., Park, C.H. and Prasad Agrawal, V. (2001) Molecular cloning and characterization of a novel jasmonate inducible pathogenesis-related class 10 protein gene, JIOsPR10, from rice (Oryza sativa L.) seedling leaves. *Biochem. Biophys. Res. Commun.* **286**, 973–983.

Karppinen, K. (2010) Biosynthesis of hypericins and hyperforins in Hypericum perforatum L.(St. John's wort)—precursors and genes involved.

Lee, M.H., Jeon, H.S., Kim, H.G. and Park, O.K. (2017) An Arabidopsis NAC transcription factor NAC4 promotes pathogen-induced cell death under negative regulation by microRNA164. *New Phytol.* **214**, 343–360.

Liu, N., Zhang, X., Sun, Y., Wang, P., Li, X., Pei, Y., Li, F. and Hou, Y. (2017) Molecular evidence for the involvement of a polygalacturonase-inhibiting protein, GhPGIP1, in enhanced resistance to Verticillium and Fusarium wilts in cotton. *Sci. Rep.* **7**, 1–18.

Matteo, A. Di, Federici, L., Mattei, B., Salvi, G., Johnson, K.A., Savino, C., Lorenzo, G.

De, Tsernoglou, D. and Cervone, F. (2003) The crystal structure of polygalacturonase-inhibiting protein (PGIP), a leucine-rich repeat protein involved in plant defense. *Proc. Natl. Acad. Sci.* **100**, 10124–10128.

Mazid, M., Khan, T.A. and Mohammad, F. (2011) Role of secondary metabolites in defense mechanisms of plants. *Biol. Med.* **3**, 232–249.

Meng, C., Zhang, S., Deng, Y.S., Wang, G.D. and Kong, F.Y. (2015) Overexpression of a tomato flavanone 3-hydroxylase-like protein gene improves chilling tolerance in tobacco. *Plant Physiol. Biochem.* **96**, 388–400.

Miedes, E., Vanholme, R., Boerjan, W. and Molina, A. (2014) The role of the secondary cell wall in plant resistance to pathogens. *Front. Plant Sci.* **5**, 1–13.

Nazari, F., Safaie, N., Soltani, B.M., Shams-Bakhsh, M. and Sharifi, M. (2017) Bacillus subtilis affects miRNAs and flavanoids production in Agrobacterium-Tobacco interaction. *Plant Physiol. Biochem.* **118**, 98–106.

Navarro, L., Dunoyer, P., Jay, F., Arnold, B., Dharmasiri, N., Estelle, M., Voinnet, O., and Jones, J.D. (2006) A plant miRNA contributes to antibacterial resistance by repressing auxin signaling. *Science*. **312**(5772):436-9.

Pitzschke, A. (2013) Agrobacterium infection and plant defense—transformation success hangs by a thread. *Front. Plant Sci.* **4**, 1–12.

Prasad, N.K., Vindal, V., Kumar, V., Kabra, A., Phogat, N. and Kumar, M. (2011) Structural and docking studies of Leucaena leucocephala Cinnamoyl CoA reductase. *J. Mol. Model.* **17**, 533–541.

Pruss, G.J., Nester, E.W. and Vance, V. (2008) Infiltration with Agrobacterium tumefaciens induces host defense and development-dependent responses in the infiltrated zone. *Mol. Plant. Microbe. Interact.* **21**, 1528–1538.

Raak, C., Büssing, A., Gassmann, G., Boehm, K. and Ostermann, T. (2012) A systematic review and meta-analysis on the use of Hypericum perforatum (St. John's Wort) for pain conditions in dental practice. *Homeopathy* **101**, 204–210.

Raes, J. (2003) Genome-wide characterization of the lignification toolbox in Arabidopsis. *Plant Physiol.* **133**, 1051–1071.

Rodriguez-Palenzuela P, Burr TJ, Collmer A. (1991) Polygalacturonase is a virulence factor in Agrobacterium-tumefaciens biovar 3. *J. Bacteriol.* **173 (20)**, 6547–6552

Saddiqe, Z., Naeem, I. and Maimoona, A. (2010) A review of the antibacterial activity of Hypericum perforatum L. *J. Ethnopharmacol.* **131**, 511–521.

Shrivastava, M. and Dwivedi, L.K. (2015) Therapeutic potential of Hypericum perforatum: A review. *Int. J. Pharm. Sci. Res.* **6**, 1000–1006.

Srivastava, N. and Meshram, A. (2013) An insight into the molecular structure and function of Polygalacturonase inhibiting protein (PGIP). *Journal of Proteins and Proteomics*. **4**, 175–181.

Tatsis, E.C., Boeren, S., Exarchou, V., Troganis, A.N., Vervoort, J. and Gerothanassis, I.P. (2007) Identification of the major constituents of Hypericum perforatum by LC/SPE/NMR and/or LC/MS. *Phytochemistry* **68**, 383–393.

Wang, X., Zhu, X., Tooley, P. and Zhang, X. (2013) Cloning and functional analysis of three genes encoding polygalacturonase-inhibiting proteins from Capsicum annuum and transgenic CaPGIP1 in tobacco in relation to increased resistance to two fungal pathogens. *Plant Mol. Biol.* **81**, 379–400.

Yahyaa, M., Ali, S., Davidovich-Rikanati, R., Ibdah, M., Shachtier, A., Eyal, Y., Lewinsohn, E. and Ibdah, M. (2017) Characterization of three chalcone synthase-like genes from apple (Malus x domestica Borkh.). *Phytochemistry* **140**, 125–133.

Zhang, C., Feng, C., Wang, J., Kong, F. and Sun, W. (2016) Cloning , expression analysis and recombinant expression of a gene encoding a polygalac- turonase-inhibiting protein from tobacco , Nicotiana tabacum. *Hly*.

Zhang, L., Yao, L., Zhang, N., Yang, J., Zhu, X., Tang, X., Calderón-Urrea, A. and Si, H. (2018) Lateral root development in potato is mediated by Stu-mi164 regulation of NAC transcription factor. *Front. Plant Sci.* **9**, 383.

Zhang, R., Wang, Y., Liu, G. and Li, H. (2010) Cloning and characterization of a pathogenesis-related gene (ThPR10) from Tamarix hispida. Acta Biol. Cracoviensia Ser. Bot. 52, 17–25.

Zheng, S.J., Snoeren, T.A., Hogewoning, S.W., van Loon, J.J., and Dicke, M. (2010) Disruption of plant carotenoid biosynthesis through virus-induced gene silencing affects

oviposition behaviour of the butterfly Pieris rapae. *New Phytol* 733–745.

Zhou, B., Wang, Y., Zhan, Y., Li, Y. and Kawabata, S. (2013) Chalcone synthase family genes have redundant roles in anthocyanin biosynthesis and in response to blue/UV-A light in turnip (Brassica rapa; Brassicaceae). *Am. J. Bot.* **100**, 2458–2467.

Chapter 5

Transcriptional responses of *H. perforatum* L. cells upon co-cultivation with *A. tumefaciens* and comparison of gene expression in *H. perforatum* L. leaves and glands

This chapter is included in the following publication:

Weina Hou, Rupesh Kumar Singh, Viviana Martins, Francisco Tenllado, Alberto Carlos Pires Dias. (2018) Transcriptional responses of *Hypericum perforatum* L. cells upon co-cultivation with *Agrobacterium tumefaciens* and comparison of gene expression in *Hypericum perforatum* L. leaves and glands. To be submitted.

Chapter 5 Transcriptional responses of *H. perforatum* L. cells upon co-cultivation with *A. tumefaciens* and comparison of gene expression in *H. perforatum* L. leaves and glands

5.1 Summary

H. perforatum L., a perennial medicinal plant, is valued for its important therapeutic compounds produced as defense responses upon elicitation with *A. tumefaciens*, consisting of a good model for studying the molecular mechanisms underlying the recalcitrance of this plant species to infection. In the present study, the expression of core genes involved in plant defense pathways including secondary metabolism, gene silencing and ROS pathways was investigated by qRT-PCR, using as model *H. perforatum* L. suspension cells challenged with *A. tumefaciens*. Besides, the transcripts of two genes specifically associated to the defense response to *A. tumefaciens* infection, *Hyp-1*and *HpPGIP*, isolated from a forward subtractive cDNA library of *H. perforatum* L. cells elicited with *A. tumefaciens* were analyzed also. Results indicated that resistance of *H. perforatum* L. cells to infection by *A. tumefaciens* involves the overexpression of several genes encoding key enzymes of secondary metabolism, including those mediating not only the synthesis of xanthones, but also hypericin and melatonin. In addition, defense against infection by *A. tumefaciens* was influenced by inducing the transcripts expression of *HpAOX* from ROS pathway. *RNA-dependent RNA polymerases 6* (*RDR6*) and *Suppressor of Gene Silencing 3* (*SGS3*) associated gene silencing pathway, sense-post-transcriptional gene silencing (S-PTGS) and trans acting siRNAs (ta-siRNA) pathway together with *HpAGO5* were independent from *H. perforatum* L. defense against *A. tumefaciens* pathways. The two *A. tumefaciens* defense genes *Hyp-1* and *HpPGIP* were significant induced at 12h and reduced at 24h. This study was complemented by determining the expression of the same defense genes in *H. perforatum* L. plants with or without dark glands which are known to accumulate large amounts of secondary metabolites, hence contributing to plant defense ability. Gene expression data showed that gift host plant the resistance to pathogens by accumulation of secondary metabolites of xanthone and hypericin, moreover, by increasing the expression of the ROS pathway gene *HpCAT* and the defense genes *Hyp-1* and *HpPGIP*, respectively, was upregulated

in glands, suggesting that these genes may be involved in the resistance of *H. perforatum* L. to biotic stress.

5.2 Introduction

H. perforatum L. as a well-known medicinal plant, contains a wide range of biologically active secondary metabolites, which include hypericin, hyperforin, xanthones, melatonin, essential oils and a broad array of flavonoids (Butterweck *et al*., 2003; Tatsis *et al*., 2007; Karppinen, 2010; Saddiqe *et al*., 2010). The presence of glands is characterized as the secretory structure in *H. perforatum* L. plants, which are visible in leaf margins, stems, flower petals and stamens appear as black or dark-red multicellular nodules (Zobayed *et al.*, 2006). Some of the biologically active components are highly accumulated in glands in *H. perforatum* L. (Karppinen *et al*., 2008; Beerhues, 2011). *H. perforatum* L. has attracted attention due to its pharmacological properties like anti-depressant, anti-inflammatory, anti-viral, anti-cancer, and anti-bacterial activities (Patočka J, 2003; Tatsis *et al*., 2007; Saddiqe *et al*., 2010). The increased accumulation of important biocompounds was observed upon *A. tumefaciens* interaction as defense response in *H. perforatum L.* in our previous reports (Franklin *et al*., 2009; Hou *et al*., 2016). *H. perforatum* L. recalcitrance against *A. tumefaciens* was studied in suspension cell cultures using *A. tumefaciens* which could infect the cells while mortality of *A. tumefaciens* was observed as well as browning of cell cultures (Franklin *et al*., 2008; 2009; Hou *et al*., 2016). Previous findings suggested the production of antimicrobial secondary metabolites in *H. perforatum* L. may be reason of mortality and inability of *A. tumefaciens* to infect suspension cells.

Plant secondary metabolites have an essential role in defense against pathogens (Mazid *et al*., 2011; Goyal *et al*., 2012). The major active secondary metabolites-flavonoid, xanthone, hyperforin and hypericin are involved into polyketide derivatives, and the key reactions of their biosynthetic pathways are catalyzed by type III Polyketide synthases (PKSs) (Beerhues, 2011; He *et al.*, 2012). To date, five type III PKS proteins have been reported from genus *Hypericum*, include Chalcone synthase (CHS), Benzophenone synthase (BPS), Octaketide synthase (OKS), PKS1 and PKS2 (Karppinen and Hohtola, 2008; He *et al.*, 2012). CHS a superfamily of PKSs, is a key enzyme catalyzes the first committed step in the flavonoid biosynthesis pathway (El-

kereamy *et al*., 2011; Zhou *et al*., 2013; Meng *et al*., 2015; Yahyaa *et al*., 2017). Besides, PAL is the first enzyme of phenylpropanoid pathway, which involves the plant flavonoid biosynthetic pathways (Gaid *et al.*, 2012; Klejdus *et al.*, 2013). The biosynthesis of xanthone also occurs though phenylpropanoid pathway and BPS another superfamily of PKSs is employed as the critical enzyme to catalyze the carbon skeleton of xanthone (Liu *et al.*, 2003; Tocci *et al*., 2010; Belkheir *et al*., 2016). In previous study, the increased production of xanthone in *H. perforatum* L. cell suspension responded to *A. tumefaciens* co-cultivation had been reported and northern bot results showed the transcritional expression of *PAL*, *4CL* (*4-coumarate:CoA ligase*) and *BPS* were upregulated during this defense reaction (Franklin *et al.*, 2009; Hou *et al.*, 2016). OKS, is considered to form the precursor of hypericin in *H. perforatum* L. (El-kereamy *et al.*, 2011). *In situ hybridization* results confirmed the role of PSK2 as an OKS specifically expressed in the dark glands and participates in the synthesis of hypericin in *H. perforatum* L. (Karppinen *et al.*, 2008; Karppinen and Hohtola, 2008). PKS1 was identified highly correlated with hyperforin synthesis in *H. perforatum* L. (Rubin-Pitel *et al*. 2010; Crispin 2014). Belonging to another majoy group of secondary metabolites in *H. perforatum* L. is melatonin, which is considerd as an antioxidant or growth promoter; a putative melatonin biosynthetic pathway including 9 enzymes was described. In this pathway, Phosphoribosylanthranilate transferase (PAT) and Indole-3-glycerol phosphate synthase (IGPS) are two enzymes related with melatonin biosynthetic pathway (He *et al.*, 2012).

Plant defense against *A. tumefaciens* is very complicated and multifaceted, which includes not only secondary metabolites pathway, but also the gene silencing pathway. RNA silencing has an important role in defending against pantheon infection in plants. RNA silencing is induced by double-stranded RNA (dsRNA) which is subsequently processed by dsRNA-specific RNase III enzyme (Dicer-like protein) into 21-25 nucleotide (nt) long small interfering RNAs (siRNAs). Then the siRNAs are recruited into the RNA-induced silencing complex (RISC), including ARGONAUTE (AGO) proteins, to guide the sequence-specific degradation of complementary RNAs. In plants, RNA-dependent RNA polymerases (RDRs) have been reported to generate secondary siRNAs in order to amplify defense signals (Ahlquist, 2002; Li *et al.*, 2017). In RDRs-mediated RNA silencing pathway, Suppressor of Gene Silencing (SGS) is required to convert single-stranded to dsRNA to produce siRNAs (Li *et al.*, 2017). In Aribidopsis, RDR6 conjunction with SGS3 synthesis dsRNAs, diced by Dicer-like protein (DCLs) to produce siRNAs in sense-post-transcriptional gene silencing (S-PTGS) and trans

acting siRNAs (ta-siRNA) pathway to induce the gene silencing in plant host (Csorba *et al.*, 2009; Shimura and Pantaleo, 2011; Parent *et al.*, 2015).

Plant defense themselves from pathogens has another hallmark is generation of ROS both pathogenic, as well as symbiotic causes the hypersensitive reaction (HR). ROS comprise of enzymatic and non-enzymatic components, AOX and CAT are the key enzymatic components (Velada *et al*., 2016; Pandey *et al*., 2017).

Defense activation of *H. perforatum* L. against *A. tumefaciens* elicitation involves many signaling pathways and activation of various genes yet to be understood. In this study, the transcripts of the core genes encoding enzymes involved in the plant defense pathways described above were analyzed by quantitative real-time PCR in *H. perforatum* L. cell suspensions challenged with *A. tumefaciens.* Moreover, two genes specifically involved in the defense against *A. tumefaciens* encoding *Hyp-1* and *HpPGIP* which were selected from the forward subtractive cDNA library of *H. perforatum* L. suspensions elicited with *A. tumefaciens*, were also a target of study. In addition, gene expression was analyzed in dark glands obtained from *H. perforatum* L. seedlings to further understand their involvement in the plant defense responses.

5.3 Results

5.3.1 Expression of key genes involved in the defense of *H. perforatum* L. cells to *A. tumefaciens* elicitation

The production of secondary metabolites has been developed by plants as an important defense mechanism to protect themselves from pathogens in the natural world. To evaluate the possible involvement of *H. perforatum* L. defense against *A. tumefaciens* in this pathway, the expression of a series of genes involved in secondary metabolite synthesis was investigated. The transcriptional expression of *HpPAL*, the first enzyme of phenylpropanoid pathway, which involves flavonoid and xanthone biosynthetic pathways in *H. perforatum* L. was increased up 16 folds after 12 h of co-cultivation with *A. tumefaciens*, but no modifications were observed after 24 h compared to control (Fig. 5.1 A). The expression of the gene *HpCHS* involved in the

flavonoid synthesis pathway was downregulated by 25% after 12 h and this effect decreased by 77.5% after 24 h (Fig. 5.1 B). The expression of xanthone synthesis pathway-encoding gene *HpBPS* was upregulated by 29 folds in cell cultures after 12 h but this effect was not observed after 24 h (Fig. 5.1 C), having the same pattern as *HpPAL* (Fig. 5.1 A). The transcriptional level of *HpPKS1,* which encodes an hyperforin pathway enzyme, was downregulated significantly by 75% after 12 h and reached its lowest level reduced by 99% after 24 h (Fig. 5.1 D). The expression of the hypericin synthesis pathway genes *HpOKS* (Fig. 5.1 E) and *HpPKS2* (Fig. 5.1 F) both were increased up 6.5 folds and 39 folds, after 12 h, respectively, the latter being downregulated even after 24 h, as the same expression level as control of *HpOKS* and 4 folds compared with control of *HpPKS2*. The expression of two key genes involved in the melatonin synthesis pathway *HpPAT* (Fig. 5.1 G) and *HpIGPS* (Fig. 5.1 H) was also evaluated. Results showed that there were no significant differences in *HpPAT* expression during *A. tumefaciens* infection. Nevertheless, the transcriptional level of *HpIGPS* was increased significantly by 85.7% after 12 h elicitation with *A. tumefaciens*.

Besides, the putative biosynthesis pathways of flavonoids, xanthone, hyperforin, hypericin, and melatonin in *H. perforatum* L, was described respectively, in Fig. 5.2 A. Relative level expression of transcripts of core genes in those secondary methanolic biosynthesis pathways in *H. perforatum* L. showed by fold variation to present the intuitive results (Fig. 5.2 B). The core genes expression from xanthone, hypericin and melatonin are increased, while the gene from hypericin is decreased as well as one gene *PAL* is increased but *CHS* is reduced in flavonoids synthesis pathway.

The gene silencing pathway takes a significant role in plant defense against pathogens, hence the expression of several key genes involved in this process was evaluated, namely *HpRDR6* (Fig. 5.3 A) and *HpSGS3* (Fig. 5.3 B) and *HpAGO5* (Fig. 5.3 C). The results showed that *HpRDR6* transcript levels increased by 25% after 12 h elicitation. In contrast, the expression of *HpSGS3* was significantly downregulated 85% or 77.5% after12 or 24 h, respectively, whereas there was no significant difference of the expression of *HpAGO5* upon elicitation. And the relative level expression of transcripts of those genes was showed by fold variation in Fig. 5.3 D.

The ROS pathway is a major process underlying plants response to biotic stress. In this present study, the expression of *HpCAT* (Fig. 5.4 A) and *HpAOX* (Fig. 5.4 B), two genes encoding core

enzymes of the ROS pathway was studied. The transcriptional expression of *HpAOX* was upregulated 2 folds after 12 h of co-cultivation with *A. tumefaciens* but not after 24 h, while *HpCAT* expression was not significantly affected. The fold variation of those two gene is present in Fig. 5.4 C.

Two genes specifically associated to the defense response to *A. tumefaciens* infection were also a target in the present study, namely *Hyp-1* (Fig. 5.5 A) and *HpPGIP* (Fig. 5.5 B). Both genes were strongly upregulated by 24 folds and 9 folds from *HpHyp-1* and 24 folds and 3.8 folds from *HpPGIP* after 12 h or 24 h elicitation with *Agrobacterium*. The fold variation of those two gene is also present in Fig. 5.5 C.

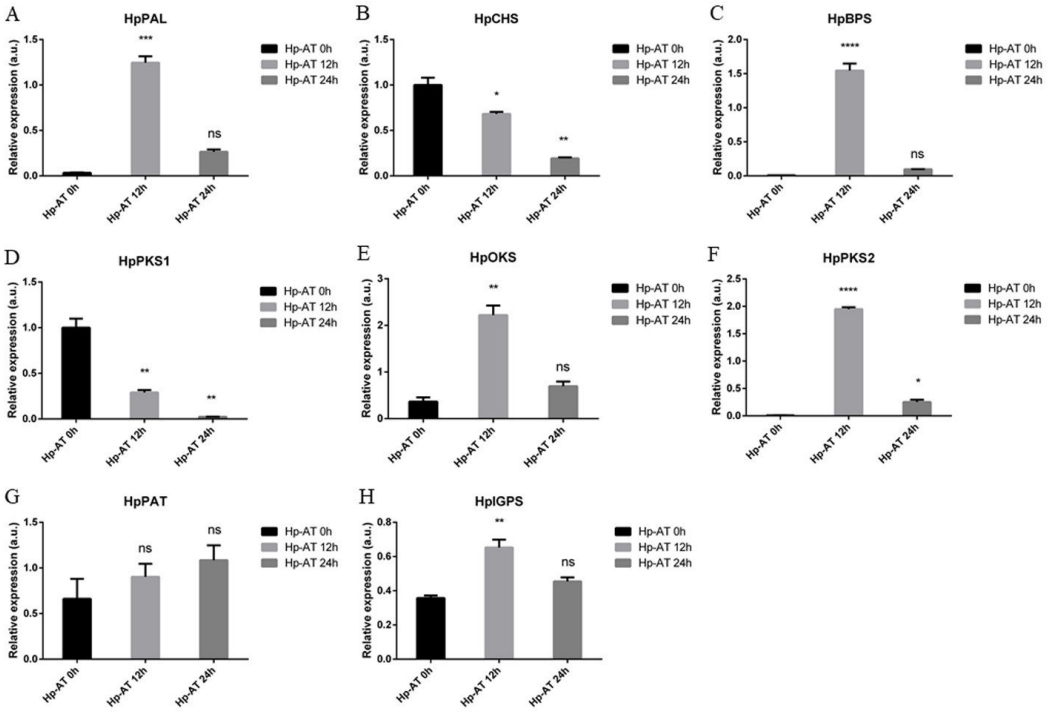


Fig. 5.1 Gene expression of key genes involved in secondary metabolites defense pathway detected by qRT-PCR. (A-B) Relative transcript level of *HpPAL* and *HpCHS* from flavonoid biosynthesis pathway. (C) Relative transcript level of *HpBPS* from xanthone biosynthesis pathway. (D) Relative transcript level of *HpPKS1* from hyperforin biosynthesis pathway. (E-F) Relative transcript levels of *HpOKS* and *HpPKS2* from hypericin biosynthesis pathway. (J-H) Relative transcript levels of *HpPAT* and *HpIGPS* from melatonin biosynthesis pathway. Asterisks denote the significance levels compared with control: *, $P \leq 0.05$; **, $P \leq 0.01$; ***, $P \leq 0.001$; ****, $P \leq 0.0001$ and ns denotes not significant.

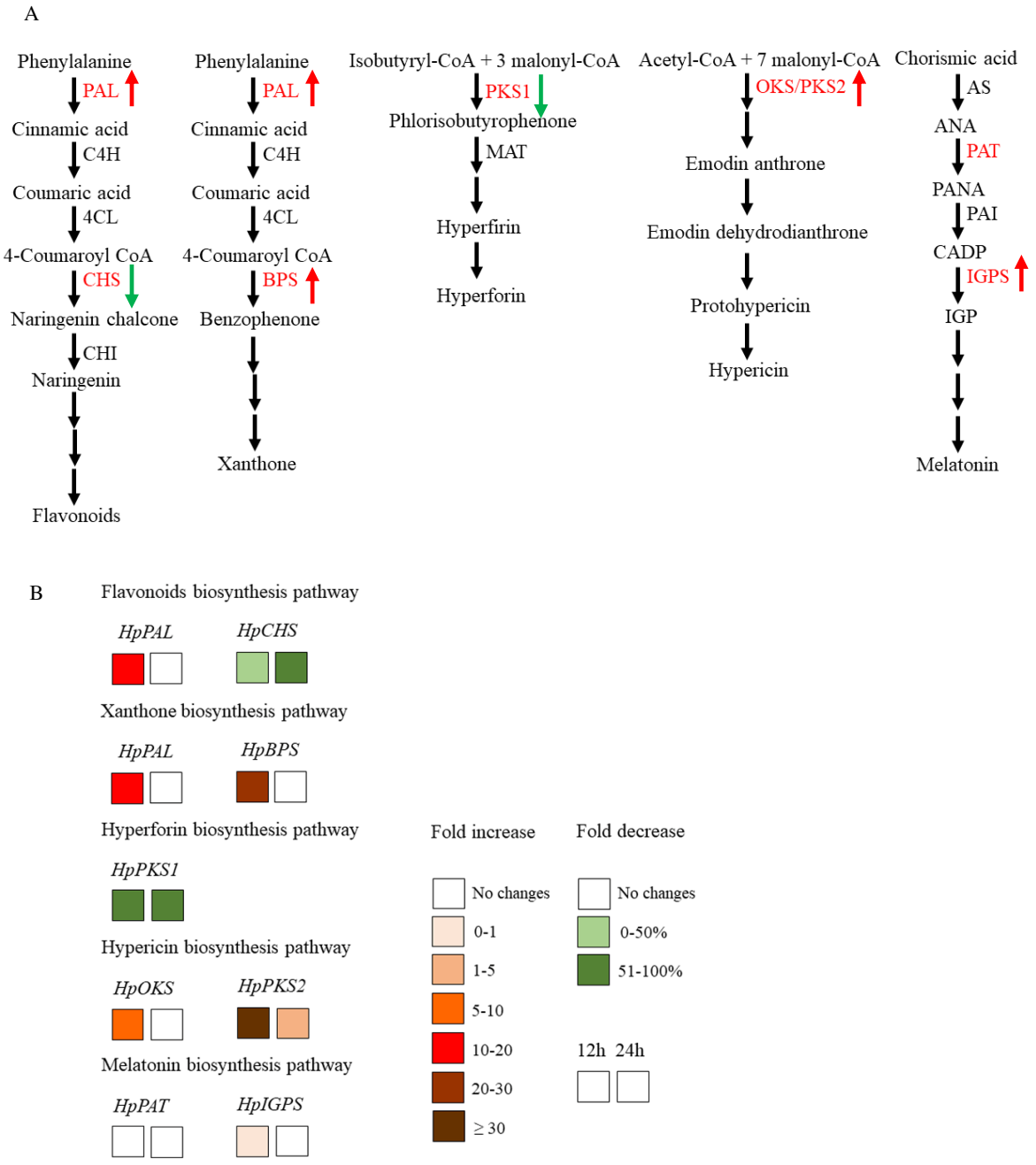


Fig. 5.2 Putative secondary metabolite synthesis pathway and fold variation in relative key genes from those pathways in *H. perforatum* L. (A) Putative biosynthesis pathways of flavonoids, xanthone, hyperforin, hypericin, and melatonin in *H. perforatum* L. PAL, Phenylalanine ammonia-lyase; C4H, Cinnamate 4-hydroxylase; 4CL, 4-coumarate-CoA ligase; CHS, Chalcone synthase; CHI, Chalcone isomerase; BPS, Benzophenone synthase; PKS1, Polyketide synthase 1; MAT, Dimethylallyltranstransferase; OKS, Octaketide synthase; PSK2, Polyketide synthase 2; AS,

Anthranilate synthase; PAT, Phosphoribosylanthranilate transferase; PAI, Phosphoribosylanthranilate isomerase; IGPS, Indole-3-glycerol phosphate synthase. The transcript levels of core enzymes from those pathways mark in red. Red arrow, denotes the increased expression of transcripts; Green arrow, denotes reduced the expression of transcripts. (B) Fold variation in relative transcript levels of key genes in flavonoids, xanthone, hyperforin, hypericin, and melatonin biosynthesis pathways in *H. perforatum* L.

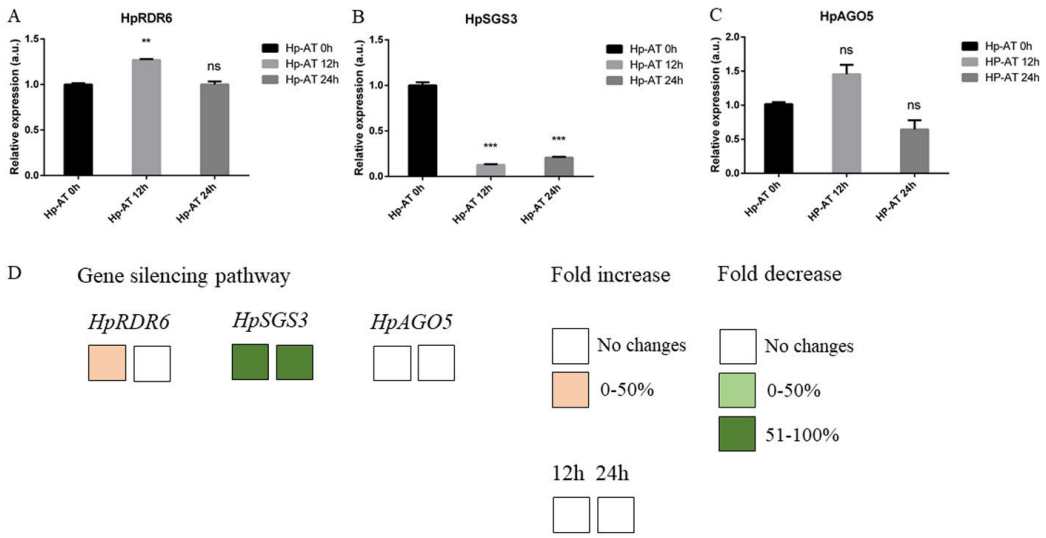


Fig. 5.3 Gene expression variation of key genes involved in gene silencing pathway. (A) Relative transcript level of *HpRDR6* detected by qRT-PCR. (B) Relative transcript level of *HpSGS3* detected by qRT-PCR. (C) Relative transcript level of *HpAGO5* detected by qRT-PCR. (D) Fold variation in relative level expression of transcripts in gene silencing pathway. Asterisks denote the significance levels compared with control: **, $P \leq 0.01$; ***, $P \leq 0.001$ and ns denotes not significant.

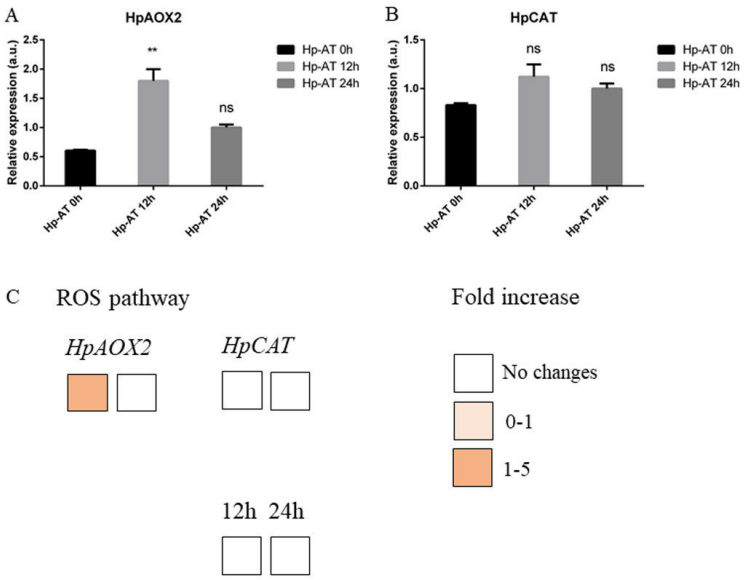


Fig. 5.4 Gene expression variation in ROS pathway. (A) Relative transcript level of *HpAOX2* detected by qRT-PCR. (B) Relative transcript level of *HpCAT* detected by qRT-PCR. (C) Fold variation in relative level expression of transcripts in ROS pathway. Asterisks denote the significance levels compared with control: **, $P \leq 0.01$ and ns denotes not significant.

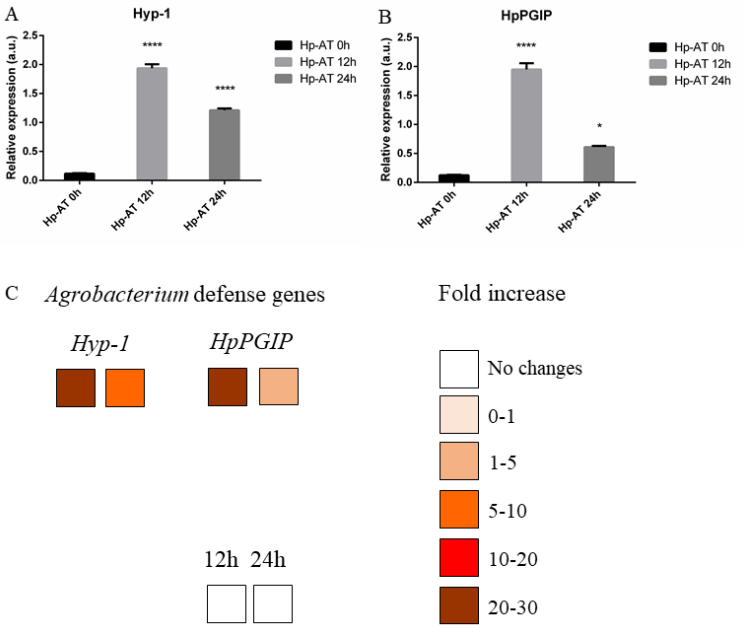


Fig. 5.5 Gene expression variation of *Agrobacterium* defense genes. (A) Relative transcript level of *Hyp-1* detected by qRT-PCR. (B) Relative transcript level of *HpPGIP* detected by qRT-PCR. (C) Fold variation in relative level expression of transcripts of *Agrobacterium* defense genes. Asterisks denote the significance levels compared with control: *, $P \leq 0.05$; ****, $P \leq 0.0001$ and ns denotes not significant.

5.3.2 Comparison the expression of key genes involved in the defense of *H. perforatum* L. plants in glands

To contribute the knowledge of the molecular mechanisms of *H. perforatum* L. defense against pathogens, the seedlings of *H. perforatum* L. with and without glands were collected and the expression of the target genes studied previously was investigated. The expression of *HpPAL* (Fig. 5.6 A) was present in both *H. perforatum* L. seedlings without and with glands samples, but not significantly different between them. The expressions of *HpCHS* (Fig. 5.6 B), showed lower expression by 25% in plants containing glands, while the xanthone pathway gene *HpBPS* (Fig. 5.6 C) was higher by 5 folds in glands. The transcriptional expression of hyperforin-responsive gene *HpPKS1* (Fig. 5.6 D) accumulated less by 25% in gland-containing plants; conversely the other two hypericin-responsive genes *HpOKS* (Fig. 5.6 E) and *HpPKS2* (Fig. 5.6 F) had highly accumulation in plants containing glands around 99 folds. Moreover, the transcriptional expression of melatonin-responsive genes *HpPAT* (Fig. 5.6 G) and *HpIGPS* (Fig. 5.6 H) was expressed in seedlings with and without glands samples without significantly difference. And the comparison of relative level expression of transcripts in secondary metabolite biosynthesis pathways described above in *H. perforatum* L. was showed by fold variation in Fig. 5.7.

The genes of *HpRDR6, HpSGS3* and *HpAGO5*, which were involved into gene silencing pathway, were equally expressed in seedlings with or without glands samples (Fig. 5.8).

Moreover, the ROS pathway gene *HpAOX2* (Fig. 5.9 A) was equally expressed in seedlings with or without glands, while *HpCAT* (Fig. 5.9 B) more expressed by 20% in plants containing glands, and the fold variation of those two gene is present in Fig. 5.9 C.

Finally, transcripts of both defense genes *HpHyp-1* (Fig. 5.10 A) and *HpPGIP* (Fig. 5.10 B) were accumulated in both plant samples with higher accumulation by 20% and 70% in plants containing glands, respectively. The fold variation of those two gene is shown in Fig. 5.10 C.

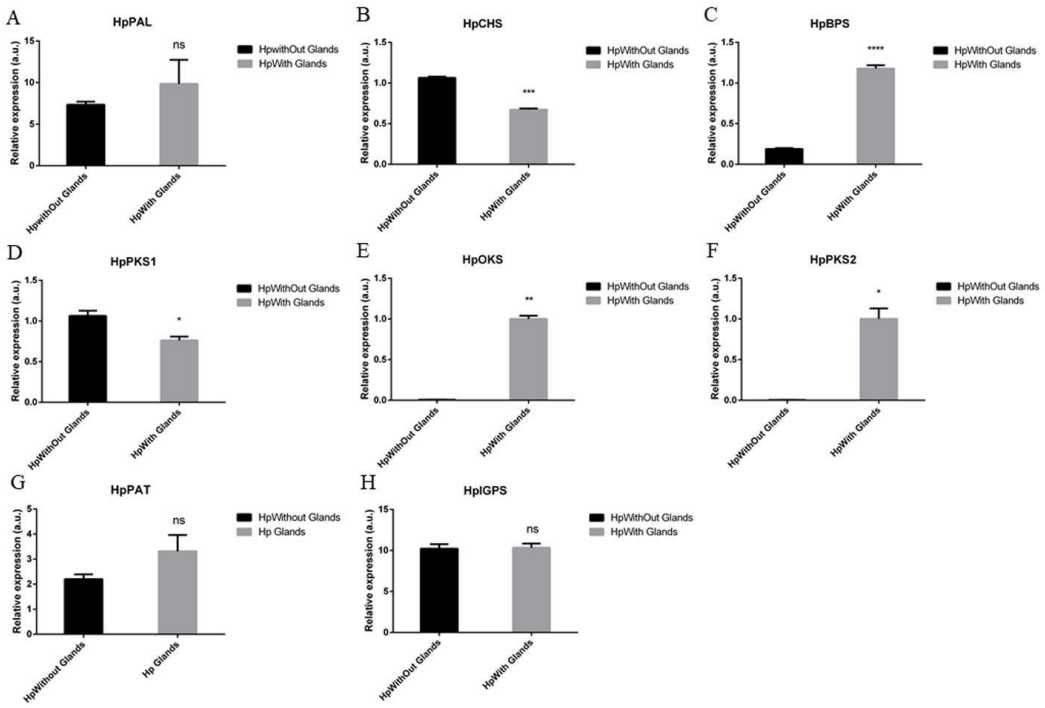


Fig. 5.6 Comparison the accumulation of core value genes from secondary metabolites pathways in *H. perforatum* L. leaves and glands by qRT-PCR. (A-B) Relative transcript level of *HpPAL* and *HpCHS* from flavonoid biosynthesis pathway. (A-C) Relative transcript level of *HpPAL* and *HpBPS* from xanthone biosynthesis pathway; d Relative transcript level of *HpPKS1* from hyperforin biosynthesis pathway. (E-F) Relative transcript levels of *HpOKS* and *HpPKS2* from hypericin biosynthesis pathway. (J-H) Relative transcript levels of *HpPAT* and *HpIGPS* from melatonin biosynthesis pathway. Asterisks denote the significance levels compared with control: *, $P \leq 0.05$; **, $P \leq 0.01$; ***, $P \leq 0.001$; ****, $P \leq 0.0001$ and ns denotes not significant.

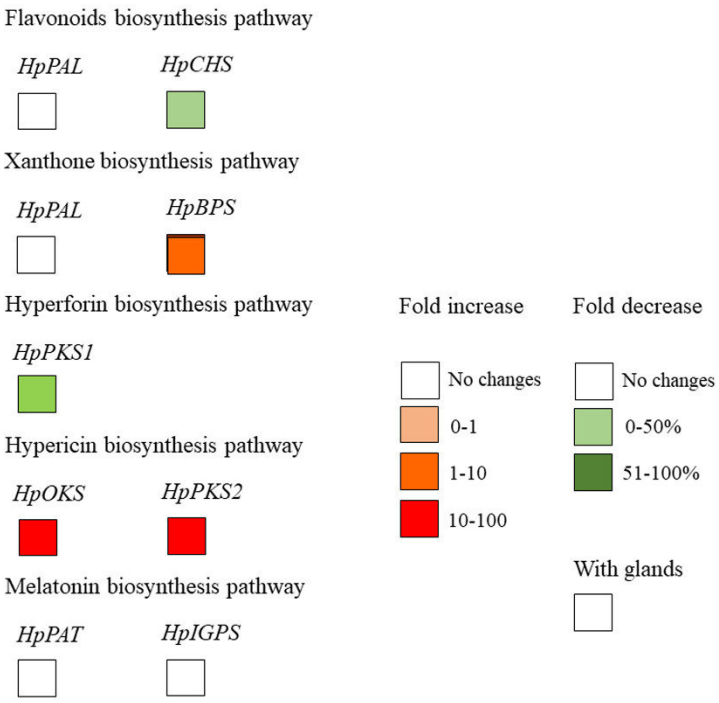


Fig. 5.7 Fold variation in comparison of relative level expression of transcripts in flavonoids, xanthone, hyperforin, hypericin, and melatonin biosynthesis pathways in *H. perforatum* L.

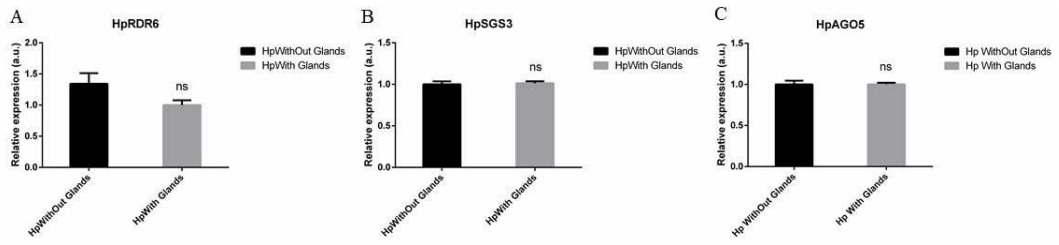


Fig. 5.8 Comparison of relative level expression of genes from gene silencing pathway in *H. perforatum* L. leaves and glands by qRT-PCR. (A) Relative transcript level of *HpRDR6*, (B) *HpSGS3* and (C) *HpAGO5* from gene silencing pathway. ns denotes not significant.

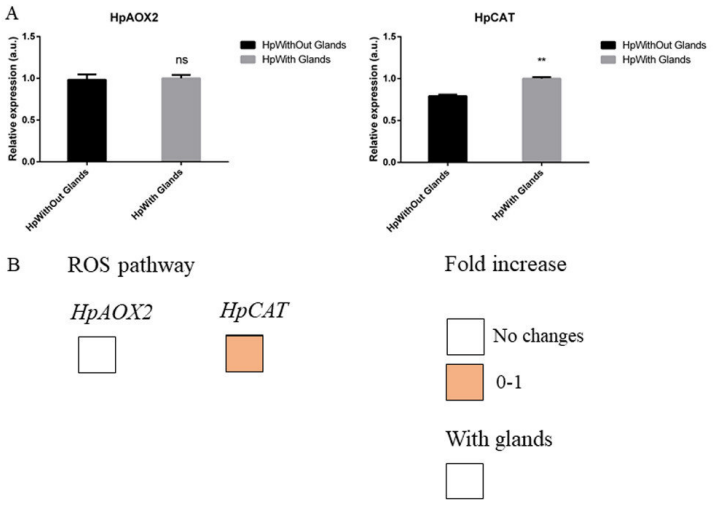


Fig. 5.9 Comparison of relative level expression of ROS pathway genes transcripts in *H. perforatum* L. leaves and glands by qRT-PCR. (A) Relative transcript level of *HpAOX2* and (B) *HpCAT* from ROS pathway. (C) Fold variation in comparison of relative level expression of transcripts in ROS pathways in *H. perforatum* L. Asterisks denote the significance levels compared with control: **, $P \leq 0.01$ and ns denotes not significant.

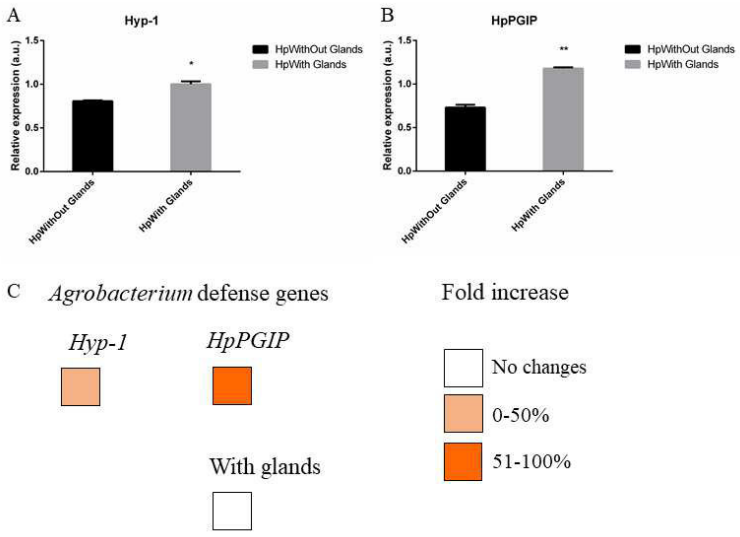


Fig. 5.10 Comparison of relative level expression of *Agrobacterium* defense genes in *H. perforatum* L. leaves and glands by qRT-PCR. (A) Relative transcript level of *Hyp-1* and (B) *HpPGIP*. (C) Fold variation in comparison of relative level expression of transcripts in *Agrobacterium* defense genes of *H. perforatum* L. Asterisks denote the significance levels compared with control: *, $P \leq 0.05$ and **, $P \leq 0.01$.

5.4 Discussion

A. tumefaciens is widely used to transfer genes into plant systems for functional genomics and genetic engineering purposes. However, as a bacterial pathogen, *A. tumefaciens* evokes a series of plant defense responses in *H. perforatum* L. and plant remains recalcitrant with still unclear mechanisms. So, the goal of this study was to understand the molecular mechanisms of *H. perforatum* L. defense at molecular level in reference to metabolite pathways against *A. tumefaciens.* In the present study, the results of qRT-PCR from *H. perforatum* L. cell suspension culture indicate that *H. perforatum* L. defense against *A. tumefaciens* go through the secondary metabolites pathway by synthesizing not only xanthone, but also hypericin and melatonin, which enriched the knowledge discovered previously (Franklin *et al.*, 2009). Moreover, ROS pathway has been verified that involve into *H. perforatum* L. resist to *A. tumefaciens* by inducing the key gene expression of *HpAOX2*. In addition, the transcripts of defense genes in glands reveal that glands gift *H. perforatum* L. the resistance to pathogens by accumulation of secondary metabolites of xanthone and hypericin, meanwhile, increasing the expression of ROS pathway gene *HpCAT* and *A. tumefaciens* defense genes *HpHyp-1* and *HpPGIP.*

In our previous report, *A. tumefaciens* interaction with *H. perforatum* L. suspension cell cultures showed 99% mortality of bacterium after 12 h cocultivation period by biphasic ROS burst and leading to browning of *Hypericum* cells (Franklin *et al.*, 2008). Additionally, some important genes (*HpPAL*, *HpBPS*) were observed being upregulated and may lead to differential metabolic profile in invaded cells. Results of our previous and present study support the direct involvement of xanthones in this mechanism while still independent of flavonoid pathway. Hyperforin was also unaffected in present study. *HpOKS*, *HpPKS2* and *HpIGPS* gene expression were observed increasingly expressed and suggested that hypericin and melatonin biosynthesis pathways may be key pathways to maintain recalcitrance in *H. perforatum L.* too. In addition, in RDR6 and SGS3 associated gene silencing pathways, the significant decreasing of *HpSGS3* indicates that S-PTGS and ta-siRNA pathways are independent from *A. tumefaciens* defense pathway in *H. perforatum L.* Besides, AGO5 which associate with short RNAs containing a 5-terminal cytosine and has been reported responses antiviral in Arabidopsis (Shimura and Pantaleo, 2011; Zhang *et al.*, 2015). In our study, there is no significant changes in the samples which revealed *HpAGO5* has no contribution to *H. perforatum L.* resist to *A.*

tumefaciens. Besides, the highly expression of *HpHyp-1* and *HpPGIP* which were selected from *H. perforatum L.* defense against *A. tumefaciens* cDNA library confirmed the *A. tumefaciens* defense function of those two genes. Moreover, the genes *HpPAL*, *HpBPS*, *HpOKS*, *HpPKS2*, *HpIGPS*, *HpAOX2*, *HpHyp-1* and *HpPGIP* were present increasing expression at 12 h and reduced by 24 h indicates the roles in mortality of *A. tumefaciens* by producing antibacterial compounds from secondary metabolites pathways, producing ROS burst and inducing defense genes expression as 99% bacterium morality was reported at 12 h.

Pathway engineering of important biocompounds in *H. perforatum* L. has major limitations due to very less information about their regulations at molecular level. For instance, hypericin was reported decades ago but genes involved behind production and accumulation in dark glands is still unclear. In this direction, present study sheds light and increase knowledge about this interaction mechanism at molecular level. *HpPAL* high expressed in both *H. perforatum* L. leaves and glands, together with *HpBPS*, *HpOKS* and *HpPKS2* were increasingly expressed in dark glands and suggested their role in increasing production of xanthones and accumulation of hypericin in dark glands. *HpCHS* and *HpPKS1* were found low expressed in dark glands, while *HpPAT*, *HpIGPS* showed no significant difference in their expression in dark glands, suggested their exclusion from biocompound accumulation of flavonoids neither melatonin specifically in dark glands. Besides, there was no significant difference expression of *HpRDR6*, *HpSGS3* and *HpAGO5* between *H. perforatum* L. leaves and glands, indicated that gene silencing pathways of S-PTGS and ta-siRNA pathway as well as *HpAGO5* were excluded out *H. perforatum* L. tissue specific defense mechanisms especially in glands. In addition, the induced expression of *HpCAT* in glands, indicated that the ROS pathway was employed by black glands. Most interesting genes were *HpHyp-1* and *HpPGIP* which were found in subtracted cDNA library of *H. perforatum* L. suspension cells challenged with *A. tumefaciens*. Both genes were found expressed in *H. perforatum* L. leaves and glands and upregulated in dark glands as well as against *A. tumefaciens* invasion. The present study, indicate that the black glands make the contribution to *H. perforatum* L. resists the *A. tumefaciens* not only producing xanthones and accumulation of hypericin but also inducing the *A. tumefaciens* defense genes expression.

Our results indicate that glands as the characterized secretory structure of *H. perforatum* L. empowered the plant defense activities. In short, glands of *H. perforatum* L. gift the resistance

to pathogens by accumulation of secondary metabolites of xanthone and hypericin, by increasing the expression of ROS pathway gene *HpCAT* and the defense genes *Hyp-1* and *HpPGIP*, respectively.

5.5 Acknowledgements

The author acknowledges the financial support provided by the FCT-Portuguese Foundation for Science and Technology (SFRH/BD/52561/2014), under the Doctoral Programme "Agricultural Production Chains – from fork to farm" (PD/00122/2012).

5.6 References

Ahlquist, P. (2002) RNA-dependent RNA polymerases, viruses, and RNA silencing. *Science (80-.).* **296**, 1270–1273.

Beerhues, L. (2011) Biosynthesis of the active Hypericum perforatum constituents. *Med. Aromat. Plant Sci. Biotechnol.* **5**, 70–77.

Belkheir, A.K., Gaid, M., Liu, B., Hänsch, R. and Beerhues, L. (2016) Benzophenone synthase and chalcone synthase accumulate in the mesophyll of Hypericum perforatum leaves at different developmental stages. *Front. Plant Sci.* **7**, 1–9.

Butterweck, V., Christoffel, V., Nahrstedt, A., Petereit, F., Spengler, B. and Winterhoff, H. (2003) Step by step removal of hyperforin and hypericin: Activity profile of different Hypericum preparations in behavioral models. *Life Sci.* **73**, 627–639.

Crispin, M.C. (2014) Metabolism and localization of polyketides in the genus Hypericum. *ProQuest Diss. Theses*, 251.

Csorba, T., Pantaleo, V. and Burgyán, J. (2009) RNA Silencing: An Antiviral Mechanism. **75**, 35–230.

El-kereamy, A., El-sharkawy, I., Ramamoorthy, R., Taheri, A., Errampalli, D., Kumar, P. and Jayasankar, S. (2011) Prunus domestica pathogenesis-related protein-5 activates

the defense response pathway and enhances the resistance to fungal infection. *PLoS One* **6**, 1–11.

Franklin, G., Conceição, L.F.R., Kombrink, E. and Dias, A.C.P. (2008) Hypericum perforatum plant cells reduce Agrobacterium viability during co-cultivation. *Planta* **227**, 1401–1408.

Franklin, G., Conceição, L.F.R., Kombrink, E. and Dias, A.C.P. (2009) Xanthone biosynthesis in Hypericum perforatum cells provides antioxidant and antimicrobial protection upon biotic stress. *Phytochemistry* **70**, 60–68.

Gaid, M.M., Sircar, D., Muller, A., Beuerle, T., Liu, B., Ernst, L., Hansch, R. and Beerhues, L. (2012) Cinnamate:CoA ligase initiates the biosynthesis of a benzoate-derived xanthone phytoalexin in Hypericum calycinum cell cultures. *Plant Physiol.* **160**, 1267–1280.

Galla, G., Vogel, H., Sharbel, T.F. and Barcaccia, G. (2015) De novo sequencing of the Hypericum perforatum L. flower transcriptome to identify potential genes that are related to plant reproduction sensu lato. *BMC Genomics* **16**, 1–22.

Goyal S., Lambert C., Cluzet S., Mérillon J.M., and Ramawat K.G. (2012) Secondary metabolites and plant defence. In: Mérillon J., Ramawat K. (eds) Plant Defence: Biological Control. Progress in Biological Control, vol 12. Springer, Dordrecht

He, M., Wang, Y., Hua, W., Zhang, Y. and Wang, Z. (2012) De novo sequencing of Hypericum perforatum transcriptome to identify potential genes involved in the biosynthesis of active metabolites. *PLoS One* **7**, 1–10.

Hou, W., Shakya, P. and Franklin, G. (2016) A Perspective on Hypericum perforatum genetic transformation. *Front. Plant Sci.* **7**, 1–12.

Jepson, C., Karppinen, K., Daku, R.M., Sterenberg, B.T. and Suh, D.Y. (2014) Hypericum perforatum hydroxyalkylpyrone synthase involved in sporopollenin biosynthesis - phylogeny, site-directed mutagenesis, and expression in nonanther tissues. *FEBS J.* **281**, 3855–3868.

Karppinen, K. (2010) Biosynthesis of hypericins and hyperforins in Hypericum perforatum L.(St. John's wort)—precursors and genes involved.

Karppinen, K. and Hohtola, A. (2008) Molecular cloning and tissue-specific expression of two cDNAs encoding polyketide synthases from Hypericum perforatum. *J. Plant Physiol.* **165**, 1079–1086.

Karppinen, K., Hokkanen, J., Mattila, S., Neubauer, P. and Hohtola, A. (2008) Octaketide-producing type III polyketide synthase from Hypericum perforatum is expressed in dark glands accumulating hypericins. *FEBS J.* **275**, 4329–4342.

Klejdus, B., Kováčik, J. and Babula, P. (2013) PAL inhibitor evokes different responses in two Hypericum species. *Plant Physiol. Biochem.* **63**, 82–88.

Li, F., Wang, Y. and Zhou, X. (2017) SGS3 cooperates with RDR6 in triggering geminivirus-induced gene silencing and in suppressing geminivirus infection in Nicotiana Benthamiana. *Viruses* **9**.

Liu, B., Falkenstein-Paul, H., Schmidt, W. and Beerhues, L. (2003) Benzophenone synthase and chalcone synthase from Hypericum androsaemum cell cultures: cDNA cloning, functional expression, and site-directed mutagenesis of two polyketide synthases. *Plant J.* **34**, 847–855.

Mazid, M., Khan, T.A. and Mohammad, F. (2011) Role of secondary metabolites in defense mechanisms of plants. *Biol. Med.* **3**, 232–249.

Meng, C., Zhang, S., Deng, Y.S., Wang, G.D. and Kong, F.Y. (2015) Overexpression of a tomato flavanone 3-hydroxylase-like protein gene improves chilling tolerance in tobacco. *Plant Physiol. Biochem.* **96**, 388–400.

Pandey, S., Fartyal, D., Agarwal, A., Shukla, T., James, D., Kaul, T., Negi, Y.K., Arora, S. and Reddy, M.K. (2017) Abiotic stress tolerance in plants: Myriad roles of Ascorbate peroxidase. *Front. Plant Sci.* **8**, 1–13.

Parent, J.S., Jauvion, V., Bouché, N., Béclin, C., Hachet, M., Zytnicki, M. and Vaucheret, H. (2015) Post-transcriptional gene silencing triggered by sense transgenes involves uncapped antisense RNA and differs from silencing intentionally triggered by antisense transgenes. *Nucleic Acids Res.* **43**, 8464–8475.

Patočka J (2003) The chemistry, pharmacology, and toxicology of the biologically active constituents of the herb Hypericum perforatum L. *J. Appl. Biomed.* **1**, 61–70.

Raak, C., Büssing, A., Gassmann, G., Boehm, K. and Ostermann, T. (2012) A systematic review and meta-analysis on the use of Hypericum perforatum (St. John's Wort) for pain conditions in dental practice. *Homeopathy* **101**, 204–210.

Rubin-Pitel, S.B., Luo, Y., Lee, J.-K. and Zhao, H. (2010) A diverse family of Type III polyketide synthases in Eucalyptus species. *Mol. Biosyst.* **6**, 1444–6.

Saddiqe, Z., Naeem, I. and Maimoona, A. (2010) A review of the antibacterial activity of Hypericum perforatum L. *J. Ethnopharmacol.* **131**, 511–521.

Shimura, H. and Pantaleo, V. (2011) Viral induction and suppression of RNA silencing in plants. *Biochim. Biophys. Acta - Gene Regul. Mech.* **1809**, 601–612.

Tatsis, E.C., Boeren, S., Exarchou, V., Troganis, A.N., Vervoort, J. and Gerothanassis, I.P. (2007) Identification of the major constituents of Hypericum perforatum by LC/SPE/NMR and/or LC/MS. *Phytochemistry* **68**, 383–393.

Tocci, N., Ferrari, F., Santamaria, A.R., Valletta, A., Rovardi, I. and Pasqua, G. (2010) Chitosan enhances xanthone production in Hypericum perforatum subsp. angustifolium cell cultures. *Nat. Prod. Res.* **24**, 286–293.

Velada, I., Cardoso, H.G., Ragonezi, C., Nogales, A., Ferreira, A., Valadas, V. and Arnholdt-Schmitt, B. (2016) Alternative oxidase gene family in Hypericum perforatum L.: characterization and expression at the post-germinative phase. *Front. Plant Sci.* **7**, 1–16.

Velada, I., Ragonezi, C., Arnholdt-Schmitt, B. and Cardoso, H. (2014) Reference genes selection and normalization of oxidative stress responsive genes upon different temperature stress conditions in hypericum perforatum L. *PLoS One* **9**, 1–24.

Yahyaa, M., Ali, S., Davidovich-Rikanati, R., Ibdah, M., Shachtier, A., Eyal, Y., Lewinsohn, E. and Ibdah, M. (2017) Characterization of three chalcone synthase-like genes from apple (Malus x domestica Borkh.). *Phytochemistry* **140**, 125–133.

Zhang, C., Wu, Z., Li, Y. and Wu, J. (2015) Biogenesis, function, and applications of virus-derived small RNAs in plants. *Front. Microbiol.* **6**, 1–12.

Zhou, B., Wang, Y., Zhan, Y., Li, Y. and Kawabata, S. (2013) Chalcone synthase family

genes have redundant roles in anthocyanin biosynthesis and in response to blue/UV-A light in turnip (Brassica rapa; Brassicaceae). *Am. J. Bot.* **100**, 2458–2467.

Zobayed, S.M.A., Afreen, F., Goto, E. and Kozai, T. (2006) Plant-environment interactions: Accumulation of hypericin in dark glands of Hypericum perforatum. *Ann. Bot.* **98**, 793–804.

Chapter 6

General Discussion and Future Prospects

Chapter 6 General discussion and future prospects

6.1 General discussion

6.1.1 Hyp-1 localizes to the plasma membrane, cytoplasm and nucleus and overexpression of *Hyp-1* alters expression of defense-related genes to modulates recalcitrance to *A. tumefaciens*

In the present study, *Hyp-1* was selected from a forward subtracted cDNA library of *H. perforatum* L. suspension cells, treated with *A. tumefaciens.* The function of *Hyp-1* as a member of the PR-10 gene family has been barely studied (Košuth *et al.*, 2013). *Hyp-1* overexpression was carried out in tobacco and in lettuce to unveil its participation in defense against *A. tumefaciens*. Efficiencies of *A. tumefaciens* infection was greatly decreased in all transgenic plants by GUS staining assay, indicating that *Hyp-1* participates in defense responses against *A. tumefaciens*. Besides, transgenic tobacco plants expressing a C-terminal truncated version of the protein were used to study the contribution of the first 80 aa to the antibacterial activity of Hyp-1. Defense activities towards *A. tumefaciens* were highly reduced in GFP-Hyp-1-N transgenic plants, suggesting that the N terminal part of Hyp-1 is not enough to contribute to the biological function of the Hyp-1 protein. The importance of maintaining Hyp-1 protein integrity could be interpreted in the light of studies on the crystal structure of Hyp-1. Several structural motifs form a huge cavity within the protein interior to bound various hydrophobic ligands, like plant hormone cytokinin (Michalska *et al.*, 2010), and the characteristic Bet.v.1 domain positioned at 89-120 aa residues in Hyp-1 (Bais *et al.*, 2003), are lacking in the Hyp-1mutant which results in the loss of biological activity.

In the present study, it was demonstrated that Hyp-1 protein was localized at the plasma membrane, nucleus and cytoplasm, by the subcellular distribution of fluorescence derived from the transient expression of GFP-Hyp-1 in *N. tabacum* leaves. Moreover, confirmation of the integrity of the full-length fusion protein in GFP-Hyp-1 transgenic plants by Western blot confirmed that the nuclear visualization of GFP fluorescence was due to Hyp-1 accumulation in nucleus rather than the import of free GFP cleaved from the fusion protein. This study demonstrated for the first time the subcellular localization of Hyp-1 in nucleus. The nuclear localization of Hyp-1 might play an important role in defense responses against invading

pathogens, especially in pathogens like *A. tumefaciens*, whose virulence depends on integration of T-DNA into the nucleus.

A. tumefaciens as a microbial pathogen provokes a series of plant defense responses, while understanding how these responses affect pathogen infection is still unclear (Pitzschke, 2013). To survey which plant defense responses could be involved in *Hyp-1*-mediated defense against *A. tumefaciens*, the expression levels of core genes from different pathways including auxin metabolism, microRNA-mediated gene silencing, lignin deposition, secondary metabolites, ROS signaling, and pathogenesis-related proteins, were determined in GFP-Hyp-1 tobacco plants. In the present study, transcripts of auxin-responsive genes *NtaTIR1* and *NtaAFR8* were remarkably reduced when *Hyp-1* was overexpressed, which suggests that *Hyp-1* overexpression could contribute to antibacterial defenses by reducing auxin signaling. Besides, overexpression of *Hyp-1* in transgenic plants led to a decrease in the transcriptional levels of *NtaAGO1* and two microRNAs, *NtamiR164ab* and *NtamiR160*. A recent report suggested that miR164 and target gene *NAC4* regulate cell death during plant-pathogen interactions, possibly by repressing GDSL lipase 1 which is an important regulator of plant immune responses (Lee *et al.*, 2017). MiR160 targets *ARF10*, *ARF16* and *ARF17* to down regulate auxin signaling, which in turn protect plants against bacteria and fungi (Pinweha *et al.*, 2015; Wójcik *et al.*, 2017). The results obtained offer preliminary evidence for the involvement of those two microRNAs in the regulation of plant defense against *A. tumefaciens* that need to be further investigated. The key genes involved in the lignin and flavonoids biosynthesis pathways, *NtaPAL1,4, NtaCCR*, *NtaCAD* and *NtaCHS,* were monitored in *Hyp-1* overexpressing plants. Our findings showed that *Hyp-1* overexpression in transgenic plants downregulated the expression of genes involved in the phenylpropanoid pathway (*NtaPAL1,4* and *NtaCHS*), whereas *NtaCCR* and *NtaCAD* were not changed, suggesting that overexpressing of *Hyp-1* increased the tolerance to *A. tumefaciens* independently from synthesis of lignin and flavonoids. Similarly, ROS signaling did not seem to play a significant role in *Hyp-1*-mediated defense against *A. tumefaciens* since the transcript levels of core enzymes were unaltered (*NtaAPX*, *NtaCAT)* or repressed (*NtaFe-SOD)* in *Hyp-1* overexpressing plants. Nevertheless, although *Hyp-1* overexpression could induce wide changes in the *gene expression* pattern of defense genes, not all of these changes are necessarily involved in the molecular mechanisms underlying *Hyp-1*-mediated antibacterial defense.

To further verify the role of *Hyp-1* in defense responses against *A. tumefaciens*, the loss-of-*function* study of the *Hyp-1* homologous *CrIPR* in the recalcitrant plant *C. roseus* was carried

out by *using* a TRV-based *VIGS* approach. *Un*expectedly, *CrIPR*-silenced plants showed increased resistance to *A. tumefaciens*, which correlated with the up-regulation of *CrPR-5* but not *CrPR-1*. It was reported that *PR-10* silenced *M. truncatula* transgenic lines showed a reduced colonization of the oomycete *A. euteiches,* and a suppressed infection in the roots of transgenic plants due to *MtPr-10* silencing led to the *de novo* induction of two isoforms of thaumatin-like proteins (PR-5b) (Colditz *et al.*, 2007). Thus, antagonistic induction of PR-5 proteins, which are normally repressed due to PR-10 expression, is not an unprecedented phenomenon in plant-microbe interactions. A similar antagonistic crosstalk was observed in our *Hyp-1* overexpressing tobacco lines, where overexpression of *PR-10* from *H. perforatum* L. led to reduced expression of endogenous PR genes, *PR-1* and *PR-10*. These findings illustrate the complex crosstalk regulating plant-pathogen interactions. In parallel, the trial of VIGS in *H. perforatum* L. clearly indicated that TRV, PPV, PVX, TuMV and CMV are not able to infect *H. perforatum* L., which excluded the possibility of *H. perforatum* L. servers as the host of those viruses, and take the preliminary steps for processing VIGS in *H. perforatum* L.

Several PR-10 proteins have shown DNase and RNase activities *in vitro* and *in vivo*, which could assist to explain the role of *Hyp-1* in antibacterial defense (Chen *et al.*, 2006; Kim *et al.*, 2008; Xie *et al.*, 2010; Kim *et al.*, 2011; Krishnaswamy *et al.*, 2011; He *et al.*, 2013). DNA fragmentation was detected in rice suspension-cultured cells treated with PBZ1, a rice PR-10 family protein (Kim *et al.*, 2011). Chadha and Das (2006) reported that an RNase activity-competent version of PR-10 from peanut was internalized by hyphae of *Fusarium oxysporum* and inhibited fungal growth. Therefore, the putative DNase and RNase activities of *Hyp-1* might also play an important role in the death of *A. tumefaciens* cells observed upon co-cultivation with *H. perforatum* L. (Franklin *et al.*, 2008). In addition, our subcellular localization data suggested that Hyp-1 localized to the plasma membrane, where is important during plant-microbe interactions, since it acts as a barrier between the host and the pathogen and many pathogen-associated molecular pattern recognition receptors are localized at the plasma membrane (Boller and Felix, 2009). And other PR proteins with associated RNase activities have been localized in the cell plasma membrane (Jiang *et al.*, 2015).

6.1.2 PGIP localizes to the plasma membrane, cytoplasm and nucleus and overexpression of *HpHGIP* alters expression of defense-related genes to modulates recalcitrance to *A. tumefaciens*

The Polygalacturonase-inhibiting protein (PGIP), a cell wall binding protein, from LRR superfamily, specifically inhibits PGs produced by pathogens like *A. tumefaciens* and fungus. *PGIP* is not classified as *PR*, but the expression of *PGIP* could be induced by both biotic and abiotic stimuli, and PGIP plays an indispensable role in plant defense. For instance, overexpression of *PGIP* genes from bean, Chinese cabbage, pepper, cotton increased the tolerance to the fungi and the and the bacterium (Janni *et al*., 2008; Hwang *et al*., 2010; Wang *et al.*, 2013; Liu *et al*., 2017). In the present study, the defense-associated gene *HpPGIP* isolated from *H. perforatum* L. suspension cell cultures elicited with *A. tumefaciens* was overexpressed in *N. tabacum*. Thereafter, it was demonstrated for the first time that *HpPGIP* enhances plant resistance to *A. tumefaciens*, as confirmed by GUS staining assays.

HpPGIP protein was localized at the nucleus and cytoplasm, supported by the subcellular distribution of fluorescence derived from the transient expression of GFP-PGIP in *N. tabacum* leaves. Like Hyp-1, the nuclear localization of HpPGIP might play an important role in defense responses against *A. tumefaciens*, whose virulence depends on integration of T-DNA into the nucleus. Besides, PGIP is reported as a non-transmembrane protein targeted to the plasma membrane (Wang *et al.* 2015; Liu *et al*. 2016), the subcellular localization of HpPGIP at the plasma membrane might play an important role in defense responses as cell surface receptors that detect pathogens like *A. tumefaciens*, whose virulence depends on expression of PG (Rodriguez-Palenzuela, 1991).

To assess if *PGIP* triggers *A. tumefaciens*-induced defense pathways in plant, the critical genes from these pathways were detected in tobacco plants overexpressing *HpPGIP*, by qRT-PCR. Previous studies reported that the exogenous application of ABA, SA, JA increases the *PGIP* expression in plants (Zhang *et al.*, 2016; Liu *et al.*, 2017), indicating that these phytohormones may take a part in the *PGIP* defense function. Accordingly, our results suggested that defense responses induced by *HpPGIP* overexpression may involve JA pathway by increasing the expression of *NtaLOX*, but not in auxin pathway since *HpPGIP* overexpression increased *NtaARF8* expression. PR proteins have been defined as a group of plant specific-proteins accumulate to respond to pathogen infection. Overexpression of *HpPGIP* affected the expression levels of a series of PR genes, especially, *NtaPR-1* and *NtaPR-10*. In the present study, the expression of both PRs was reduced, while overexpressing cotton *PGIP* gene, *GhPGIP1*, in *Arabidopsis* increased *AthPR-1* and *AthPR-5* expression after inoculation with *V. dahliae* (Liu *et al.*, 2017). Moreover, microRNA-mediated gene silencing pathway involved *HpPGIP* defense against *A. tumefaciens*, since *NtaAGO1* expression was induced, and also first

time revealed that *NtamiR164*, especially *NtamiR164c* also involved into this pathway. *MiR164* have been recognized into plant response to abiotic stresses in *Arabidopsis*, *Brassica*, rice and potato (Bhardwaj *et al*., 2014; Fang *et al*., 2014; Lee *et al*., 2017; Zhang *et al*., 2018). In biotic stress, transcriptional activity of miR164a promoter was induced during plant virus infection (Bazzini *et al.*, 2009). To best of our knowledge, this is first report that *miR164c* accumulated in tobacco plants overexpressing defense genes against *A. tumefaciens*. Most importantly, *HpPGIP* overexpression increased the accumulation of genes involved in lignin biosynthesis pathways, namely *NtaPAL1,4* and *NtaCCR,* and in the flavonoid pathway namely *NtaCHS*. Furthermore, the increased expression of *NtaAPX* and *NtaFe-SOD*, demonstrated ROS pathway also participated into *A. tumefaciens*-induced defense pathway.

To further discover and expand the knowledge about plant response to the infection of *A. tumefaciens*, *Hyp-1* was fused with *HpPGIP* and the overexpressed in tobacco. As observed before, secondary metabolites and ROS pathways were confirmed to be involved the defense pathway. In contrast, those two defense pathways were enriched in *Hyp-1-PGIP* plants, where a significant increase in the expression of *NtaCAD* and *NtaCAT* was observed, in addition to an increase in the expression of *NtaPAL1,4*, *NtaCCR*, *NtaCHS*, *NtaAPX*, *NtaFe-SOD.* It is very interesting that this phenomenon is not the simple superposition of *Hyp-1* and *HpPGIP*, since lignin synthesis and ROS pathways were not involved in plants overexpressing *Hyp-1*. Moreover, the flavonoid synthesis pathway was even suppressed in these plants (Hou *et al*., unpublished results). Moreover, the increased expression of *NtaLOX* and *NtaAGO1* indicated that JA signaling pathway and miroRNA-mediated gene silencing pathway were employed in plants overexpressing *Hyp-1-PGIP*. Furthermore, *NtaARF8* and *NtaTIR1* were particularly induced by the fusion genes in transgenic plants indicating that auxin signaling pathway is not recruited as described previously that up-regulate the expression of those two genes could causes cell wall expansion and stomata opening that allows some pathogens to gain access to the interior of plant tissues (Fu and Wang, 2011; Nazari *et al.*, 2017), conversely, which is employed by *Hyp-1*overexpression plant lines (Hou *et al*., unpublished results). Overexpression of *Hyp-1-PGIP* also interfered with the PR proteins and microRNA expression compared with *PGIP* single expressed plant samples.

To further investigate the functional characterization of *HpPGIP*, VIGS was performed to knock-down the *PGIP* expression, and *BoPGIP* from *B. oleracea* was selected as the homologous gene of *HpPGIP* by phylogenetic analysis. Unfortunately, as the marker of gene silencing, the bleach symptom induced by silencing of *BoPDS2* was neither observed in *B.*

oleracea or *B. nigra*, unlike reports described previously (Zheng *et al*., 2010). So, in our study, *N. benthamiana* plants were used to harbor the heterologous VIGS. Interestingly, silencing of *BoPGIP* in *N. benthamiana* resulted in enhanced tolerance to *A. tumefaciens* rather than reducing the resistance. These findings are supported by the increase in *NbPRs* expression, in agreement with the silencing of PR-10-like proteins in *M. truncatula* which results in *MtPR-5* accumulation in order to tolerate upon with *A. euteiches* infection (Colditz *et al.*, 2007) and it is consistent with our other data of silencing *Hyp-1* in *C. roseus* described above (Hou *et al*., unpublished results).

In summary, *Agrobacterium*-mediated genetic transformation approaches that reduce *HpPGIP* expression in *H. perforatum* L. could give a better chance at efforts aimed at the genetic manipulation of this recalcitrant and medicinal plant spp. However, antagonistic regulation of PR proteins and that of other inducible defense-related proteins that result in enhanced resistance to *A. tumefaciens* should be taken into consideration. The present study provides a better understanding regarding the functional characterization of *PGIP* gene from *H. perforatum* L., and adds significant knowledge about the molecular mechanism of the *H. perforatum* L.-*A. tumefaciens* interaction.

6.1.3 A networking of genes involved in secondary metabolism, ROS pathways and other defense mechanisms is recruited in *H. perforatum* L. upon elicitation with *A. tumefaciens*

In previous reports, *A. tumefaciens* treated with *H. perforatum* L. suspension cell cultures showed 99% mortality of bacterium after a 12 h cocultivation period, through a biphasic ROS burst, which led to browning of *Hypericum* cells (Franklin *et al.*, 2008). Additionally, some important genes (*HpPAL*, *HpBPS*) were upregulated and may have led to differential metabolic profile in invaded cells. Together with the present study, these results supported the direct involvement of xanthones in this mechanism while still independent of flavonoid pathway. Hyperforin was also unaffected in present study. *HpOKS*, *HpPKS2* and *HpIGPS* gene expression were observed increasingly expressed and suggested that hypericin and melatonin biosynthesis pathways may be key pathways to maintain recalcitrance in *H. perforatum L.* too. In addition, in *RDR6*- and *SGS3*-associated gene silencing pathways, the significant decrease in *HpSGS3* transcripts indicated that S-PTGS and ta-siRNA pathways are not involved in

defense pathways of *H. perforatum L* against *A. tumefaciens*. Moreover, in the present study there was no alteration in the expression of *HpAGO5*, which is known for associating with short RNAs containing a 5-terminal cytosine and has been reported in antiviral responses in Arabidopsis (Shimura and Pantaleo, 2011; Zhang *et al.*, 2015), suggesting that it has no contribution in *H. perforatum L.* resistance to *A. tumefaciens*. Moreover, the overexpression of *Hyp-1* and *HpPGIP* which were selected from a cDNA library of *H. perforatum L.* cells elicited with *A. tumefaciens* confirmed the defense function of these two genes. Furthermore, the overexpression of the genes *HpPAL*, *HpBPS*, *HpOKS*, *HpPKS2*, *HpIGPS*, *HpAOX2*, *Hyp-1* and *HpPGIP* after 12 h and the reduction in gene expression after 24 h, supports their roles in mortality of *A. tumefaciens*, likely by promoting the production of antibacterial compounds such as secondary metabolites and ROS. A 99% bacteria mortality rate after 12 h of co-cultivation supports this conclusion (Franklin *et al.*, 2008).

Pathway engineering of important bio-compounds in *H. perforatum* L. has major limitations due to the lack of information about the regulation of these pathways at molecular level. For instance, hypericin production was reported decades ago, but genes involved in its production and accumulation in dark glands is still unclear (Karppinen, 2010). In this direction, the present study shed light on this matter at molecular level. *HpPAL* highly expressed in both *H. perforatum* L. leaves and glands, together with *HpBPS*, *HpOKS* and *HpPKS2* suggests their roles in the increased production of xanthones and accumulation of hypericin in dark glands. *HpCHS* and *HpPKS1* were found lowly expressed in dark glands, while *HpPAT*, *HpIGPS* showed no significant difference in their expression, indicating that they may not be involved in accumulation of flavonoids neither melatonin, specifically in dark glands. Besides, there was no significant difference in the expression patterns of *HpRDR6*, *HpSGS3* and *HpAGO5* among *H. perforatum* L. leaves and glands, indicating that gene silencing pathways of S-PTGS and ta-siRNA pathway as well as *HpAGO5* were not involved in *H. perforatum* L. defense responses. In addition, the induced expression of *HpCAT*, indicated that the ROS pathway was occurring in black glands. The genes isolated and characterized in this study, *Hyp-1* and *HpPGIP*, were found to be expressed both in *H. perforatum* L. leaves and glands, being upregulated in dark glands as well as upon *A. tumefaciens* invasion. Hence, the present study indicated that the black glands play a major role in *H. perforatum* L. resistance to *A. tumefaciens*, not only producing xanthones and hypericin, but also producing high levels of transcripts of key genes underlying plant defense.

In summary, qRT-PCR results indicated that several pathways are involved in the defense of *H. perforatum* L. cell suspensions to *A. tumefaciens* infection, including the secondary metabolism pathways that lead to the production of xanthone, hypericin and melatonin, complementing the knowledge discovered previously (Franklin *et al.*, 2009). Moreover, ROS pathway was confirmed to be involved in these defense responses by inducing the expression of key genes such as *HpAOX2*. In addition, the transcripts of defense genes in *H. perforatum* L. glands revealed these structures are responsible for the resistance to pathogens, by accumulating a wide array of secondary metabolites, namely, xanthone and hypericin, while increasing the expression of *HpCAT* and of *A. tumefaciens* defense genes *Hyp-1* and *HpPGIP*.

6.2 Future prospects

In the present study, the identification and characterization of two *Agrobacterium* defense genes *Hyp-1*and *HpPGIP* have been carried out. It provides a better understanding of the biofunction of those two defense genes and adds significant knowledge about the molecular mechanism of the *H. perforatum* L.-*A. tumefaciens* interaction.

Several PR-10 proteins have shown DNase and RNase activities *in vitro* and *in vivo*, which could assist to explain the role of *Hyp-1* in antibacterial defense. Future research on the characterization of RNase and DNase activities of Hyp-1 might shed light on its protective role in degrading DNA or RNA of invading pathogens in *H. perforatum* L. *Agrobacterium*-mediated genetic transformation approaches that reduce *Hyp-1* expression in *H. perforatum* L. could give a better chance at efforts aimed at the genetic manipulation of this recalcitrant and medicinal plant spp. However, antagonistic regulation of PR proteins and that of other inducible defense-related proteins that result in enhanced resistance to *A. tumefaciens* should be taken into consideration.

HpPGIP from *H. perforatum* L. was characterized for the first time, and it was provided evidence that *HpPGIP* overexpressing results in enhances tolerance of tobacco plants to *A. tumefaciens*, revealing the possible defense pathways involved. Numerous studies about PGIP have been done in plants so far, especially in the interaction between plant and fungus, but very few researches have been carried out to discover the function of PGIP-PGs between plant and bacterium, even though it has been reported in 1991 that *A. tumefaciens* produces PGs to infect

plants (Rodriguez-Palenzuela *et al*., 1991). PGIPs belong to the superfamily of LRR protein, a group of proteins that are believed to be specialized for recognition of non-self-molecules and protein-protein interaction. LRR motif has been found in the proteins with the functions of resistance and defense against microbial pathogens in plants. The crystal structure of a PGIP from Phaseolus vulgaris reveals a negative charge on the surface of the LRR concave face, which probably participates in binding of PGs (Di Matteo *et al*., 2003). Moreover, PGIPs are well-known for their functions in limiting cell wall degradation and pathogens invasion. In particular, PGIP specifically recognizes and inhibits PGs which are produced by bacteria and fungus to limit their destructive action and accumulate OGs, which activate a wide range of defense responses. Future studies regarding the interaction between *HpPGIP- A. tumefaciens* will further elucidate the pathways involved in *HpPGIP*-mediated defense against bacterial infection.

Furthermore, besides the defense genes, it is well-known that plant secondary metabolites have an essential role in defense against pathogens, and *H. perforatum* L., is a reservoir of high-value secondary metabolites. In the present study (chapter 5) provided a better understanding on the molecular mechanisms underlying the resistance of *H. perforatum* L. cells to *A. tumefaciens* infection. Further studies including identification and characterization of the genes from secondary methanolic pathways, will help elucidate the particular role of each gene in plant defense, and contribute to the assembly of the network of events underlying these responses.

6.3 References

Bais, H.P., Vepachedu, R., Lawrence, C.B., Stermitz, F.R. and Vivanco, J.M. (2003) Molecular and biochemical characterization of an enzyme responsible for the formation of hypericin in St. John's wort (Hypericum perforatum L.). *J. Biol. Chem.* **278**, 32413–32422.

Bazzini, A.A., Almasia, N.I., Manacorda, C.A., Mongelli, V.C., Conti, G., Maroniche, G.A., Rodriguez, M. C., Distéfano, A. J., Hopp, H.E., Vas, M., and Asurmendi, S. (2009) Virus infection elevates transcriptional activity of miR164a promoter in plants. *BMC Plant Biol.* **9**.

Bhardwaj, A.R., Joshi, G., Pandey, R., Kukreja, B., Goel, S., Jagannath, A., Kumar, A., Katiyar-Agarwal, S. and Agarwal, M. (2014) A genome-wide perspective of miRNAome in response to high temperature, salinity and drought stresses in Brassica

juncea (Czern) L. *PLoS One* **9**.

Boller, T. and Felix, G. (2009) A renaissance of elicitors: perception of microbe-associated molecular patterns and danger signals by pattern-recognition receptors. *Annu. Rev. Plant Biol.* **60**, 379–406.

Chadha, P. and Das, R.H. (2006) A pathogenesis related protein, AhPR10 from peanut: An insight of its mode of antifungal activity. *Planta* **225**, 213–222.

Chen, Z.-Y., Brown, R.L., Rajasekaran, K., Damann, K.E. and Cleveland, T.E. (2006) Identification of a maize kernel pathogenesis-related protein and evidence for its involvement in resistance to Aspergillus flavus infection and aflatoxin production. *Phytopathology* **96**, 87–95.

Colditz, F., Niehaus, K. and Krajinski, F. (2007) Silencing of PR-10-like proteins in Medicago truncatula results in an antagonistic induction of other PR proteins and in an increased tolerance upon infection with the oomycete Aphanomyces euteiches. *Planta* **226**, 57–71.

Fang, Y., Xie, K. and Xiong, L. (2014) Conserved miR164-targeted NAC genes negatively regulate drought resistance in rice. *J. Exp. Bot.* **65**, 2119–2135.

Franklin, G., Conceição, L.F.R., Kombrink, E. and Dias, A.C.P. (2008) Hypericum perforatum plant cells reduce Agrobacterium viability during co-cultivation. *Planta* **227**, 1401–1408.

Franklin, G., Conceição, L.F.R., Kombrink, E. and Dias, A.C.P. (2009) Xanthone biosynthesis in Hypericum perforatum cells provides antioxidant and antimicrobial protection upon biotic stress. *Phytochemistry* **70**, 60–68.

Fu, J. and Wang, S. (2011) Insights into auxin signaling in plant-pathogen interactions. *Front. Plant Sci.* **2**, 1–7.

He, M., Xu, Y., Cao, J., Zhu Z, Jiao Y, Wang Y, Guan X, Yang Y, Xu W and Fu Z. (2013) Subcellular localization and functional analyses of a PR10 protein gene from Vitis pseudoreticulata in response to Plasmopara viticola infection. *Protoplasma* **250**, 129–140.

Hwang, B.H., Bae, H., Lim, H.S., Kim, K.B., Kim, S.J., Im, M.H., Park, B.S., Kim, D.S. and Kim, J. (2010) Overexpression of polygalacturonase-inhibiting protein 2 (PGIP2) of

Chinese cabbage (Brassica rapa ssp. pekinensis) increased resistance to the bacterial pathogen Pectobacterium carotovorum ssp. carotovorum. *Plant Cell. Tissue Organ Cult.* **103**, 293–305.

Janni, M., Sella, L., Favaron, F., Blechl, A.E., Lorenzo, G. De and D'Ovidio, R. (2008) The expression of a bean PGIP in transgenic wheat confers increased resistance to the fungal pathogen *Bipolaris sorokiniana*. *Mol. Plant-Microbe Interact.* **21**, 171–177.

Jiang, L., Wu, J., Fan, S., Li, W., Dong, L., Cheng, Q., Xu, P. and Zhang, S. (2015) Isolation and characterization of a novel pathogenesis-related protein gene (GmPRP) with induced expression in soybean (*Glycine max*) during infection with *Phytophthora sojae*. *PLoS One* **10**, e0129932.

Karppinen, K. (2010) Biosynthesis of hypericins and hyperforins in Hypericum perforatum L.(St. John's wort)—precursors and genes involved.

Kim, S.G., Kim, S.T., Wang, Y.M., Yu, S., Choi, S.I., Kim, Y.C., Kim,W.T., Agrawal,G.K., Rakwal, R., and Kang, K.Y,. (2011) The RNase activity of rice probenazole-induced protein1 (PBZ1) Plays a key role in cell death in plants. *Mol. Cells* **31**, 25–31.

Kim, S.T., Yu, S., Kang, Y.H., Kim, S.G., Kim, J.Y., Kim, S.H. and Kang, K.Y. (2008) The rice pathogen-related protein 10 (JIOsPR10) is induced by abiotic and biotic stresses and exhibits ribonuclease activity. *Plant Cell Rep.* **27**, 593–603.

Košuth, J., Hrehorová, D., Jaskolski, M. and Čellárová, E. (2013) Stress-induced expression and structure of the putative gene hyp-1 for hypericin biosynthesis. *Plant Cell. Tissue Organ Cult.* **114**, 207–216.

Krishnaswamy, S., Baral, P.K., James, M.N.G. and Kav, N.N.V. (2011) Site-directed mutagenesis of histidine 69 and glutamic acid 148 alters the ribonuclease activity of pea ABR17 (PR10.4). *Plant Physiol. Biochem.* **49**, 958–962.

Lee, M.H., Jeon, H.S., Kim, H.G. and Park, O.K. (2017) An Arabidopsis NAC transcription factor NAC4 promotes pathogen-induced cell death under negative regulation by microRNA164. *New Phytol.* **214**, 343–360.

Liu, N., Zhang, X., Sun, Y., Wang, P., Li, X., Pei, Y., Li, F. and Hou, Y. (2017) Molecular evidence for the involvement of a polygalacturonase-inhibiting protein, GhPGIP1, in enhanced resistance to Verticillium and Fusarium wilts in cotton. *Sci. Rep.* **7**, 1–18.

Matteo, A. Di, Federici, L., Mattei, B., Salvi, G., Johnson, K.A., Savino, C., Lorenzo, G. De, Tsernoglou, D. and Cervone, F. (2003) The crystal structure of polygalacturonase-inhibiting protein (PGIP), a leucine-rich repeat protein involved in plant defense. *Proc. Natl. Acad. Sci.* **100**, 10124–10128.

Michalska, K., Fernandes, H., Sikorski, M. and Jaskolski, M. (2010) Crystal structure of Hyp-1, a St. John's wort protein implicated in the biosynthesis of hypericin. *J. Struct. Biol.* **169**, 161–171.

Nazari, F., Safaie, N., Soltani, B.M., Shams-Bakhsh, M. and Sharifi, M. (2017) Bacillus subtilis affects miRNAs and flavanoids production in Agrobacterium-Tobacco interaction. *Plant Physiol. Biochem.* **118**, 98–106.

Pinweha, N., Asvarak, T., Viboonjun, U. and Narangajavana, J. (2015) Involvement of miR160/miR393 and their targets in cassava responses to anthracnose disease. *J. Plant Physiol.* **174**, 26–35.

Pitzschke, A. (2013) Agrobacterium infection and plant defense—transformation success hangs by a thread. *Front. Plant Sci.* **4**, 1–12.

Rodriguez-Palenzuela P, Burr TJ, Collmer A. (1991) Polygalacturonase is a virulence factor in Agrobacterium-tumefaciens biovar 3. *J. Bacteriol.* **173 (20)**, 6547–6552

Shimura, H. and Pantaleo, V. (2011) Viral induction and suppression of RNA silencing in plants. *Biochim. Biophys. Acta - Gene Regul. Mech.* **1809**, 601–612.

Wang, X., Zhu, X., Tooley, P. and Zhang, X. (2013) Cloning and functional analysis of three genes encoding polygalacturonase-inhibiting proteins from Capsicum annuum and transgenic CaPGIP1 in tobacco in relation to increased resistance to two fungal pathogens. *Plant Mol. Biol.* **81**, 379–400.

Wójcik, A.M., Nodine, M.D. and Gaj, M.D. (2017) MiR160 and miR166/165 contribute to the LEC2-mediated auxin response involved in the somatic embryogenesis induction in Arabidopsis. *Front. Plant Sci.* **8**, 1–17.

Xie, Y.R., Chen, Z.Y., Brown, R.L. and Bhatnagar, D. (2010) Expression and functional characterization of two pathogenesis-related protein 10 genes from Zea mays. *J. Plant Physiol.* **167**, 121–130.

Zhang, C., Feng, C., Wang, J., Kong, F. and Sun, W. (2016) Cloning , expression analysis and recombinant expression of a gene encoding a polygalac- turonase-inhibiting protein from tobacco , Nicotiana tabacum. *Hly*.

Zhang, C., Wu, Z., Li, Y. and Wu, J. (2015) Biogenesis, function, and applications of virus-derived small RNAs in plants. *Front. Microbiol.* **6**, 1–12.

Zhang, L., Yao, L., Zhang, N., Yang, J., Zhu, X., Tang, X., Calderón-Urrea, A. and Si, H. (2018) Lateral root development in potato is mediated by Stu-mi164 regulation of NAC transcription factor. *Front. Plant Sci.* **9**, 383

Zheng, S.J., Snoeren, T.A., Hogewoning, S.W., van Loon, J.J., and Dicke, M. (2010) Disruption of plant carotenoid biosynthesis through virus-induced gene silencing affects oviposition behaviour of the butterfly Pieris rapae. *New Phytol* 733–745.